UNIVERSIDADE DE LISBOA
FACULDADE DE CIÊNCIAS
DEPARTAMENTO DE BIOLOGIA ANIMAL

Role of RHBDD2 in Membrane Trafficking Regulation

Mestrado em Biologia Evolutiva e do Desenvolvimento

Tianyi Hu

Dissertação orientada por:
Dr. Colin Adrain
Prof. Dr. Gabriela Rodrigues

2014/2015

Summary

RHBDD2 é parcialmente relacionada com romboides, protéases intra-membranares que degradam substratos na via secretora. Curiosamente, um subgrupo da família romboide, incluindo a RHBDD2, não tem resíduos catalíticos essenciais. Estas "pseudo-proteases" são conservadas, o que implica uma pressão seletiva para manter a sua função durante a evolução. Recentemente, uma mutação pontual (R85H) foi identificada no gene humano que codifica para a proteína RHBDD2, e está associada a uma doença neuro-degenerativa chamada Retinitis Pigmentosa (RP). Esta mutação pontual de G para A, alterou o aminoácido codificado de arginina para histidina no códão 85 do Segundo exão. No entanto a relevância fisiológica da RHBDD2 e a sua contribuição para a doença acima referida não é clara.

Os dois maiores focos deste estudo foram (1) a investigação de como a mutação R85H na RHBDD2 contribui para a doença a nível celular; (2) investigar a função da RHBDD2 nativa a nível da célula e do organismo.

Vários programas de alinhamento (ClustalO, muscle, tcoffee ferramentas de alinhamento) foram usados para prever a topologia da RHBDD2. Com base na comparação com outros membros da superfamília romboide, os domínios transmembranares (TMD) da RHBDD2 foram previstos. Após identificar cuidadosamente todos os aminoácidos chave nos alinhamentos, eu previ que a RHBDD2 é uma proteína transmembranar com 6 TMD, com ambas as terminações N- e C- presentes na face citoplasmática.

Devido ao conhecimento prévio de que a RHBDD2 é expressa em níveis elevados na retina, consistente com a expressão a nível do mRNA na base de dados bioGPS, células de ratinho RPE foram selecionadas como materiais essenciais para as seguintes experiências. Plasmídeos para a sobre-expressão da RHBDD2 WT e da mutação R85H com uma tag de HA no C-terminal foram gerados no vector pLEX MCS, e usados para gerar células estáveis por transdução

lentiviral. Estas linhas celulares juntamente com a linha celular com o vector vazio (EV) foram usadas para investigar a função da RHBDD2 a nível bioquímico e da biologia celular.

Surpreendentemente, a expressão da forma mutante da RHBDD2 em células RPE, não induziu um stress constitutivo do retículo endoplasmático (RE). Não houce degradação da proteína mutante na linha celular R85H. Isto permitiu-me propor de forma preliminar, que o fenótipo da mutação R85H não é causado por stress do (RE).

Por forma a analisar a localização do Et e mutante R85H, células RPE foram marcadas com um anticorpo anti-HA (para detectar RHBDD2 WT e mutante R85H) e com o marcador de stress do RE Calreticulin ou o marcador do cis-Golgi GM130. Imagens de imuno-fluorescência e co-localização mostraram que tanto a WT como a mutante RHBDD2 localizam predominantemente no aparelho de Golgi. Indicando que a mutante R85H localiza-se no mesmo compartimento celular que a proteína nativa, sugerindo que o fenótipo da doença não é causado por stress do RE ou por falta de folding da proteína.

Ratinhos com deleção genética (KO) na RHBDD2 foram gerados pelo sistema CRISPR/Cas9 para definir a função da RHBDD2 e o fenótipo dos animais mutantes. Infelizmente, 5 animais fundadores morreram no primeiro dia de vida. Analise do tecido revelou que dois deles tinham INDELs e três deles eram nativos. Logo, a morte dos animais é pouco provável estar relacionada com o genótipo RHBDD2. A experiência foi repetida e 17 potencias fundadores foram obtidos. Resultados de sequênciaçao indicaram que dois animais fundadores tinham a mutação desejada, provavelmente como quimeras. Identificamos também animais fundadores com INDELs de 6 e 9 pares de bases.

Experiências de imuno-precepitação acopladas a espectrometria de massa foram realizadas para identificar novos interactores da RHBDD2. Três IPs foram efetuados em diferentes condições (com ou sem crosslinker, acoplado com diferentes tampões de lavagem). Golgins (GM160, Golgin-84, Golgin-45), que atuam como plataformas de acoplamento membranar, foram co-immuno-precepitadas coma RHBDD2 em ambas as experiências com cross-linker, indicando que a RHBDD2 pode ter um papel na manutenção da estrutura do aparelho de Golgi. Componentes chaves das vesículas COPII foram

também capturados nos IPs crosslinked e não crosslinked, indicando que a RHBDD2 pode contribuir para o transporte ER para Golgi dependente de COPII. Estes dois grupos apareceram tanto nos IPs da proteína RHBDD2 nativa como mutante R85H. De notar, o número total de identificações de peptídeos está diminuído em IPs de R85H em condições de crosslinking ou na sua ausência, indicando talvez que o mutante R85H, exibe uma alteração conformacional que resulta numa mudança de repertório de interactores.

De acordo com as IPs, experiências de fragmentação do Golgi e da sua reorganização, foram efectuadas com RNA de interferência curto (siRNA) para fazer a atenuação da expressão (KD) de RHBDD2 em células HeLa. /2 horas após a transfecçao, as células foram tratadas com BFA, e depois a droga foi removida do meio. De seguida, as células foram fixadas a diferentes pontos de incubação. Esta experiência não resultou em nenhuma diferença óbvia, na cinética de da morfologia do aparelho de Golgi entre as células tratadas control ou com o KD, mas é importante notar que o siRNA não promove a atenuçao complete da expressão da RHBDD2, logo a presença de alguma RHBDD2 residual pode ter prevenido a observação de um fenótipo mais marcado.

O papel fisiológico da RHBDD2 permanece desconhecido. Considerando os possíveis parceiros de ligação da RHBDD2 e a localização da RHBDD2, eu proponho que trabalho future se deva focar no teste do tráfego celular e da glicosilação em células sem expressão de RHBDD2 (KO). Também seria útil gerar um mutante R85H endógeno nas células RPE para avaliar a patologia da mutação, e claro, para avaliar o fenótipo dos ratinhos mutantes.

Palavras chave: RHBDD2, superfamília romboide, controlo de qualidade do RE, fragmentação do Golgi, Retinitis Pigmentosa

Index

1. Introduction

1.1 The Secretory pathway

About one third of all proteins enter the secretory pathway, a route that allows a cell to regulate delivery of newly synthesized proteins, carbohydrates, and lipids to the cell surface and intracellular vesicular organelles. In brief, secretory cargoes are synthesized and assembled in the endoplasmic reticulum (ER); subsequently they are transported to the Golgi apparatus for further processing and maturation. After that, these proteins are distributed to their final destination (Fig.1). This directional membrane flow is called membrane trafficking[1].

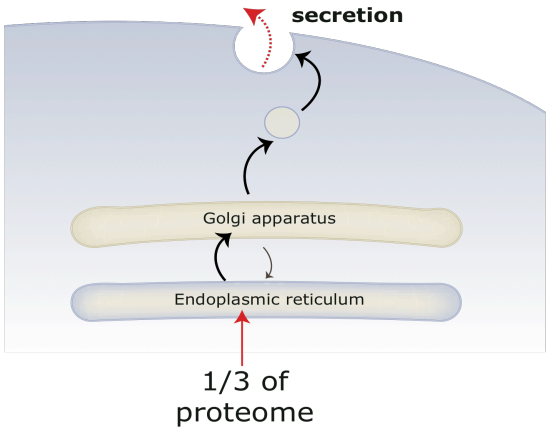

Figure 1 The secretory pathway
The secretory molecules are synthesized and assembled in the ER, then further modified in Golgi. Afterwards, they are distributed to their final destination (for example, the plasma membrane). The ER is the first line of defense in quality control, a mechanism that prevents the transit of misfolded folded proteins to the later secretory pathway. If any of the misfolded proteins inadvertantly escaped, they can be retrieved by retrograde transport from the Golgi apparatus to ER.

One of the most important roles of secretory proteins is to serve in cell signaling, which governs fundamental cellular activities and coordinates cell actions. Basically, the signal-sending cells produce secretory proteins that

change the cellular behavior of other cells (the signal-receiving cells)[30]. For instance, fibroblast growth factor (FGF) can induce limb development in specific tissues; Notch signaling can inhibit their neigbouring cells from becoming neurons; the Ephrin-Eph signaling can lead to repulsion and segregation of cells and tissues etc.

The receptors on the surface of the signal-receiving cells in the signaling pathway are transmembrane proteins. They are physically attached to the membrane and span across the entire lipid bilayer with their transmembrane domains at least once. As a result, they can perceive the information carried by extracellular signaling molecules and transfer it to the intracellular side, and vice versa.

The EGFR signaling pathway in *Drosophila* is a prominent example of how membrane proteins are used to control signaling. Spitz, a membrane-tethered EGFR ligand is synthesized in the ER and is transported to Golgi by the help of a chaperone, called star. Thereafter, Rhomboid-1, a serine protease that localizes to the Golgi, cleaves Spitz within the upper part of its transmembrane domain with the help of the serine-histidine catalytic dyad. Subsequently, Spitz is secreted from the cell. Now it can bind to the EGF receptor on the surface of a neighboring cell and activate the EGFR[2].

1.2 Protein quality control in the early secretory pathway

Protein folding in the ER involves complex folding intermediates and is therefore intrinsically error prone[3]. Namely, if the folding capacity of the ER is exceeded, or a mutant protein is expressed, they risk misfolding and aggregation of proteins. In severe cases, the stress to the ER caused by misfolded protein results in apoptosis of the secretory cell in question, which can impact on the functionality of the secretory tissue or organ. Therefore a robust quality control of protein folding, which is monitored by the ER at the first stage, is critical in organisms to ensure that nascent cargo is retained and not recognized by the export machinery until the cargo is fully folded and assembled.

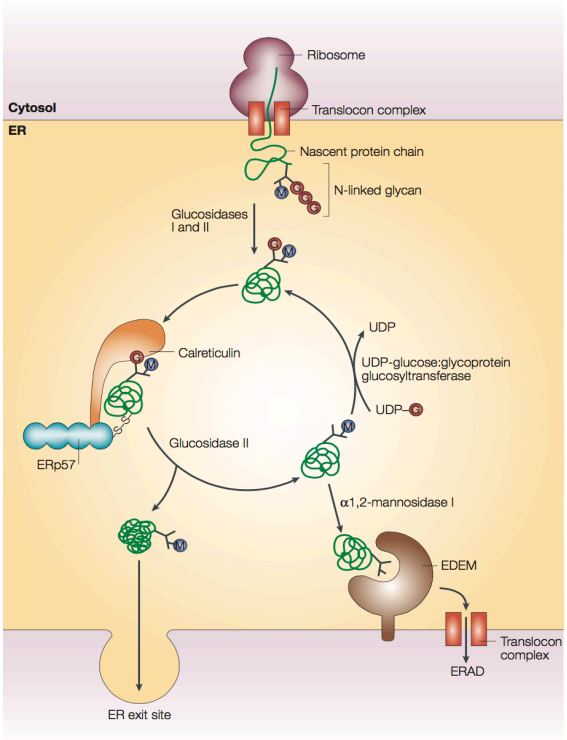

Figure 2 The calreticulin/calnexin ER folding cycle
Calreticulin and calnexin assist the folding of glycoproteins in the ER. They bind to monoglucosylated proteins during their synthesis and then associate with the thiol-disulphide oxidoreductase ERp57 to allow it form interchain disulphide bonds with bound glycoproteins. Cleavage of the remaining glucose by glucosidase II terminates the interaction with calreticulin and calnexin. On their release, correctly folded glycoproteins can exit ER, otherwise, a single glucose would be put back on the glycan and thereby promotes another calreticulin/calnexin cycle. (Adapted from Ellgaard & Helenius et al., 2003[4])

For example, glycoprotein quality control is fulfilled by the calreticulin and calnexin ER folding cycle. Glycoprotein synthesis proceeds via sequential addition and and removal of glycans (Fig.2). Calreticulin interacts with a monoglucosylated protein in the early steps. Cleavage of glucose in later step terminates the interaction with calreticulin. At this moment, if the protein is correctly folded, it would be released from the ER. By contrast, if the protein is not correctly folded, it is be recognized by glycoprotein glucosyltransferase, which places a single glucose back on the glycan and thereby promotes a renewed association with calreticulin. Calnexin is a similar quality-control molecular chaperone that performs the same service for soluble glycoproteins as does calreticulin[4].

Proteins that pass ER quality control are transported to the Golgi apparatus by anterograde transport in COPII (coat protein complex II) vesicles (Fig.3). However unfolded or misfolded proteins are retained in the ER and degraded by ER-associated degradation (ERAD)(Fig.4). Some partially folded proteins may escape from the ER; some proteins need export chaperones or export receptors to enable their transport from ER to Golgi. These export factors and escaped misfolded proteins must all be retrieved from the Golgi apparatus[6]. This so called

'retrograde transport' is achieved by the COPI (coat protein complex I) vesicles to balance the anterograde transport[7](Fig.3). Thus, although the ER is the major center of secretory protein quality control, the COPII, COPI vesicles and cis-Golgi compartments also contribute.

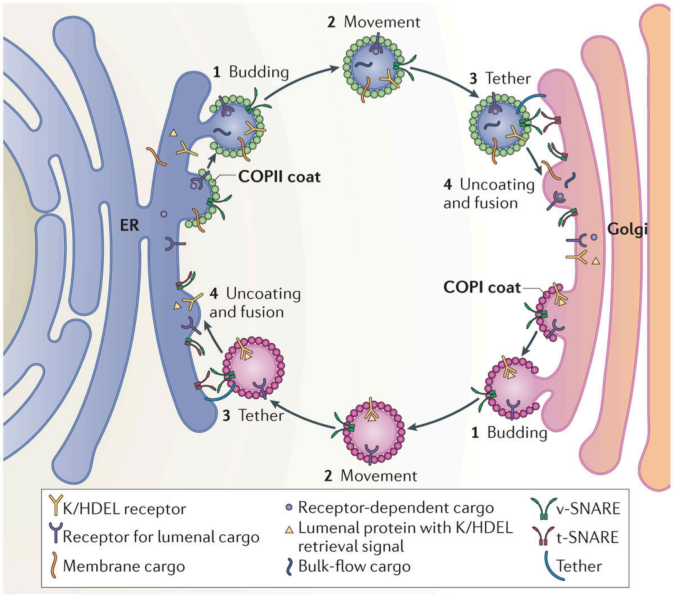

Figure 3 COPI and COPII mediated bidirectional transport between ER and Golgi apparatus
COPII vesicles mediate ER-to-Golgi anterograde transport. COPI vesicles facilitate Golgi-to-ER retrograde transport, including retrieval of escaped ER resident proteins. (Adapted from Brandizzi & Barlowe et al., 2013[5])

During ERAD, the molecular chaperones and associated 'sensors' in the ER recognize and target their client proteins for retrotranslocation into the cytoplasm, where the proteins are degraded by the ubiquitin-proteasome machinery[8]. Thus, ERAD counteracts the possibility of ER stress by removing misfolded proteins from the ER lumen and targeting them for degradation. In general, ubiquitination of proteins is a multistep process, involving activation, conjugation and ligation, performed by ubiquitin-activating enzyme (E1), ubiquitin-conjugating enzyme (E2) and ubiquitin ligase (E3), respectively. In the ubiquitination cascade, E1 can bind with dozens of E2s, which can bind with hundreds of E3s in a hierarchical way, hence the E3s involved in recognition and ubiquitination of highly specific target proteins[9]. In the specific case of ERAD, dedicated membrane-tethered E3 ligases (eg Hrd1, gp78) mediate ubiquitylation of ERAD substrates, acting on the cytoplasmic side of the membrane.

Derlin, a catalytically inactive member of the rhomboid family, is required for the extraction of certain aberrantly folded proteins from the ER[10] and has been proposed, based on yeast mutant studies to serve as a central component of the ERAD machinery. Specifically, Derlin has been proposed to provide a channel

for misfolded proteins to be retrotranslocated into the cytoplasm[11]. Derlins form heteromultimeric complexes with E3 ligases. During ERAD, the dislocation of proteins that contain one or several hydrophobic transmembrane domains, from the ER into the cytoplasm is clearly thermodynamically unfavourable. Therefore, transit across the ER membrane and into the cytoplasm is difficult, so needs to be fuelled by p97/VCP, an ATPase that binds to Derlins and the E3 ligases. Eventually, the dislocated proteins undergo proteasomal degradation in the cytoplasm[10,12] (Fig.4).

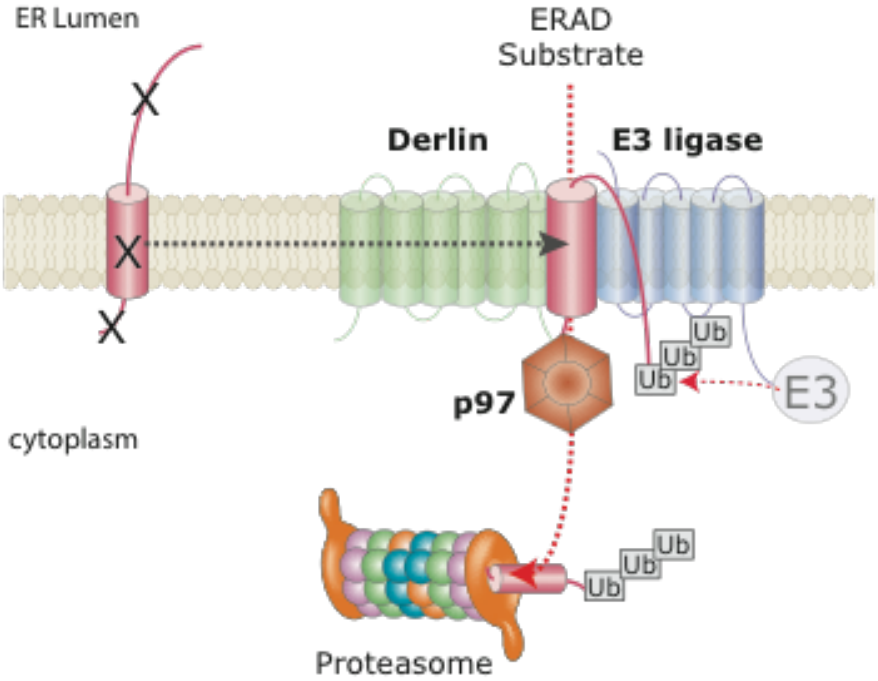

Figure 4 ERAD model
This is a simplified schematic diagram illustrating ERAD of a misfolded client protein (left red, x indicates misfolding that could occur within the ER lumen, ER membrane or cytoplasm). Right side is the multimeric membrane protein complex consisting of Derlin, E3 ligase and p97 ATPase. Ultimately, the ERAD substrate will be degraded by the proteasome.

1.3 Excessive accumulation of misfolded proteins triggers ER stress

If the ERAD machinery is insufficient, unfolded proteins accumulate in the ER

lumen, undermine the function of the organelle, and initiate ER stress. The term "unfolded protein response (UPR)" is a protective mechanism against ER stress in cells. At least four ER stress response outcomes have been identified. Three of them are designed to alleviate stress: upregulation of folding chaperones, translational attenuation and enhancing ERAD. However, the sustained or excessive stress will result in apoptosis[13].

There are three arms in the ER stress response pathway. First, the protein kinase RNA-like ER kinase (PERK)-mediated phosphorylation of eukaryotic translation initiator factor 2α (elF2α) can block translation and selectively upregulate the activating transcription factor 4 (ATF4) as well. Afterward, ATF4 enters the nucleus and activates ER stress response target genes. Second, during ER stress, the activating transcription factor 6 (ATF6) is cleaved, releasing an N-terminal cytosolic domain (p50ATF6), which thereafter enters the nucleus. Third, IRE1 is a kinase and endoribonuclease that dimerizes and autotransphosphorylates under ER stress conditions. Activated IRE1 catalyses the excision of a 26 nucleotide unconventional intron from the transcription factor X box-binding protein 1 (XBP1) mRNA, shifting the coding reading frame to generate an active transcription factor that translocates to the nucleus to induce the upregulation of its target genes[14].

Given the importance of the secretory pathway, it is unsurprising that many diseases are associated with membrane trafficking defects. The ER quality control machinery can contribute to diseases in diverse ways. (1) ER retention of mutated protein prevents the protein from reaching its final destination, thus causes diseases. Cystic fibrosis(CF) where a single point mutation results in a failure to traffic CFTR, a chloride channel, to the plasma membrane in CF patients. CFTR is instead retained in the ER and degraded [15]. (2) Misfolded proteins triggers ER stress that causes diseases. A prominent example is Retinitis Pigmentosa (RP)[16], in which misfolding mutations in important photoreceptor proteins trigger ER stress, causing photoreceptor death and thus blindness. (3) Chronic ER stress in particular has been implicated in numerous human diseases. In type II diabetes, the excess nutrient intake demands increased insulin secretion. This large amount of insulin secretion pushes the ER folding and quality control capacity to the limit[17]. In summary, the discovery of many

diseases that are associated with trafficking defects, ER quality control and ER stress highlights the importance of this pathway. [1]

1.4 Golgi Apparatus

The Golgi apparatus is one of the most important organelles in membrane trafficking. It is a huge network that consists of stapled cisternae, the membranous stacks, which contain a variety of resident enzymes that modify the secretory proteins by addition of carbohydrates (glycosylation) and phosphates (phosphorylation). Thus, Golgi plays a key role in intracellular trafficking, processing and secretion of glycoproteins, glycolipids and proteoglycans (proteins that are heavily glycosylated).

Based on the distribution of different resident proteins appearing in the Golgi stacks, it can be divided into three regions: cis, medial and trans. The movement and maturation of cisternae from cis to trans is called anterograde membrane flow. On the contrary the transport of cargoes from the Golgi to ER is referred as retrograde transport (Fig.1).

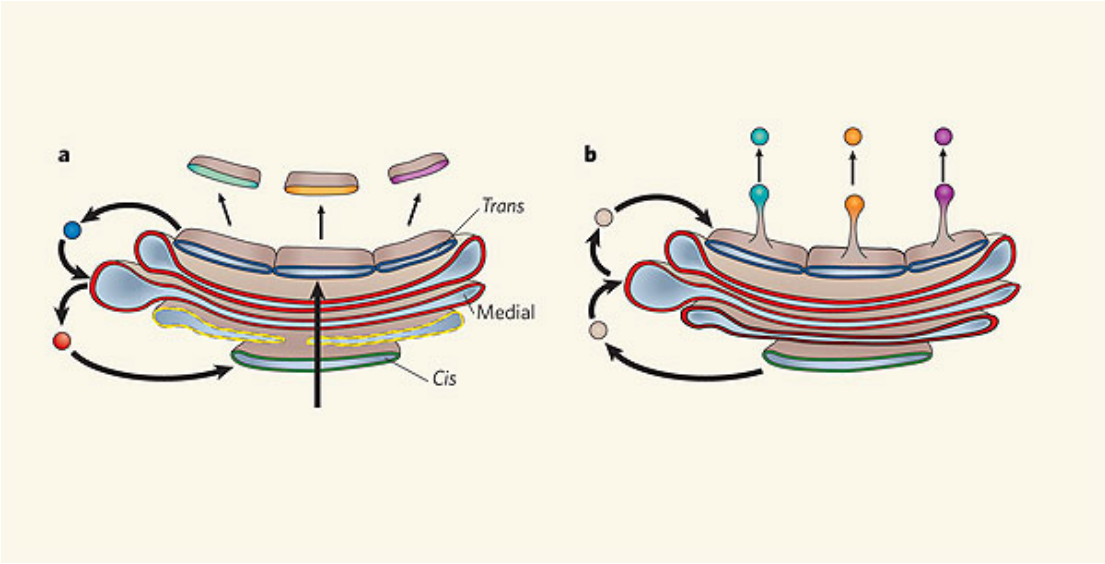

Figure 5 Two Golgi apparatus models
(a) The cisternal maturation model. (b) The anterograde vesicular transport model (Adapted from Malhotra and Mayor et al., 2006[18])

There are two models of intra-Golgi transport (Fig.5): Anterograde vesicular transport and cisternal maturation. The major difference is the movement of resident and cargo proteins. In the first model, cargo molecules will move through the stack passively as the cisternae move forward, while resident proteins will be recycled by retrograde transport to establish differential concentrations across the stack. In the second model, molecules will move forward in transport vesicles, while resident proteins are specifically retained. These two models are not mutually exclusive and may occur simultaneously[19].

At the cis-Golgi, where incoming vesicles undergo fusion with the cisterna COPII and COPI vesicles mediate the anterograde transport and retrograde transport respectively between the ER and the Golgi apparatus. The trans-Golgi, the exit point of the Golgi, is the major site of sorting secretory proteins and lipids to various cellular locations: another key role of the Golgi apparatus. It still remains to be established how many types of distinct vesicular trafficking destinations there are[20].

In addition to the enzymatic and sorting activities of the Golgi, a cohort of resident Golgi proteins maintain the Golgi structure, and also play an important role in the disassembly and reassembly of Golgi during mitosis, such as golgins[21].

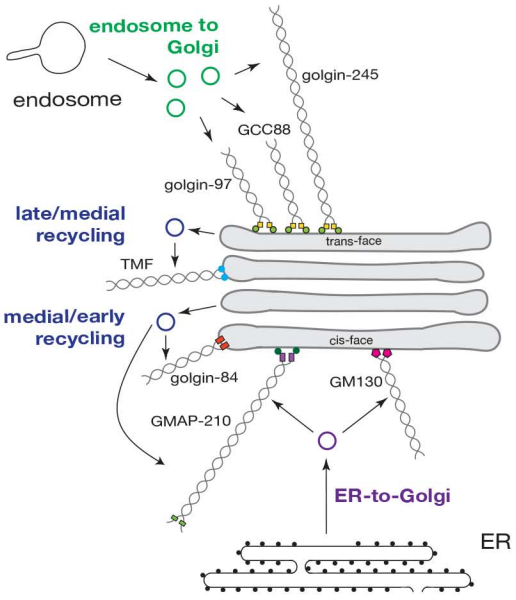

Figure 6 Schematic golgins model
All of the molecules shown are golgins. They appear to tether the different sets of vesicles arriving at the Golgi. (Adapted from Wong and Munro et al., 2014[22])

The fractionation experiments of Golgi apparatus suggested the presence of a Golgi matrix[23]. Golgin and GRASP family membranes are identified as the major components of this putative matrix[24]. Golgins usually are anchored to the Golgi

by their C termini with the majority of the protein exposed to the cytoplasm[24]. Golgins are membrane tethers throughout the whole Golgi apparatus that capture transport vesicles and help them attach to the Golgi apparatus, which drive membrane fusion[22]. Specific golgins can tether specific classes of vesicles more efficiently (Fig.6), thus leads to a selective transfer of contents between Golgi cisternae[22].

Following the tethering of the captured vesicles, SNARE proteins mediate fusion between donor and acceptor membranes. SNAREs are soluble NSF (N-ethyl-maleimide-sensitive fusion protein) attachment protein receptors, which have been implicated as central in most intracellular membrane trafficking events. SNAREs were initially considered to confer specificity of intracellular membrane trafficking, which now remains controversial[25]. And intuitively it is most likely to be defined at the tethering stages, by golgins described above.

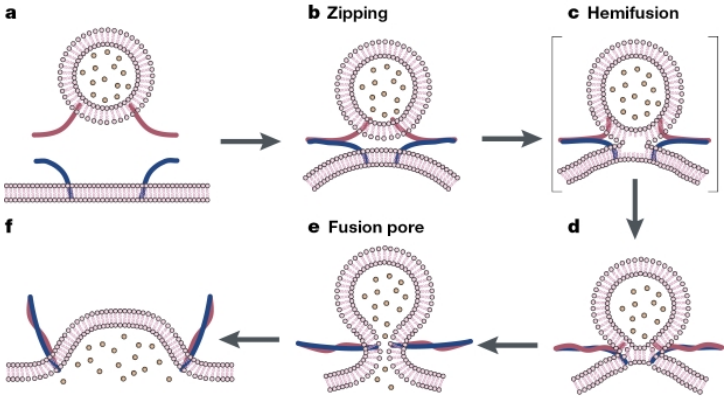

Figure 7 Model of SNARE-mediated lipid fusion
The SNARE core complex forms the "zippers" to overcome energetically unfavourable lipid fusion. (Adapted from Chen and Scheller et al., 2014[25])

The current model of SNARE mediated model is the "zipper" model (Fig.7) [25]. The SNARE core complex "zips" two membrane compartments from the membrane-distal amino termini to the membrane-proximal carboxyl termini to overcome the energetically unfavourable process. Once two membranes are close enough, the hemifusion occurs. Afterward, the membrane breakdown (fusion pore) is induced by the lateral tension of the "zippers". In the end, the fusion pore expands and the membrane relaxes.

1.5 The Rhomboid family contains several catalytically inactive homologs

The Rhomboid gene was first discovered in genetic screens in *Drosophila*[26]. Subsequently, Rhomboids were found to exist in almost all species, and they are highly conserved throughout evolution from archaea to humans, implying selective pressure (Fig.8). Until now, Rhomboids are discovered to have diverse biological functions[27]. Rhomboids are intramembrane-cleaving proteases, whose unique property is that their active sites are buried in the lipid bilayer of cell membranes, which is unsatisfactory for the water-requiring hydrolysis reaction. Crucially, structural studies revealed the presence of a central cavity that allows water molecules to access and converge near the critical serine[28]. Rhomboids are serine proteases that cleave other transmembrane proteins within their transmembrane domains[27,29]. The Rhomboid-1 protease mentioned above is a typical example for this.

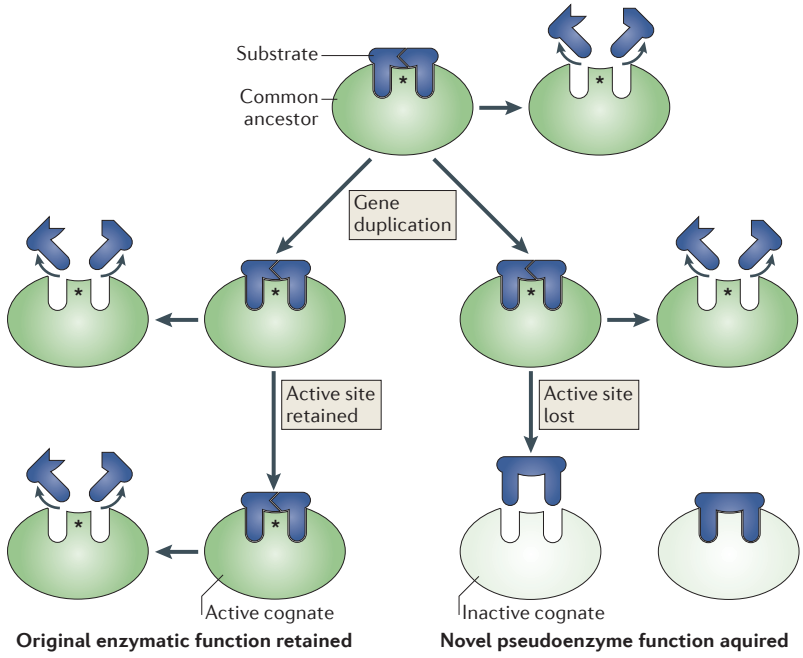

Figure 8 Evolutionary model for inactive enzyme evolving from a catalytically active ancestor
Through gene duplication, the enzyme guarantees its original function and gains an extra copy to have the potential evolving force. Once the enzyme acquired novel pseudoenzyme function that was favored by nature selection, it could be fixed in the population. (Adapted from Adrain and Freeman et al., 2012[30])

Intriguingly, bioinformatic analysis identified that some members of the rhomboid family lack the amino acid residues essential for proteolysis (Fig.11A green asterisk position)[31]. Derlins, TMEM115, UBAC2, iRhoms and RHBDDs belong to these "pseudoproteases". However, they are conserved in mammals (and some in yeast), implying a selective pressure to retain them during evolution (Fig.8). There are other dead enzymes that have atypical catalytic mechanisms. For example, WNK1 is a mammalian protein kinase that lacks the catalytic lysine, which in most cases functions to anchor and orient ATP[32]. As mentioned before, Derlin is heavily implicated in ERAD. Although the roles of the other rhomboid pseudoproteases are only now emerging, below I summarize known functions and highlight the emerging themes.

1.5.1 Tmem115

TMEM115 predominantly localizes to the Golgi apparatus. It is shown to interact with the conserved oligomeric Golgi complex (COG), which is implicated in the tethering of retrograde transport vesicles[33]. It is experimentally proved that knockdown or overexpression of TMEM115 would delay Brefeldin A induced Golgi-to-ER retrograde transport[33]. Thus it is likely to regulate Golgi-to-ER retrograde transport and perhaps other Golgi functions. TMEM115-deficient cells also showed a decline in the binding of lectins (peanut agglutinin and Helix pomatia agglutinin), which highly specific for glycoprotein binding, indicating defects in the Golgi glycosylation machinery[33].

1.5.2 iRhoms

iRhoms have diverse roles in different species. They are essential for ADAM17/TACE maturation and trafficking in mammals[34]. Meanwhile in *Drosophila*, they bind EGF ligands and direct them towards ERAD[35].

1.5.3 UBAC2

UBAC has a ubiquitin-binding motif and it is identified as a central element in the gp78 complex [36]. This is interesting because gp78 is an E3 ligase associated with ERAD. This predicts an ERAD-like role for UBAC2 similar to Derlins, although this remains to be fully investigated[37]. Interestingly, there appears to be a genetic association between UBAC and Behçet's disease, an inflammatory condition[38].

1.5.4 RHBDD1

RHBDD1, also known as RHBDL4, localizes in ER. RHBDD1 has been shown to cleave ERAD substrates with unstable membrane helices; it interacts with the ATPase p97. This role has been proposed to assist in conventional ERAD by cleaving membrane ERAD substrates, thus making their dislocation via the conventional ERAD pathway more efficient[39].

1.5.5 RHBDD3

RHBDD3 directly binds the modulator NEMO via the ubiquitin-binding-association (UBA) domain. Afterward, it is modified by an unknown E3 ligase to recruit the deubiquitinase, A20. Thus RHBDD3 facilitates the interaction of A20 with NEMO, which suppresses the transcription factor NF-kB in dendritic cells, whose overactivation can cause autoimmune and inflammatory diseases[40].

1.5.6 RHBDD2

The focus of this thesis is on RHBDD2, which as the name suggests is related to RHBDD3 and more distantly, to RHBDD1[41]. Little is known about RHBDD2, except that it is overexpressed in breast cancer[42] and colorectal cancer patients[43]. It is however not yet clear whether elevated RHBDD2 expression plays a role in the development, maintenance or progression of tumors. Or even if it is rather a consequence of tumor development.

Notably, a mutation[16] in RHBDD2 has been observed in patients suffering from Retinitis Pigmentosa (Fig.11C). The function of RHBDD2 is still unknown. However, Ahmedli reported that RHBDD2 locates to the cis-Golgi[16], which implies a role in trafficking or quality control in the early secretory pathway.

In summary, the rhomboid superfamily members interact with membrane proteins and control the fate of these binding partners. Their diverse functions are implicated in Golgi-to-ER retrograde transport, glycosylation, TACE trafficking, and ERAD. This is what we know so far about the biological role of rhomboids. However, the biological role of RHBDD2 remains obscure and many questions remain unanswered.

1.6 RHBDD2 is mutated in Retinitis Pigmentosa

As mentioned above, Ahmedli and colleagues reported a point mutation in human RHBDD2, the G to A transition changed arginine to histidine at codon 85 at the second exon (Fig.11C) leads to Retinitis Pigmentosa (RP), a disease that causes photoreceptor death[16]. This mutation is homozygous in Retinitis Pigmentosa patients, but not all patients have this mutation, meaning RP can be caused by mutations in several other genes. Consistent with a role in the retina, Ahmedli and colleagues reported the RHBDD2 expression pattern in adult mouse

retina to support their view (Fig.9).

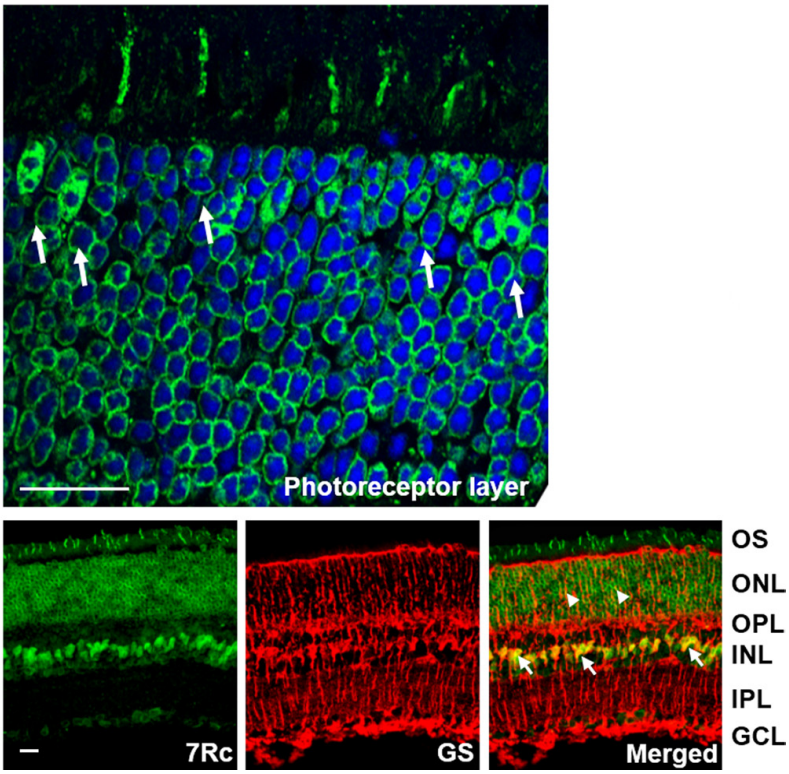

Figure 9 RHBDD2 expression pattern in adult mouse retina
Upper panel shows the vertical section of ONL, labeled with 7RC (anti-RHBDD2 antibody). The arrows point to the irregularly shaped heterochromatin, one of hallmarks of mature cone photoreceptors. Lower panel shows the horizontal section of mouse retina. Images show the RHBDD2 localization (green), glutamine synthetase (GS, a marker for Müller glial cells) localization (red), and their co-localization in the somas of many Müller glial cells (arrows) and some of their processes (arrowheads). OS, outer segments; ONL, the outer nuclear layer; OPL, outer plexiform layer; INL, inner nuclear layer; IPL, inner plexiform layer; GCL, the ganglion cell layer. (Adapted from Ahmedli et al., 2013[16])

Retinitis pigmentosa is a common name given to a group of genetically and clinically heterogeneous inherited retinal dystrophies presented with a loss of photoreceptors and retinal pigment deposits. Retinitis pigmentosa first affects rod photoreceptors (retinal cells that detect dim light) and cone photoreceptors (retinal cells that detect light and color) in the retina. Patients usually begin with night blindness then experience progressive vision loss because of the gradual breakdown of rods and cones[44].

More than 45 genes were identified to be associated with retinitis pigmentosa. Among those genes, rhodopsin is the capital one in which more than 140 mutations have been identified[45]. Mutations can have a variety of effects on gene

function, which can be difficult to predict *a priori*. For example, mutations can partially reduce normal gene function (in the case of a hypomorph) or completely (in the case of a null). In addition some mutations can result in increased WT gene function (for example, rendering a molecule constitutively active), whereas neomorphic mutations can create a new function not encoded by the WT gene. This is examplified by rhodopsin, a transmembrane glycoprotein with 7 TMDs, the T17, P23, G51, T58, V87, G89, G106, C110, L125, A164, C167, P171, Y178, E181, G182, C187, G188, D190, H211, C222, P267, S270, K296 mutants are all misfolding and retained in the ER[46].

Why does R85H mutation cause Retinitis Pigmentosa? What is the normal physiological role? Does RHBDD2 play an ER quality control role? Does it control trafficking in the early secretory pathway? Since it is not a protease, what kind of molecules does it bind to to exert its function? Does this reveal any common themes about the role of the mammalian rhomboids in the secretory pathway? This master thesis is dedicated to answer these questions.

2. Material and Methods

2.1 Mice

C57BL/6J mice were obtained from Instituto Gulbenkian de Ciência (IGC) and maintained at the IGC animal facility.

2.2 Cell culture

The HeLa-GalT-GFP stable cell line was a gift from Dr. Jack Rohrer (Friedrich Miescher Institut, Basel, Switzerland). Mouse RPE cell line was a gift from Professor Heping Xu (Centre for Experimental Medicine, Queen's University Belfast).

HEK cells, Hela cells were cultured in Dulbecco's modified Eagle's medium (DMEM; Biowest) supplemented with 10% fetal bovine serum (FBS) and 1% penicillin/streptomycin at 37°C and 5% CO2. RPE cells were cultured in the same conditions with additional 116.6 mg/ml sodium bicarbonate.

2.3 Sequence data

Rhomboid sequences were retrieved from Uniprot[61]. These sequences of the full-length proteins were automatically aligned by online multiple sequence

alignment tools, including ClustalO[58], Muscle[59] and Tcoffee[60]. The alignments were then manually corrected to remove gaps. The Rhomboid topology models were constructed by TMD predictions from Uniprot database[61].

2.4 Generation of RPE cell lines expressing empty vector (EV), WT RHBDD2 and RHBDD2 R85H mutant.

R85H point mutagenesis was executed by KOD Hotstart DNA polymerase from Novagen (using primers: GAAGTTGCCAGCAAAGTGCCAGATGATGATGGC and GCCATCATCATCTGGCACTTTGCTGGCAACTTC) based on the WT RHBDD2 construct with a triple HA tag on C termini. Both constructs were cloned into the lentiviral expression vector pLEX MCS. After verification of the nucleotide sequences, these constructs, plus the empty vector, were used to produce lentivirus in HEK cells. The resultant virus was then used to infect RPE cells, which were selected for puromycin resistance.

2.5 Cell lysis

Cells were washed twice in PBS, pH 7.2 (137mM NaCl, 2.7mM KCl, 10mM Na_2HPO_4, 1.8mM KH_2PO_4) lysed on ice for 10min in lysis buffer (1% Triton X-100, 150 mM NaCl, 50 mM Tris-HCl, pH 7.4). Following centrifugation to remove insoluble material, and other manipulations (such as immunoprecipitations), samples were denatured in LDS buffer (LDS from Novex®#NP0007, 141mM Tris base, 106mM Tris HCl, 2% LDS, 10% Glycerol, 0.51mM EDTA, 0.22mM SERVA Blue G, 0.175mM Phenol Red, pH 8.5, 50mM DTT).

2.6 Western blot

Samples were loaded in SDS-Page gels, which were prepared according to "GEL CASTING INSTRUCTIONS" from Novex® by life technologies (Pub.no. MAN0001660). Proteins were subsequently transferred to PVDF membranes. The membranes were blocked for 45 min in 5% non fat dried milk in TBST (100mM Tris pH 7.4, 3.0M NaCl, 1% Tween). Incubation with primary antibodies were done in 5% milk at 4℃ overnight. Membranes were then washed 5x for 6 minutes each in TBST and incubated with secondary antibodies labeled with HRP for 1 hour if necessary. Enhanced chemiluninescence (ECL) was used to reveal signals, which were captured on photographic film.

Used antibodies:

anti-HA-HRP antibody (Roche, 12013819001)

7RC (a gift from Ahmedli et al., 2013[16])

anti-β-actin (Abcam, Ab8227)

anti-CHOP (GADD153, santa cruz, sc-7351)

2.7 Induction of ER stress

RPE cells were incubated in 1μg/ml thapsigargin (Tg) (Santa Cruz, #sc-24017), 0.33μg/ml tunicamycin (Tm) (Santa Cruz, #sc-3506) or 1μg/ml Brefeldin A (BFA) (Santa Cruz, # sc-200861) for 8h to induce ER stress.

2.8 Golgi fragmentation and Golgi reassembly

Hela cells were treated with 0.25μg/ml BFA and fixed with 4% Formaldehyde (made from Bio-Connect BV, #PIER28908) at different time points. After an one

hour incubation with BFA, cells were rinsed twice in complete medium (DMEM, supplemented with 10% FBS and 1% penicillin/streptomycin) to washout the BFA and fixed with 4% Formaldehyde at different time points.

2.9 Image acquisition and analysis

Fluorescent images were obtained on Leica DMRA2 microscopy. In order to be semi-quantified by the colocalization program Imaris, images were deconvoluted by Huygens Workstation. The image shown in Figure 3 is one representative stack out of the 20 Z stacks. The brightness and contrast is adjusted by Fiji to visualize the signals. Note the statistical analysis was done on the original signal.

2.10 CRISPR/Cas9

CRISPR (Clustered Regularly Interspaced Short Palindromic Repeats)/Cas9 system is a genome engineering machinery endogenous to bacteria. The discovery of CRISPR originates with the identification of repetitive palindromic elements in bacteria, juxtaposed beside so called 'spacer' sequences which were found to often match sequences of bacteriophages, viruses that infect bacteria. It was subsequently discovered that bacteria incorporate phage DNA into their own genomic CRISPR loci (the spacers); in turn these are a template for transcription of RNA, which can destroy the foreign DNA from phage[47]. In bacterial immune defense, these spacers and palindromic DNA are transcribed, then processed to produce short spacer-derived RNAs, called tracrRNA, which subsequently works with Cas9 (an RNA-guided endonuclease specialized for cutting DNA) to produce the crRNA[48], the element that confers the sequence specificity. Later, Jinek and colleagues combined the tracrRNA and spacer RNA into a "guide RNA", achieving the goal to enables a nuclease (Cas9) to be programmable by only editing of this sequence specific guide RNA[49]. Jinek and

colleagues also found that Cas9 can only bind to the DNA target if it is followed by the PAM sequence (5'-NGG-3') and the cleavage site is at three base pairs upstream of the PAM sequence[49].

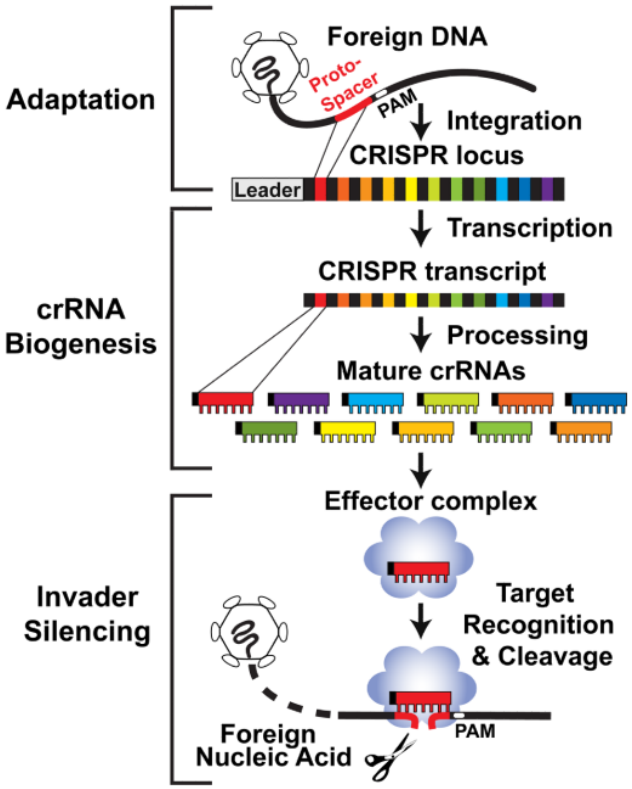

Figure 10 Overview of the CRISPR/Cas9 invader defense pathway
In the adaptation phase, short fragments of foreign DNA (protospacer, adjacent to PAMs) are acquired. In the crRNA biogenesis phase, CRISPR locus transcripts are processed to release individual mature crRNAs. In the invader silencing phase, crRNA-Cas protein effector complexes recognize foreign DNA and cleave it. (Adapted from Terns and Terns et al., 2011[65])

Taking advantage of the versatility of CRISPR/Cas9 system, a strategy was devised to generate mice null for RHBDD2. A gRNA sequence (CGACACCAGCAGCGAGAGCA) was designed using a CRISPR prediction resource[63] and one of these was chosen for cloning into the gRNA basic plasmid (a gift from Dr. Moises Mallo, IGC) (Supplementary Fig.S1). The 200 bp homology template was synthesized by IDT DNA Ultramer Oligos (Fig.17A).

The microinjection was done by Ana Nóvoa in IGC transgenics facility. 52 occytes were injected, and 34 of them were survived and transferred into pseudopregnant females at the 1-cell stage.

2.11 Genotyping of CRISPR mice

Screening primers (Fig.17B primer 1 - AAATTGAGGAGGGAGGCGGGGAGT, primer 2 - ATCCCCGCCCCGCCTCTTCTCACCT, primer 3 - ACCGCCCTGTAATGATAGGGTACCCT, primer 4 – AGGGTACCCTATCATTACAGGGCGGT) were used to genotype the putative founder animals. PCR products were loaded on 4% agarose gel. A part of PCR products were heated to 95℃ and slowly cool down to room temperature, then loaded on 8% acrylamide gel.

Emma Burbridge was using another outer primer 2 (TGAGGAAGCGCGCCATCCCCGCC) for the screening procedure.

2.12 Immunoprecipitation (IP)

HEK cells transduced with pLEX empty vector or pLEX plasmid containing iRhom1, iRhom2, iRhom1 N termini, RHBDD2, RHBDD3, UBAC2, unc93b1 by lentiviral transduction were used in IP experiments. Live cells were exposed to the crosslinker DSP(Thermo #22585) in the first and second experiments but not the third one. After making lysates, irrelevant control antibodies conjugated to magnetic beads (Thermo #21354) were added to the lysates to pre-clear non-specific binding proteins from the extract during a one hour rotation at 4℃. At this point, the precipitated beads were discarded, the supernatant recovered and 50 ul supernatant was saved as the 'Input' sample. Then the lysates were incubated with anti-HA resin (Thermo #88837) for 1.5 hour rotation at 4℃. Subsequently, the precipitated beads were kept and washed four times in different wash conditions (for experiments with crosslinker, using IP wash buffer; for experiment without crosslinker, using RIPA buffer) to remove contaminants that bound non-specifically. Three-quarters of the precipitated beads were put in UREA buffer (8M Urea, 4% CHAPS, 100mM DTT, 0.05%SDS)

and sent to Professor Christopher Gerner (University of Vienna) for mass spectrometry analysis. One-quarter of the beads and the Input sample were put in LDS buffer (Novex®#NP0007, 50mM DTT), then heated to 65℃ for 15 mins. This part of sample was used in the Western blots.

Used buffer:

IP Lysis buffer: 1% Triton X-100, 150 mM NaCl, 50 mM Tris-HCl, pH 7.4, 1,10-phenanthroline, protease inhibitor from Roche

SDS/buffer: 5% Sodium Deoxycholate and 2% SDS

IP wash buffer: 1% Triton X-100, 300mM NaCl, 50mM Tris-HCl, pH 7.4, 1,10-phenanthroline, protease inhibitor from Roche

RIPA buffer: 1% Triton X-100, 0.1% SDS, 0.25% deoxycholate, 150mM NaCl, 50mM Tris-HCl, pH 7.4, 1,10-phenanthroline, protease inhibitor from Roche

2.13 siRNA knockdown (KD)

An siRNA pool of 4 different siRNAs (ON-TARGETplus) was ordered from GE Healthcare to knock down human RHBDD2 (targeting sequences: GGATATCCGTGTTCAAGTA, CCCCATGCCCTGAGAGAAT, ACGGCAGCCCTGTGGAGTA and ATGCAGAAAGCGAGACGTT). A mock siRNA was ordered as well to KD Unc93b1. 5nmol siRNA was solubilized into 250ul in RNAse-free water. Hela cells were plated one day before transfection on 6-well-plates, as described below.

Transfection for 6-well-plate (per well scale): 7.5ul siRNA was mixed with 125ul Opti-MEM (Life Technologies, #25200-072). 15ul Oligofectamine (Life Technologies, #LTI 12252-011) was incubated with 60ul Opti-MEM for 5min at room temperature. There two above were combined and incubated for 20min at room temperature. Add the solution to each well.

A double knockdown was performed in all experiments; hence a second transfection was executed 19 hours following the first transfection. Experiments were performed post 72 hours after the first transfection.

2.14 Reverse transcription PCR

Reverse transcription PCR was performed by Transcriptor One-Step RT-PCR Kit (Roche, #04655877001), using primers in Figure 20 (red primers for isoform 1 and 2: AAGGAGCAGAGGACCGGCAG and AGCTTCGGGGTGGATTGAGTG; blue primers for all three isoforms: CTTCAGCCGAGAGGAGGGCAGCCCAGAG and GTTCACAGGCGTGGGGGGCTGGATGCC) PCR products were collected after 30x and 35x themocycles and loaded on 2% agarose gel.

3. Results

3.1 Prediction of the transmembrane topology of RHBDD2

RHBDD2 is a 39 kDa protein which is highly conserved amongst vertebrate species. However, to date the topology of RHBDD2 is unclear. Based on different transmembrane domain prediction algorithms[16] RHBDD2 has been proposed to contain five or seven possible transmembrane domains(TMDs)[16]. As an understanding of the RHBDD2 transmembrane topology is an important prerequisite to understand function, we revisited this issue. Based on a careful comparison with residues conserved in other members in Rhomboid superfamily, we predicted that RHBDD2 has six TMDs, with cytoplasmic N and C termini (Fig.11C).

Bioinformatic analysis focused on the transmembrane helices of several mouse Rhomboid-like proteins suggests that all rhomboid-like proteins contain a core of 6 TMDs, with less conservation in the first TMD (Fig.11A). Where present as a C-terminal addition in some Rhomboid-like proteins, the seventh TMD is also poorly conserved (Fig.11B). In addition, the alignment performed using the Tcoffee multiple sequence alignment tool[60] revealed several highly conserved motifs and hallmark amino acids that were used as a basis to identify the equivalent TMDs in RHBDD2 (Fig.11A) Greenblatt reported a conserved “WR motif” and “GXXXG motif” in Derlins[50]; Lemberg observed the same in active Rhomboids[51]. The “WR motif” is contained in the luminal loop between helices 1 and 2; the “GXXXG motif” appears in TMD6 (Fig.11A blue asterisk). These features were used as a guide to locate the equivalent transmembrane helices, when the RHBDD2 sequence was aligned against a panel of other rhomboid

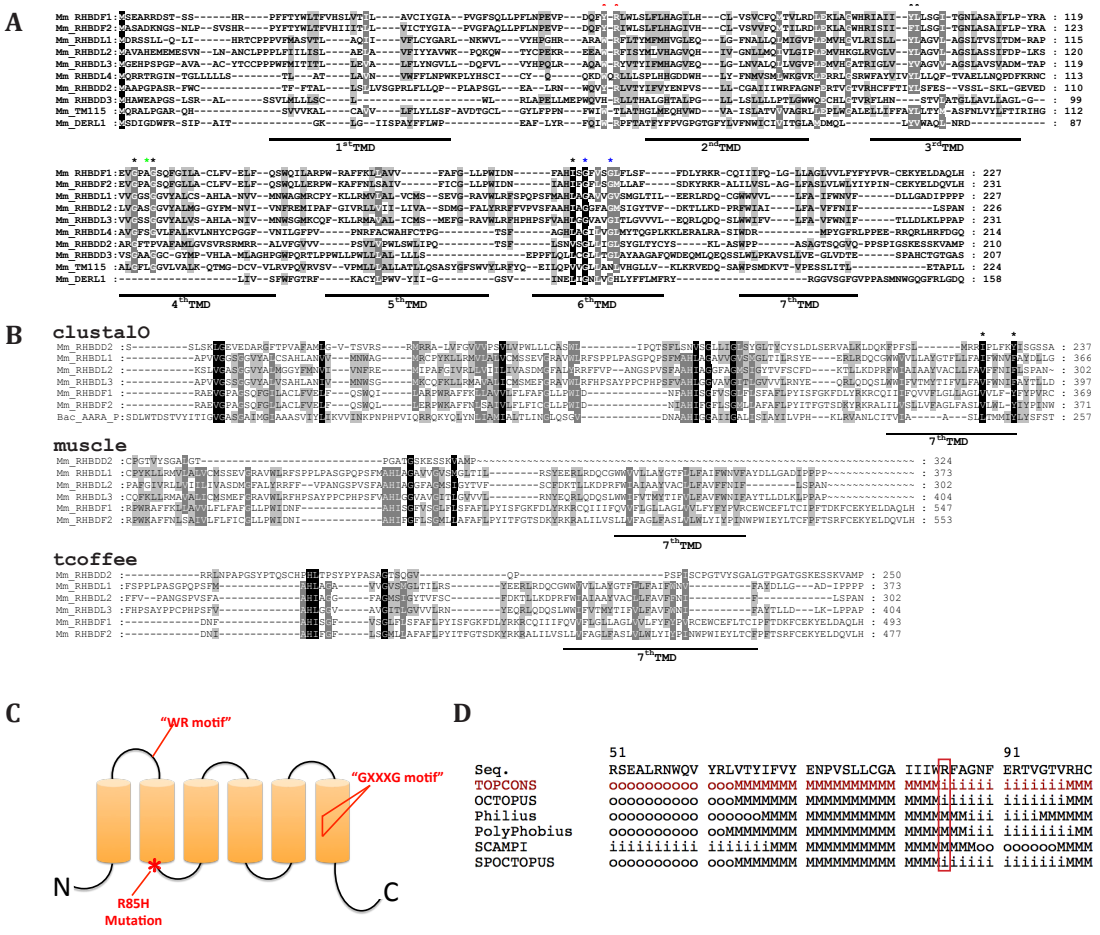

Figure 11 Topology of RHBDD2 and other rhomboid superfamily members

(A) Tcoffee alignment of the transmembrane domains of rhomboid superfamily members in mice (RHBDF1,Q6PIX5; RHBDF2,Q80WQ6; RHBDL1,Q8VC82; RHBDL2,A2AGA4; RHBDL3,P58873; RHBDL4,Q8BHC7; RHBDD2,Q8VEK2; RHBDD3,Q8BP97; TM115,Q9WUH1; DERL1,Q99J56). TMDs are labeled according to the RHBDL2 topology on UniProtKB[61]. Hallmark amino acids are indicated by black asterisk. A green asterisk indicates the catalytic serine site of Rhomboids. Red asterisks denote the "WR motif", including the highly conserved arginine residue, that is found in the luminal region between TMDs 1 & 2. The "GXXXG motif" found in TMD6 is denoted by blue asterisks. The alignment was corrected manually to remove gaps in predicted TMDs and loops. (B) Alignment of RHBDD2 and rhomboid superfamily members that have 7 TMDs was performed by three different programs (clustalO, muscle and tcoffee). The 7th TMD is highlighted according to RHBDL2 topology on UniprotKB. (C) Schematic of the RHBDD2 with 6 TMDs showing "WR motif" and "GXXXG motif" in the first loop and within the sixth TMD respectively. The red asterisk marked the position of the point mutation, R85H. (D) Prediction data from TOPCONS of arginine (red frame) of the R85H mutation.

proteins. Among the aligned proteins including inactive Rhomboids, the arginine residue in the "WR motif" was conserved in all members except TMEM115 and was identified for RHBDD2 (Fig.11 red asterisk). Notably, the tryptophan in the "WR motif" is substituted by tyrosine, an amino acid that has very close

properties to tryptophan, in iRhoms and RHBDD2 (Fig.11). The "GXXXG motif" in the putative sixth TMD is also conserved in all listed members except TMEM115, but including RHBDD2 (Fig.11). Similar results were obtained by the clustal Omega multiple sequence alignment tool (data not shown).

I then searched for the presence of additional conserved features, specifically a tyrosine adjacent to a leucine, conserved in the third TMD; two glycines in the fourth TMD; and a defined leucine or isoleucine or valine at two position before the "GXXXG motif" in the sixth TMD[50] (Fig.11). Taken together, this analysis enabled me to locate 1st TMD and 2nd TMD with the arginine in "WR motif" in between; the 3rd TMD by the conserved tyrosine and leucine; the 4th TMD by conserved glycines (indicated with black asterisks) and the 6th TMD by the "GXXXG motif" (Fig.11, black asterisks). This revealed that RHBDD2 contains the hallmark amino acids within the anticipated TMDs and indicates that the protein has a topology similar to Rhomboids containing 6 or 7 TMDs.

Having confidently assigned TMDs 1 to 6, to investigate the presence or absence of the seventh TMD, we aligned the RHBDD2 with the rhomboids known to have 7 TMDs[52] using three different programs (clustalO, muscle and tcoffee)(Fig.11B). ClustalO shows two consensus amino acids (i.e, conserved in the 7th TMD of other rhomboids) in the putative seventh TMD region, however, crucially, the alignment required a 7 amino acid gap in the equivalent region for RHBDD2, making the presence of a 7th TMD implausible. Meanwhile, muscle and tcoffee suggest that RHBDD2 cannot be aligned with the 7th TMD of other Rhomboids within this specific region. Hence, taken together, three difference alignment algorithms failed to identify conserved features of a 7th TMD. To rule out the possibility that a non-conserved 7th TMD was present, the RHBDD2 sequence was submitted to TOPCONS[62], which also failed to identify a 7th TMD. Hence, no TMD predictors nor aligment tools identify a 7th TMD, making it unlikely that RHBDD2 has a 7th TMD. In summary, I predict that RHBDD2 is a transmembrane protein that has 6 TMDs, with both N- and C-termini embedded in the cytoplasm. This prediction will be tested in future experiments.

I next examined whether the 6 TMD core predicted above applied to all RHBDD2 vertebrate orthologs. Among all vertebrates listed in Figure 12, RHBDD2 is conserved. The R85 residue contained in the 2nd TMD, that was found

to be mutated in RP patients[16], is also conserved in all species investigated (Fig.12 red asterisk). TOPCONS[62] gave the prediction that arginine of the R85H mutation (Fig.11D red frame) is on the boundry of the 2nd TMD, however whether it is marginally inside or outside of the TMD is unclear.

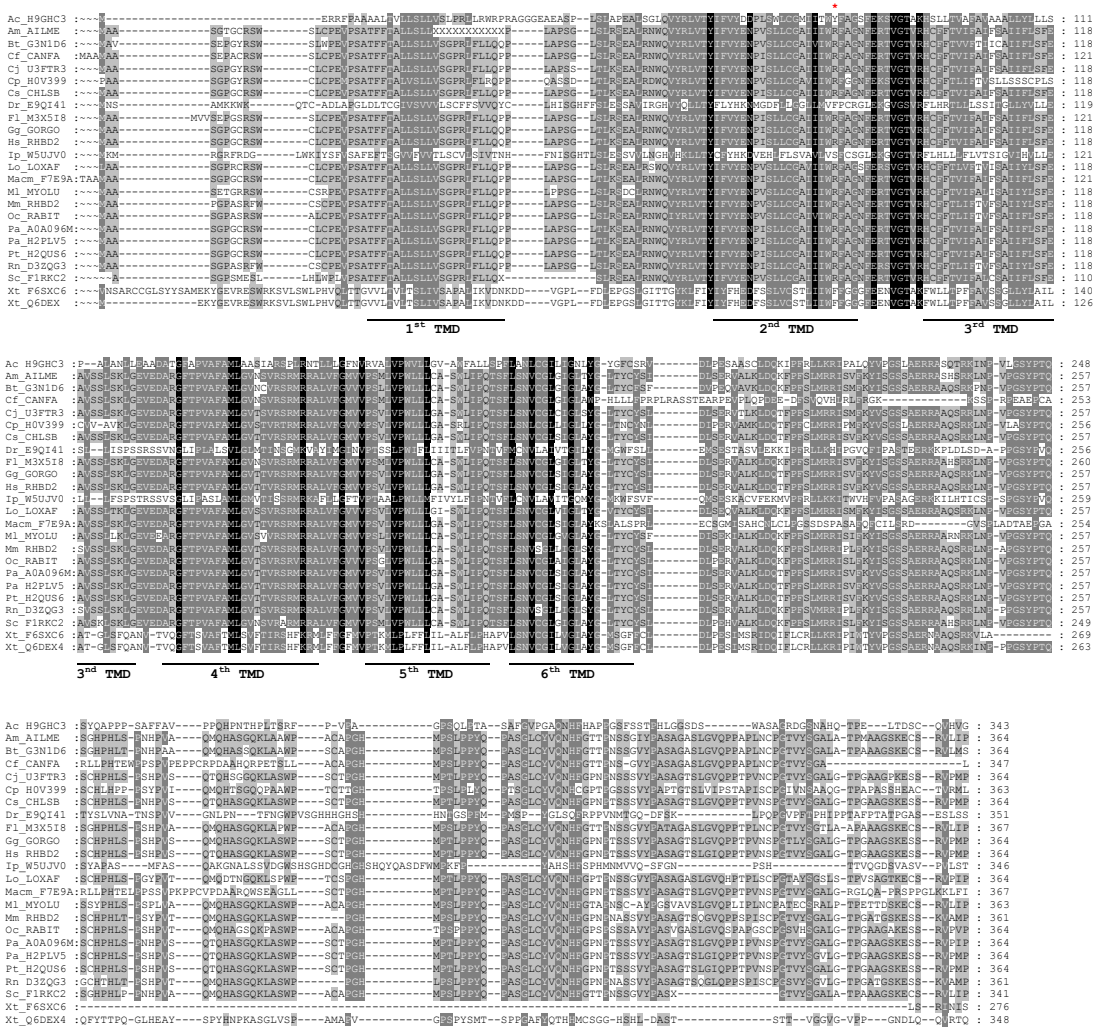

Figure 12 Alignment of RHBDD2 in vertebrates

The red asterisk donates the R85H{Ahmedli et al., 2013, #82299} point mutation position. Tcoffee alignment of RHBDD2 from *Anolis carolinensis*(Ac_H9GHC3), *Ailuropoda melanoleuca*(Am_AILME,G1LWT8), *Bos taurus*(Bt_G3N1D6), *Canis familiaris*(Cf_CANFA,F1PB04), *Callithrix jacchus*(Cj_U3FTR3), *Cavia porcellus*(Cp_H0V399), *Chlorocebus sabaeus*(Cs_CHLSB,A0A0D9RZY0), *Danio rerio*(Dr_E9QI41), *Felis catus*(Fl_M3X5I8), *Gorilla gorilla gorilla*(Gg_GORGO,G3RL85), *Homo sapiens*(Hs_RHBD2,Q6NTF9), *Ictalurus punctatus*(Ip_W5UJV0), *Loxodonta africana*(Lo_LOXAF,G3SLX9), *Macaca mulatta*(Macm_F7E9A,F7E9A1), *Myotis lucifugus*(Ml_MYOLU,G1PU74), *Mus musculus*(Mm_RHBD2,Q8VEK2), *Oryctolagus cuniculus*(Oc_RABIT,G1T655), *Papio anubis*(Pa_A0A096M,A0A096MVK2), *Pongo abelii*(Pa_H2PLV5), *Pan troglodytes*(Pt_H2QUS6), *Rattus norvegicus*(Rn_D3ZQG3), *Sus scrofa*(Sc_F1RKC2), *Xenopus tropicalis*(Xt_F6SXC6), *Xenopus tropicalis*(Xt_Q6DEX,Q6DEX4). The TMDs are highlighted according to Fig.11.

3.2 Disease Mutation R85H in RHBDD2

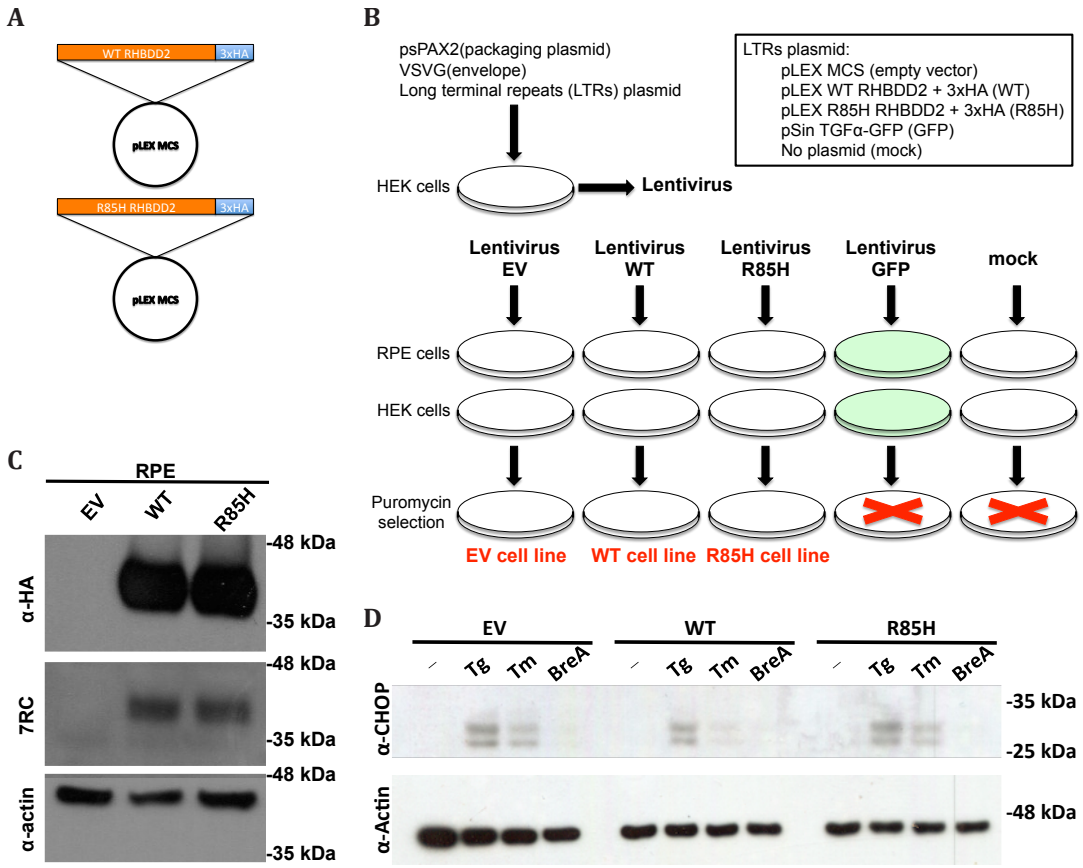

Figure 13 Generation of RHBDD2-expressing cell lines and determining the effect of RHBDD2 overexpression on induction of ER stress

(A) WT RHBDD2 and R85H mutant RHBDD2 with a triple HA tag on their C termini were inserted into pLEX MCS plasmid. The point mutagenesis was performed using KOD Hotstart Polymerase. (B) Cell lines were generated by lentiviral transduction. Viruses were made in HEK cells with packaging plasmid psPAX2, envelope plasmid VSVG and 4 different types of long terminal repeat (LTR) plasmids: pLEX MCS plasmid (empty vector), pLEX MCS plasmid inserted with WT RHBDD2 plus triple HA tag (WT), pLEX MCS plasmid inserted with R85H RHBDD2 mutation plus triple HA tag (R85H) and pSin plasmid inserted with GFP linked TGFα. One set of mock experiment without the LTR plasmid was fulfilled as well. Five sets of lentivirus were transfected into mouse RPE cells and HEK cells. The efficiency of transfection was first visualized by GFP. Then to select for the pLEX MCS-based plasmids, the positive cells were selected by adding Puromycin to the growth medium. In the end, three cell lines were generated, harbouring pLEX MCS, WT RHBDD2 and R85H mutation in RPE cells. (C) Western blots of cell line lysates mentioned in (B). (D) Western blots of three RPE cell line lysates after 8h drug treatment (thapsigargin(Tg), tunicamycin(Tm) and Brefeldin-A(BreA)) to induce ER stress. The blots were probed with antibodies specific to CHOP, transcriptional targets of the UPR. The blots were probed with actin antibody as a loading control.

As described in the Introduction, Almedli and colleagues identified a mutation within RHBDD2, R85H, that is associated with retinitis pigmentosa[16]. I reasoned that understanding the phenotype elicited by mutant RHBDD2 may help to elucidate the basis of its contribution to disease, as well as potentially help reveal the normal function of WT RHBDD2.

To examine how the R85H mutation affects RHBDD2 function, I generated overexpression constructs for WT and Mutant RHBDD2 incorporating a triple HA tag at the C terminus. These were cloned into a lentiviral expression vector pLEX MCS (Fig.13A and Fig.13B). These constructs, plus the empty vector (EV), were used to produce lentivirus in HEK cells; the resultant virus was then used to infect both mouse RPE (retinal pigment epithelium) cells, which were selected for puromycin resistance. RPE cells were selected because Almedli and colleagues showed that RHBDD2 is highly expressed in retina[16]. This is consistent with mRNA expression data from bioGPS[64], a public gene expression database (Fig.14). Using these cell lines, I could determine whether the R85H mutant is mislocalized, degraded within the ER, and if this results in triggering the UPR. The implication of this hypothesis would be that the pathology in patients harboring the R85H mutation is caused by photoreceptor loss triggered by unscheduled ER Stress.

Comparing the lysates from RPE cells expressing vector, RHBDD2 WT and RHBD2 mutant, probed with α-HA antibody and an α-RHBDD2 antibody 7RC[16], the expression of WT RHBDD2 and R85H were equivalent in RPE cells (Fig.13C).

As one possibility is that the R85H mutation may render RHBDD2 misfolded, thereby triggering the UPR(unfolded protein response). To assess the sensitivity to the UPR, I used three different drugs to induce ER stress in the RPE cell lines (Fig.13D). Thapsigargin (Tg) triggers ER stress by interfering with calcium homeostasis (it blocks the SERCA calcium pump) in the ER thereby inducing the UPR; tunicamycin (Tm) inhibits N-glycosylation thereby induces the UPR; Brefeldin A (BFA) blocks ER-to-Golgi transport hence induces ER stress and Golgi fragmentation. The RPE cell lysates were made from cells treated with Tg, Tm or BFA for 8h. The blots were probed for transcriptional target of the UPR (CHOP) and the protein level were normalized by actin. As shown in Fig.13D, there is no evidence of constitutive induction of the UPR in cells expressing the

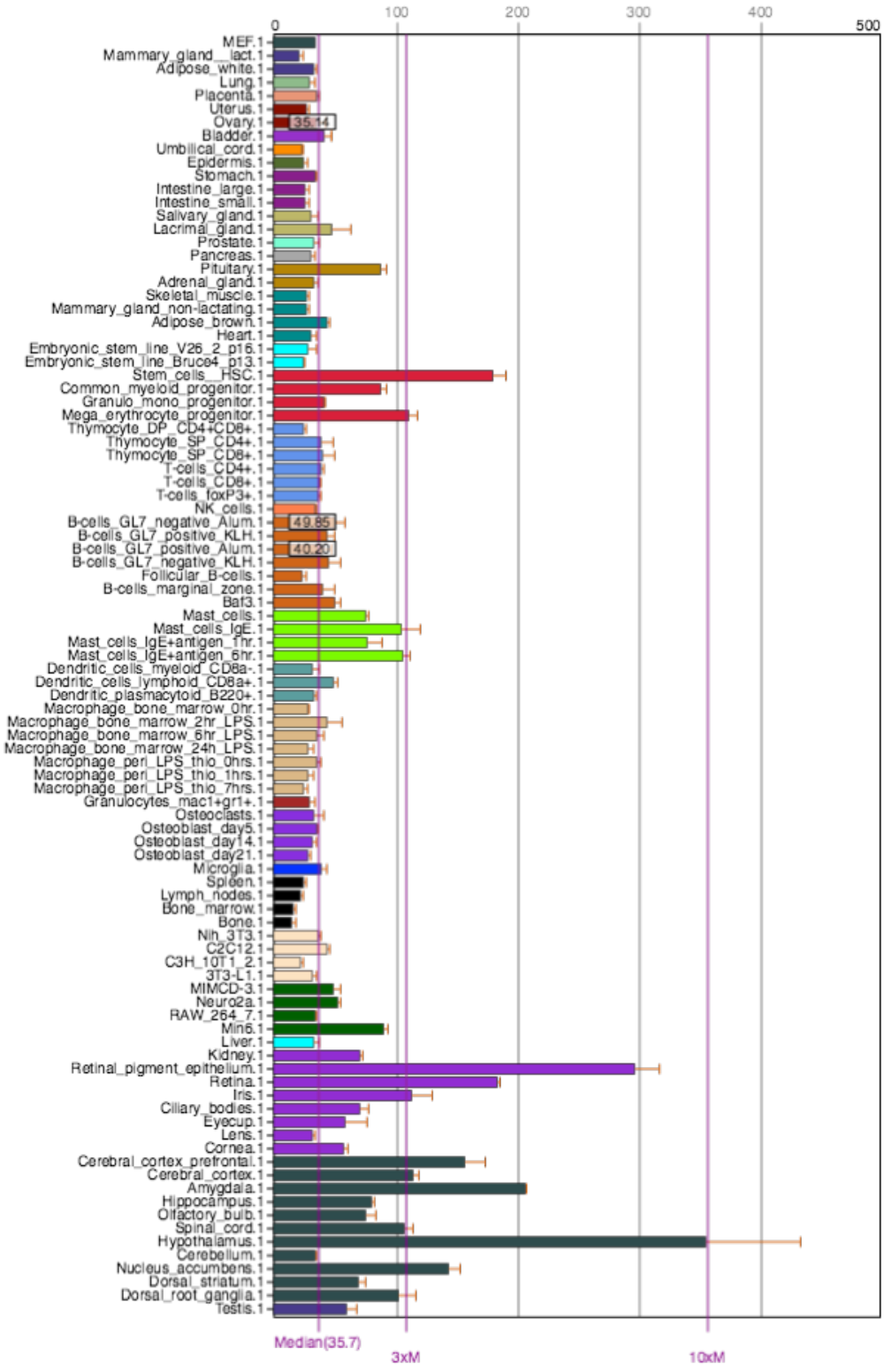

Figure 14 RHBDD2 expression level in different mouse tissues

The data was obtained from bioGPS[64] in mouse tissues.

R85H (without drug treatment) compared to vector or WT RHBDD2-expressing cells. CHOP expression levels among these cell lines shows minimal differences

in three drug treatments. A slight difference of CHOP induction was observed in Tm treatment.

All above, there is no degradation of R85H mutated protein or constitutive induction of the UPR in the mutant cell line could cause the disease. The slight difference of CHOP induction needs to be further confirmed by examining other UPR transcriptional target (Park, ATF6, ATF4, etc.). However, as there was no evidence that constitutive expression of the R85H mutant triggered ER stress, this argues against substantial misfolding of the mutant.

3.3 Localization of WT and R85H RHBDD2

I next examined the localization of WT vs mutant RHBDD2 by immunofluorescence. Notably, both WT and mutant protein was detected expressing in virtually 100% of the stably expressing cells (data not shown). EV, WT and R85H RPE cells were fixed and labelled with anti-HA antibodies (to detect RHBDD2 WT or R85H), the ER marker Calreticulin or the cis-Golgi marker GM130. Compared to the Hela cells used below, RPE cells are very flat and extended cells, thus the organelle structures are easier to identify. Twenty stacks were captured in each field, which is enough to cover the depth of the whole cell. Eight decentralized fields on each coverslip were captured to assess the localization of RHBDD2 WT or R85H. Cells were deconvoluted and semi-quantified by colocalization. Images were adjusted by Fiji to visualize the signals. Note that all the statistical analysis was done on the original data.

Imunofluorescence analysis of the localization of WT RHBDD2 and R85H suggested a Golgi-like localization (Fig.15A). In the merge channel, the green signal of GM130 overlapped substantially with the red signal of WT RHBDD2 or R85H; by contrast, there appeared almost no colocalization with calreticulin. To quantitate this observation, I next used Pearson's coefficient (r) to assess the colocalization level (Fig.15B). Compared with the EV cell line and the calreticulin marked cells, it is obvious that WT and R85H RHBDD2 colocalized with GM130 with a high Pearson's coefficient (Fig.15B). These data confirmed that RHBDD2

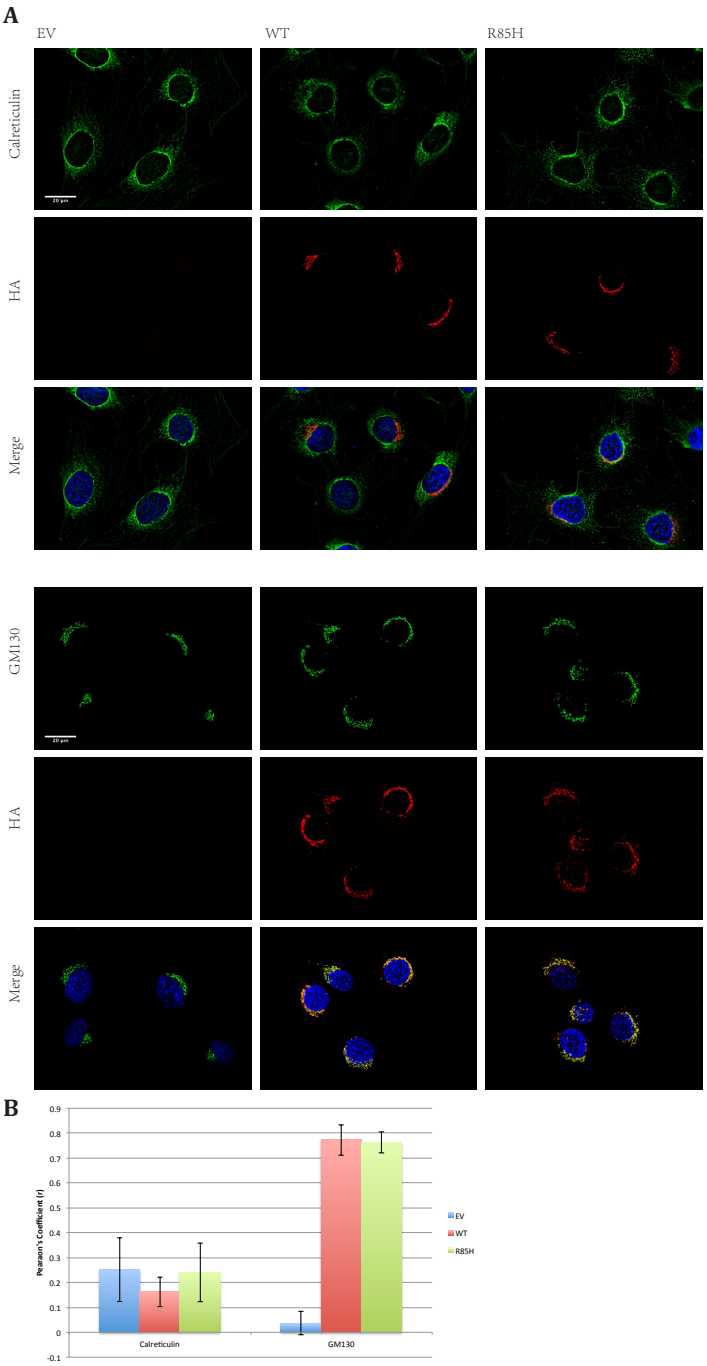

Figure 15 RHBDD2 localization
(A) Immunofluorescent detection of HA-tagged (RHBDD2 WT or R85H - red) and calreticulin (green) (top panel) or HA and GM130 (green) (bottom panel) in EV, WT and R85H RPE cell lines. Images were taken by Leica DMRA2 microscopy and deconvoluted by Huygens Workstation. (B) Histogram of colocalization semi-quantified by Pearson's coefficient (r). Ten cells were valued individually by Fiji JACop plugin in each detection. The histogram shows the average of Pearson's coefficient (r) and the error bar gives standard deviation.

WT and R85H are colocalized much more substantially with GM130 and hence localize to the Golgi apparatus. Because I was unable to obtain reliable medial and trans-Golgi marker antibodies, I was unable to ascertain whether RHBDD2 is preferentially enriched in a specific sub-compartment of the Golgi apparatus, for example, the cis-Golgi, as reported. Nonetheless, these data suggest that WT and mutant RHBDD2 both localize to the Golgi. Moreover, it implies that the disease phenotype caused by R85H is not the result of retention/degradation of the

mutant in the ER. It also suggests that RHBDD2 R85H mutant does not cause ER stress, implying that ER stress is unlikely to be the cause of photoreceptor loss in the RP patients.

3.4 Generation of Knockout Mice

One approach to define the function of RHBDD2 is to generate knockout (KO) mice harbouring a null mutation for RHBDD2 and assess the phenotype of the resulting mutant animals. Although much of this lies outside of the timescale of this thesis, contemporary gene editing techniques based on CRISPR/Cas9 make the initial design and gene targeting approaches feasible. Considering the expression levels of RHBDD2 in different tissues in mice (Fig.14), as RHBDD2 is highly expressed in the retina and brain, phenotypic defects may be anticipated in those tissues in KO mice.

A knockout strategy was designed based on CRISPR to generate mice harboring a null mutation for RHBDD2. As shown in Figure 16A, the mouse RHBDD2 gene has 4 coding exons. To prematurely terminate synthesis of RHBDD2 protein as early in the coding sequence as possible, we designed a homology directed repair based strategy to insert three stop codons, plus a restriction site (KpnI, to aid in genotyping the founder animals), into the first exon. The introduction of premature stop codons more than 50 bp upstream of the last exon-exon boundary is predicted to trigger degradation of the mRNA via non sense mediated decay[53]. However, as an additional failsafe, to avoid the possibility that a stable mutant mRNA may result, a 26 amino acid region was left intact before insertion of the premature stop codons. During translation of a resultant stable mutant mRNA, the presence of this small encoded polypeptide should prevent the ribosome reinitiating at a subsequent downstream initiator methionine[54]. Hence the prediction is that even if the mutant mRNA is stable, a small polypeptide (Figs.16B, 16C) comprising only the cytoplasmic N-terminus of RHBDD2 and a small fragment of the first TMD will be produced. Hence, this fragment completely lacks the core rhomboid domain, is highly unlikely to enter

the sec61 translocon (hence translocate into the membrane), and is therefore highly unlikely to retain significant function.

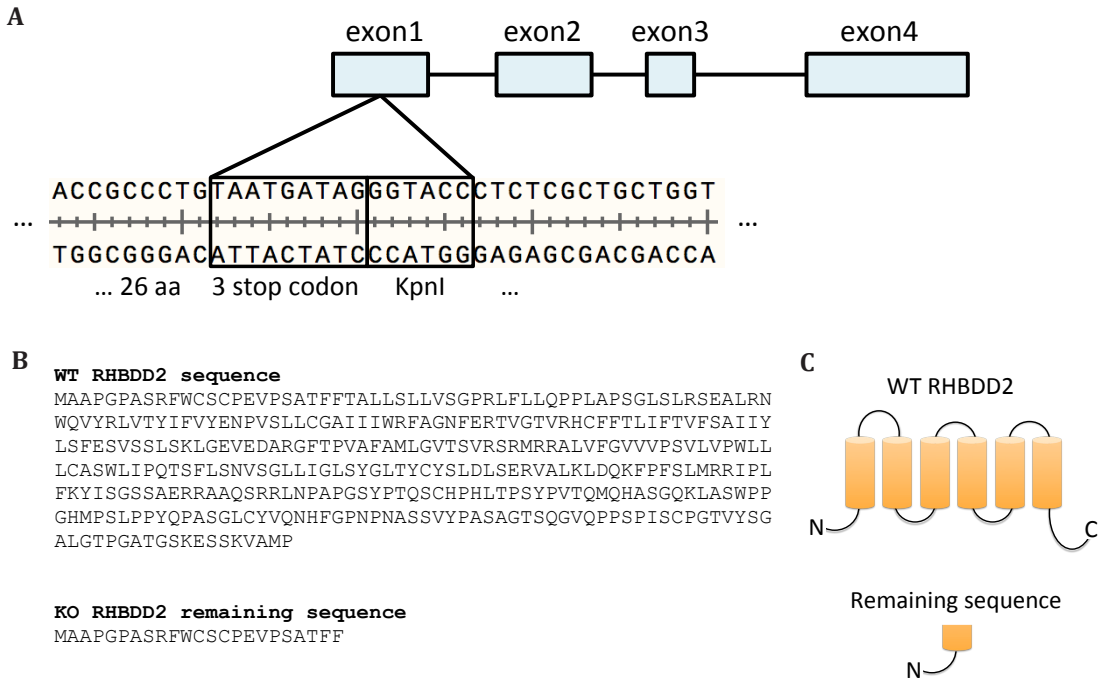

Figure 16 Design of CRISPR KO mice
(A) Schematic of RHBDD2 gene that shows 4 coding exons. Three stop codons and a KpnI restriction site were inserted into the first exon with 26 amino acid region left intact before insertion. (B) Amino acid sequences for WT RHBDD2 and the remaining sequence after RHBDD2 KO. (C) Schematic of WT RHBDD2 protein structure and the remaining structure after RHBDD2 targeting.

Guide RNA (gRNA) sequences were designed using a CRISPR prediction resource[63] and one of these was chosen for cloning into the gRNA basic plasmid (a gift from Dr. Moises Mallo) (Supplementary Fig.S1). To achieve homology-directed repair, three components were required: the gRNA, which was *in vitro* transcribed from the gRNA basic plasmid, an mRNA encoding Cas9 protein, plus the 200 bp homology directed repair template mentioned above, synthesized as a single stranded DNA oligo (Fig.17A).

As described above, the combination of Cas9 and gRNA trigger a double stranded DNA break at a site 3-4 base pair upstream of the PAM sequence[49]. The 200 bp homology template incorporating 5' and 3' homology arms on either side of the triple stop codon and KpnI restriction site (Fig.17A). Afterward, the plasmid and homology template were injected into a fertilized egg in the IGC's

transgenics facility.

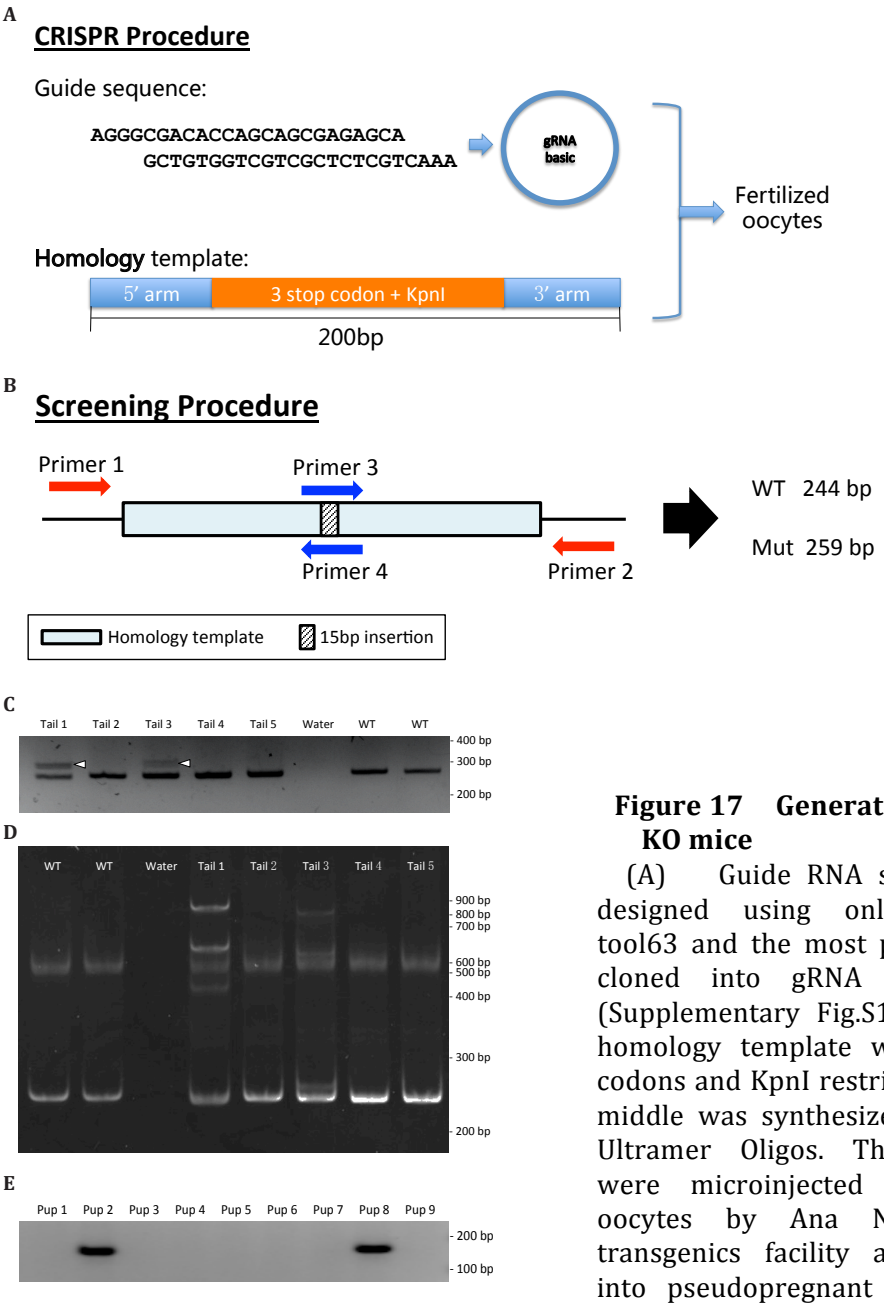

Figure 17 Generation of RHBDD2 KO mice

(A) Guide RNA sequences were designed using online prediction tool63 and the most proper one was cloned into gRNA basic plasmid (Supplementary Fig.S1). The 200 bp homology template with three stop codons and KpnI restriction site in the middle was synthesized by IDT DNA Ultramer Oligos. These constructs were microinjected into fertilized oocytes by Ana Nóvoa in IGC transgenics facility and transferred into pseudopregnant mice at 1-cell stage. (B) Four screening primers were designed to genotype the CRISPR mice. Two outer primers (red) would amplify 244 bp PCR products from WT RHBDD2 and 259 bp PCR products from the mutant RHBDD2 with the specific insertion. Another genotype strategy is to use the inner primers (blue) – primer 1 + primer 4 and primer 3 + primer 2. These two pairs of primer would only amplify the mutant RHBDD2, namely no PCR products from WT RHBDD2. (C) PCR products of DNA extracted from five putative founder mice were loaded in 4% agarose gel. The arrow heads indicate bands of higher molecular weight in addition to WT bands. (D) The same PCR products in (C) were heated to 95℃ and slowly cool down to room temperature then loaded in 8% acrylamide gel. (E) Agarose gel shows the PCR products of DNA extracted from nine pups of the second targeting experiment, using primer 3 and primer 2.

Five animals were born and died on the first day of birth. Five tails were collected to extract DNA for the screening test (Fig.17B). The 'outer' pair of screening primers (primer 1 and primer 2) were designed to anneal to an area on either side, outside of the homology template. If targeting were successful, PCR should amplify a 244 bp DNA product in WT mice and a 259 bp product in KO mice (Fig.17B). The inner primer pairs, identical forward and reverse primers identifying the mutant insertion sequences, primer 1 and 4, detect a 151 bp product in KO mice, while primer 3 and primer 2 produce a 147 product. These two pairs of primers should not produce PCR products from DNA from WT animals. Using the combination of primer pair 1 and 2'outer', on 4% agarose gel, all five founders had a WT allele band whereas two of them (founder 1 and founder 3) had an additional band of higher molecular weight (Fig.17C). It was not possible to detect the product encoded by the homology template using either combination of the 'inner' and 'outer' primers (data not shown). This suggested that the presence of INDELs accounts for the molecular weight difference. To investigate this possibility further, PCR products were heated to 95℃for 5 mins to denature double stranded DNA, then they were slowly cooled down to room temperature to randomly anneal with each other. Hence, products containing a wild type strand annealed to a strand harbouring indels can be created under these conditions. Subsequently, the products were electrophoresed on an 8% acrylamide gel, which has a very high resolving power for small fragments of DNA (Fig.17D). Consistent with the results above obtained with standard agarose electrophoresis, all five founders had banding patterns identical to the WT products. However, the DNA from founder 1 and founder 3 exhibited different additional bands, indicating they harboured INDELs and were hence heterozygous at the RHBDD2 locus.

The experiment was repeated and 17 putative founders were obtained. These founders were screened by Emma Burbridge (IGC, membrane traffic group). This analysis revealed that two founder animals (Nº2, Nº8) harboured the desired mutation, as indicated by the ability of primers 2 & 3 to recognize the mutant product (Fig 17.E). This was further confirmed by DNA sequencing, which indicated that indeed the correct targeting event had occurred.

Notably, screening genomic DNA from these two founder animals using the

outer primers (Fig.17B, primers 1&2) revealed only a WT band. This indicates firstly that the animals are certainly heterozygous at the RHBDD2 locus. As the mutant allele cannot be easily amplified with the outside primers 1&2 (Fig. 17B) that can also recognize the WT allele, this could suggest that the mutant animals are chimeric and that only a minority of the tissue contributing to the genomic DNA sample harbours the mutant allele. Nonetheless, these founders have now been setup to breed with WT mice to screen for germline transmission of the mutant allele, in order to ultimately generate RHBDD2 null animals.

3.5 Identification of RHBDD2 interactors

RHBDD2 is a pseudoprotease, therefore it must function by binding to other proteins. However, to date no RHBDD2 interactors have been reported. As it is possible to detect stable binding of iRhoms—also rhomboid-like pseudoproteases— to their client protein TACE[30] by immunoprecipitation(IP), we should be able to detect physical interactors of RHBDD2 in the same way. Hence, I reasoned that this approach, in identifying RHDD2 interaction partners, could help reveal the physiological function of RHBDD2.

HEK cell lines harbouring either the pLEX.MCS empty vector plasmid, RHBDD2 WT, RHBDD2 R85H, iRhom1, iRhom2, iRhom1 NT(N-terminus), RHBDD3, UBAC2, Unc93b1 were used in three Immunoprecipitation experiments. All proteins were tagged with a triple HA tag.

Cells were exposed to the crosslinker DSP (dithiobis[succinimidyl propionate]) in the first two experiments. The challenge of IPs is to provide buffer conditions sufficiently stringent to minimize non-specific binding. At the same time, the buffer must be gentle enough to permit specific interactions, which is often fulfilled by many weak non-covalent bonds. Hence, cross-linking with DSP was used, a reversible homo-bifunctional chemical crosslinker, that promotes inter-molecular crosslinkeages via primary amines. When DSP is used, following crosslinking, the wash buffer used can be more stringent since the bait and prey are covalently attached, allowing non-specific interactors to be washed away.

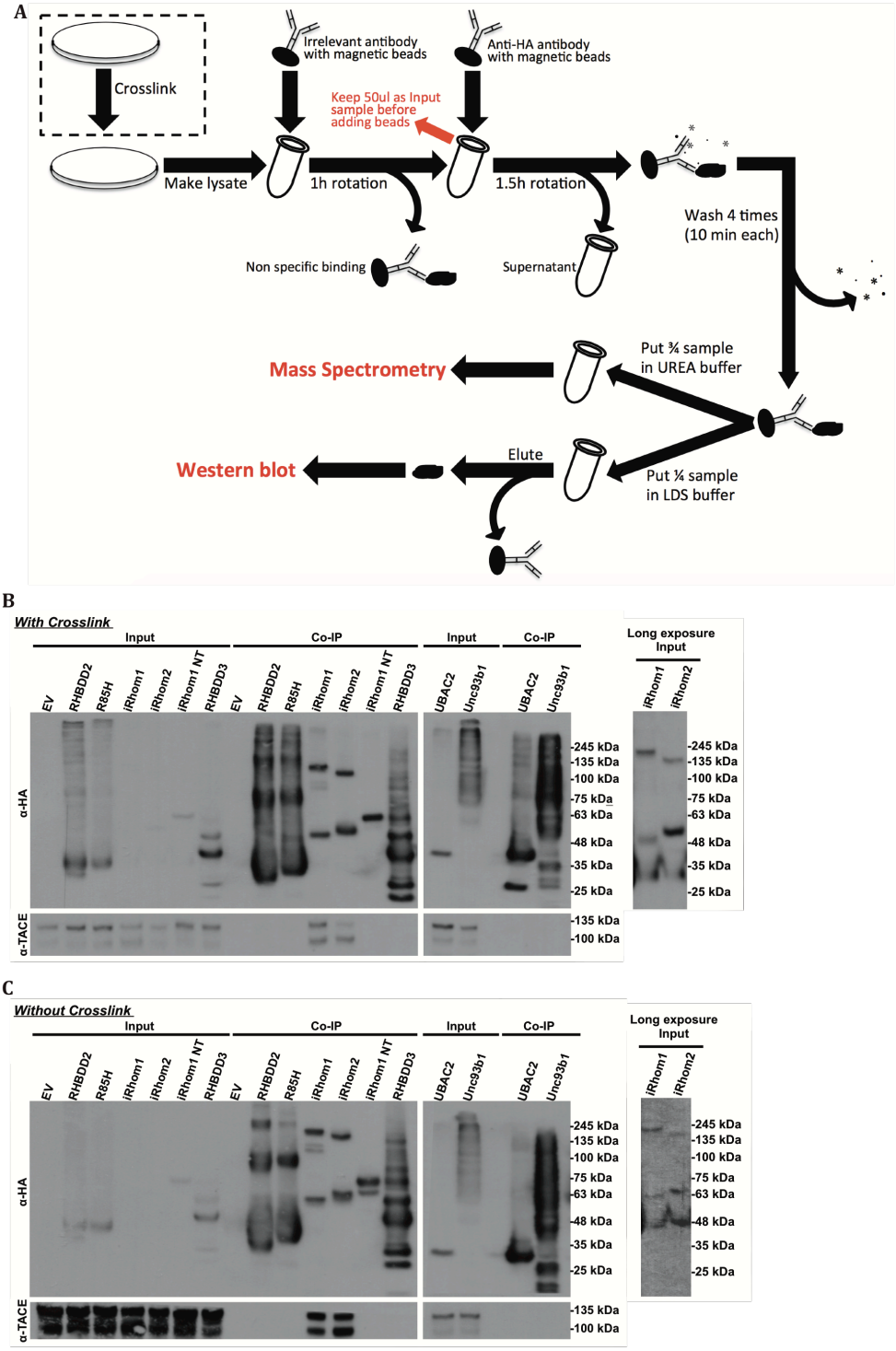

Figure 18 Immunoprecipitation (IP)
(A) The IP procedure (details in material and methods section) (B) Western blots of IP with crosslinker. The input and Co-IP samples were loaded in 6% acrylamide gel and probed with anti-HA and anti-TACE antibodies. The right panel is the same membrane with a longer exposure time. (C) Western blots of IP without crosslinker.

Subsequently, the crosslinks can be reversed by treatment with reducing agents. An alternative approach was adopted in a third experiment: this time, cells were not exposed to a crosslinker and hence the resultant IPs were exposed to much milder wash conditions. This dual approach was rationalized by a desire to balance the fact that chemical cross-linking is limited by the availability of free primary amines within a defined chemical space of 12Å, which may not be fulfilled by all genuine interactions. Hence, such interactions may instead be captured under the milder conditions of the non-crosslinking IPs. As described in methods, one-quarter of the co-IP samples were used in the following western blot experiments (Fig.18A). Three-quarters of the co-IP samples were sent to Professor Christopher Gerner, University of Vienna for mass spectrometry experiment.

With or without crosslinker, the western blots results are similar: they demonstrate expression of all overexpressed proteins with triple HA tag and no expression in EV cell lines in Co-IP samples. Although the iRhom1 and iRhom2 expression in Input samples are not visible in Figure 18B and 18C left panel, the expression can be seen with a longer exposure time (Fig.18B and 17C right panel) Detection of TACE indicates that existed in all lysates, but only been pulled down by IP in iRhom1 and iRhom2 sample, was as a positive control.

The compositions of all the hits that uniquely co-precipitated with RHBDD2 and/or R85H were classified based on the subcellular localization. Most of the RHBDD2 unique hits localize to Golgi apparatus in IPs with crosslinker (Fig.19) Note that the “other” section includes proteins from several organelles and cytoplasm). These hits were further classified by their function. Details in Supplementary Table 1~10.

Comparing the unique hits between first and second IP (both done under cross-linking conditions; Fig.19), the total number of hits in second IP is increased, which may due to an enriched protein sample (the second experiment was scaled up by 3 folds). The rough composition however did not change. Two groups of conserved hits (Supplementary Table 6) caught my attention: golgins that are involved in Golgi organization (golgin-160, golgin-84 and golgin-45) and Sec proteins (Sec24A, Sec24B and Sec24D) that are responsible for the COPII vesicle formation. These findings imply that RHBDD2 may play a role in Golgi

organization and COPII dependent ER-to-Golgi anterograde transport.

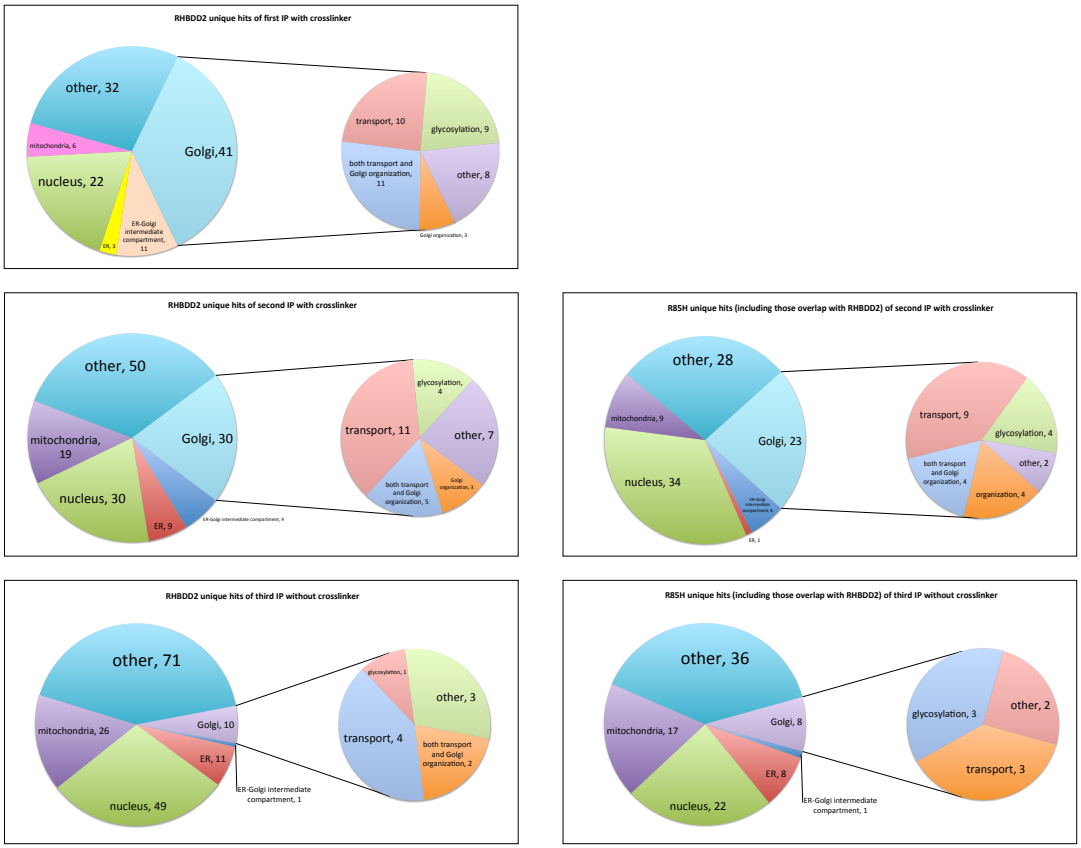

Figure 19 Pie charts of IPs
The hits that uniquely co-precipitated with RHBDD2 or R85H were first classified by the subcellular localization. The Golgi localized hits were subsequently classified by their function. (Details see Supplementary Table 1~5)

Several inferences can be made concerning the WT versus RHBDD2 mutant immunoprecipitates. First, as shown in Supplementary Table 2~5, there is a large core cohort of proteins that bind mutually to RHBDD2 WT and to the mutant protein. Second, both proteins exhibit a unique binding profile to different sets of proteins found in the WT but not the mutant, and vice versa. Third, the total number of these hits is greater for the WT than the mutant, both in experiments with and without crosslinker. This allows me to make the tentative observation that the point mutation alters the binding specificity for a cohort of interactors; understanding the difference between these two interactors may help reveal the pathological basis of the R85H disease mutation.

Comparing the experiments with and without crosslinker (Fig.19), the number

of Golgi localized hits are reduced in non-crosslinking IPs. Proteins from the nucleus and cytoplasm (and other organelles) are increased in these IPs. This may be attributable due to a milder wash conditions which could have facilitated more non-specific binding of these molecules. However, the Sec16A, Sec23A and Sec24C were captured by this IP, although they are not the same in the crosslinked IPs, they belong to the same family and are components of COPII dependent ER-to-Golgi anterograde transport. Hence, the presence of these COPII components is a common theme.

3.6 Role of RHBDD2 in homeostasis of the Golgi apparatus

Several golgin proteins were identified as specific putative interactors of WT RHBDD2 in both the first and second PI/mass spectrometry experiments: Golgin-160, Golgin-84, Golgin-45 (Supplementary Table 6). As described in introduction, golgins generally function as membrane tethers that form Golgi cisternae, but also play various respective additional roles. Golgin-160 plays a role in Golgi positioning during cell migration in wound response[55]. Golgin-84 captures cis- and trans-Golgi resident proteins to maintain the Golgi homeostasis[22]. Golgin-45 is a interactor of GRASP55, a medial-Golgi matrix protein, which functions in the stacking of Golgi cisternae[56]. As RHBDD2 binds to several Golgins, we hypothesized that RHBDD2 plays a role in the maintenance of Golgi structure or Golgi homeostasis.

A common way in which the contribution of Golgin proteins to Golgi integrity is assessed, involves triggering the disassembly of the Golgi apparatus using the drug BFA then examining the kinetics of Golgi disassembly or reassembly. BFA blocks anterograde trafficking, leading to the eventual collapse of the Golgi apparatus and its coalescence with ER membranes. There are several physiological contexts where Golgi fragmentation is physiologically relevant: during mitosis, when the Golgi apparatus must be partitioned equally into mother and daughter cells; the Golgi also undergoes fragmentation during apoptosis.

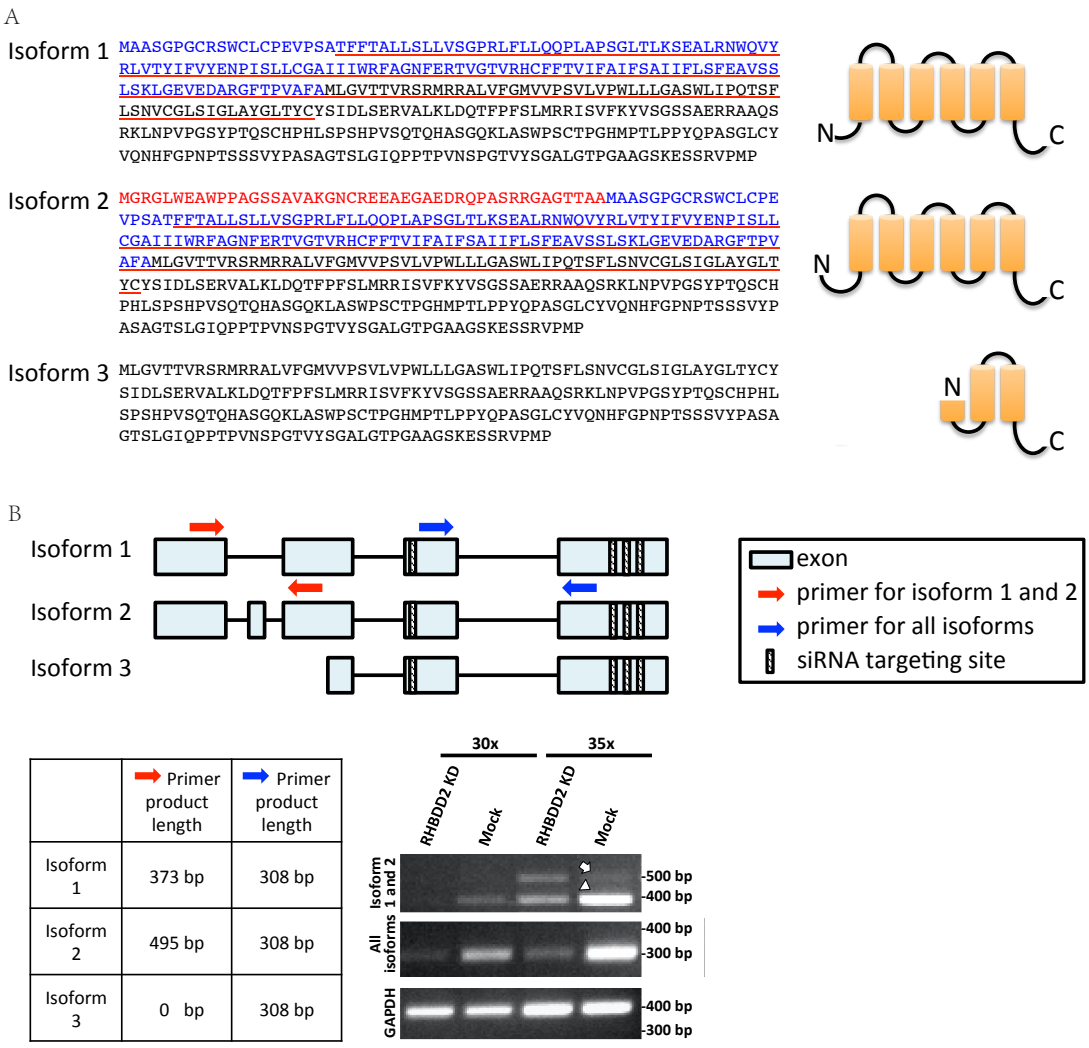

	Primer product length	Primer product length
Isoform 1	373 bp	308 bp
Isoform 2	495 bp	308 bp
Isoform 3	0 bp	308 bp

Figure 20 siRNA mediated human RHBDD2 knockdown

(A) Sequences and schematic of three isoforms of human RHBDD2. (B) Schematic gene structure of three human RHBDD2 isoforms shows four siRNA targeting site with shadowing area. This pool of four siRNAs were transfected into Hela-GalT-GFP cells to KD RHBDD2. DNA was extracted from these cells and tested by rtPCR using following primers. One pair of primers (blue) was used to amplify all three isoforms at the same size (308 bp). Another pair of primers (red) was used to amplify isoform 1 with 373 bp products and isoform 2 with 495 bp products. The PCR products from 30x and 35x thermocycles of rtPCR using primers mentioned above were loaded in 2% agarose gel. Primers for amplifying GAPDH was used as a loading control. The arrow indicates the isoform 2 band and the arrow head indicates the isoform 1 band. siRNAs for KD Unc93b1 were transfected to the same cells as a control.

Golgi fragmentation experiments were carried out in Hela-GalT-GFP cells, which stably express GalT, a trans Golgi marker, fused to GFP, enabling Golgi disassembly and assembly to be tracked (a gift from Dr. Jack Rohrer). Limited by timescale, instead of using the CRISPR/CAS9-based knockout strategy (described in methods above), siRNA-mediated knockdown of RHBDD2 was performed in

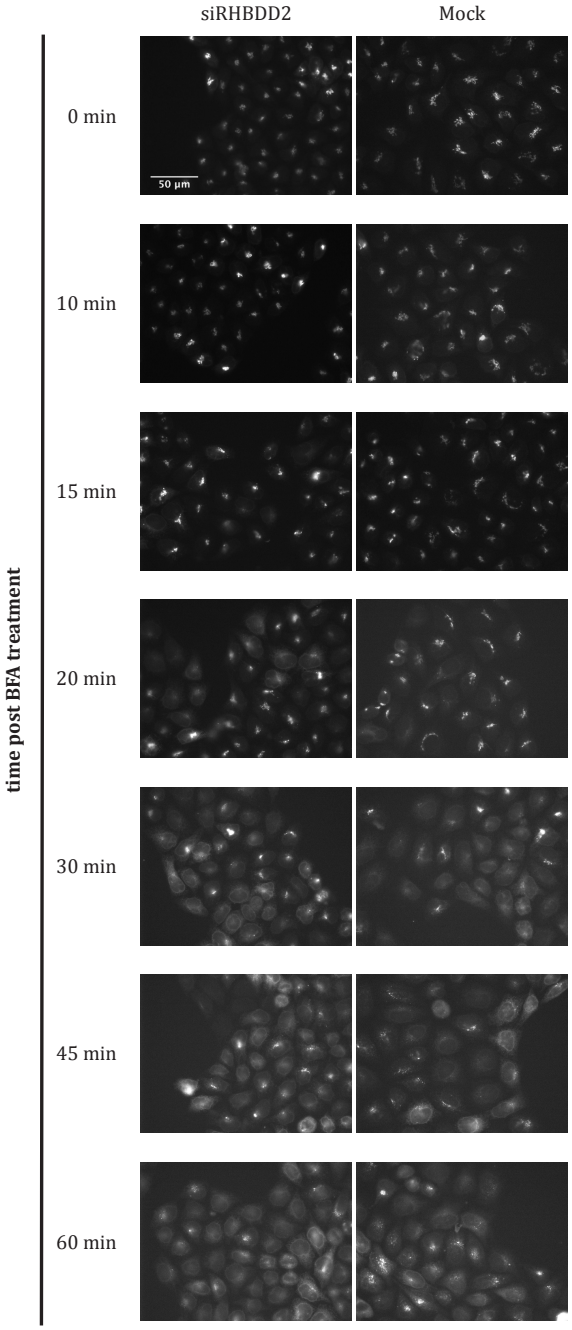

Figure 21 BFA induced Golgi fragmentation
After 72h of siRNA transfection, RHBDD2 KD Hela-GalT-GFP cells (mentioned in Fig.18B) were treated with BFA (0.25µg/ml) and fixed with 4% formaldehyde at different time points. Unc93b1 KD hela-GalT-GFP cells were used as a control.

human Hela GalT-GFP cells. Human RHBDD2 has three isoforms. Their amino acid sequences, schematic structure and genomic locus are shown in Figure 20A and 19B. All three isoforms have the same sequences near C terminus (Fig.20A black sequences). Both isoforms 1 and 2 have the Rhomboid domain core (Fig.20A black sequences). Isoform 2 has an additional 45 amino acids at the N terminus (Fig.20A black sequences).

Two pairs of primers were designed to detect mRNA expression level of remaining RHBDD2 after siRNA-mediated knockdown (a pool of four siRNA oligos, whose targeting sites are in the common area of all three isoforms, was delivered to the cells), via reverse transcriptase PCR (RT-PCR) reactions (Fig.20B). The primers indicated with red arrows can simultaneously detect isoforms 1 and 2 (each has a distinct product length). The primers denoted with blue arrows can detect all three isoforms, with the same product length. 72 hours following siRNA transfection, RNA was isolated and subjected to RT-PCR. The mRNA levels of

GAPDH were used as a loading control. RT-PCR results revealed that isoform 2 (white arrow) normally has much lower abundance than isoform 1 expression (arrow head) in control cells. Isoform 1 expression was evidently reduced by approximately 50% after 72h post siRNA transfection. The total amount of RHBDD2 was reduced by approximately 70% after 72h post siRNA transfection. However the isoform 2 band following 35x thermocycle steps is even brighter in the knockdown lane. This can be a result that less primers were occupied by isoform 1, so isoform 2 got more primers to amplify. There appeared to be a reasonable knockdown at the RNA level. Hence, this knockdown approach was used in the subsequent functional experiments.

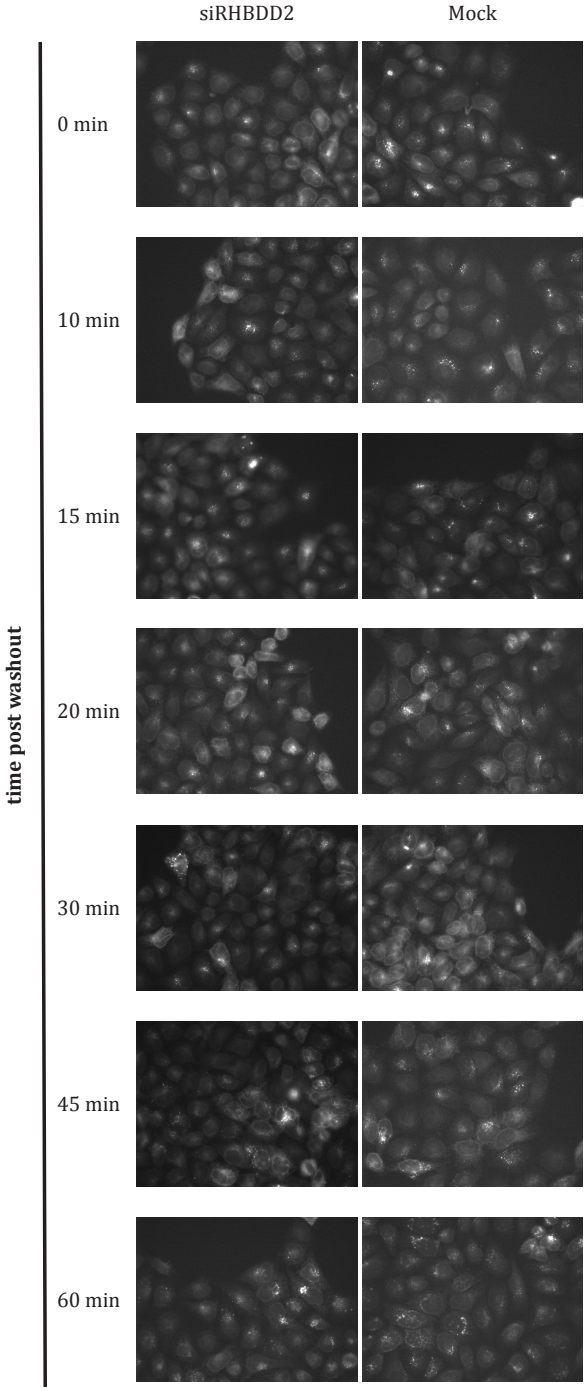

RHBDD2 KD and unc93b1 KD Hela-GalT-GFP cells were incubated with BFA (0.25μg/ml) to induce Golgi fragmentation. Cells were fixed at different time points to assess the extent of Golgi disassembly (Fig.21). There is no observable difference between the Golgi fragmentation of RHBDD2 KD versus unc93b1 KD cells in all time points.

Figure 22 BFA washout following Golgi fragmentation
This experiment followed the procedures described for Figure 19. The first two images on the top are the same images of the last two in Figure 19. Cells were rinsed twice in complete medium for BFA washout and fixed at different time points with 4% formaldehyde.

Because BFA induced blocking of ER-to-Golgi transport is reversible, the assay was adapted to examine the ability of Golgi reassembly in these cells; BFA was washed out b y normal medium after a one hour incubation. Then cells were fixed at different time points. Again there is no observable difference between RHBDD2 KD and mock cells in all time points (Fig.22).

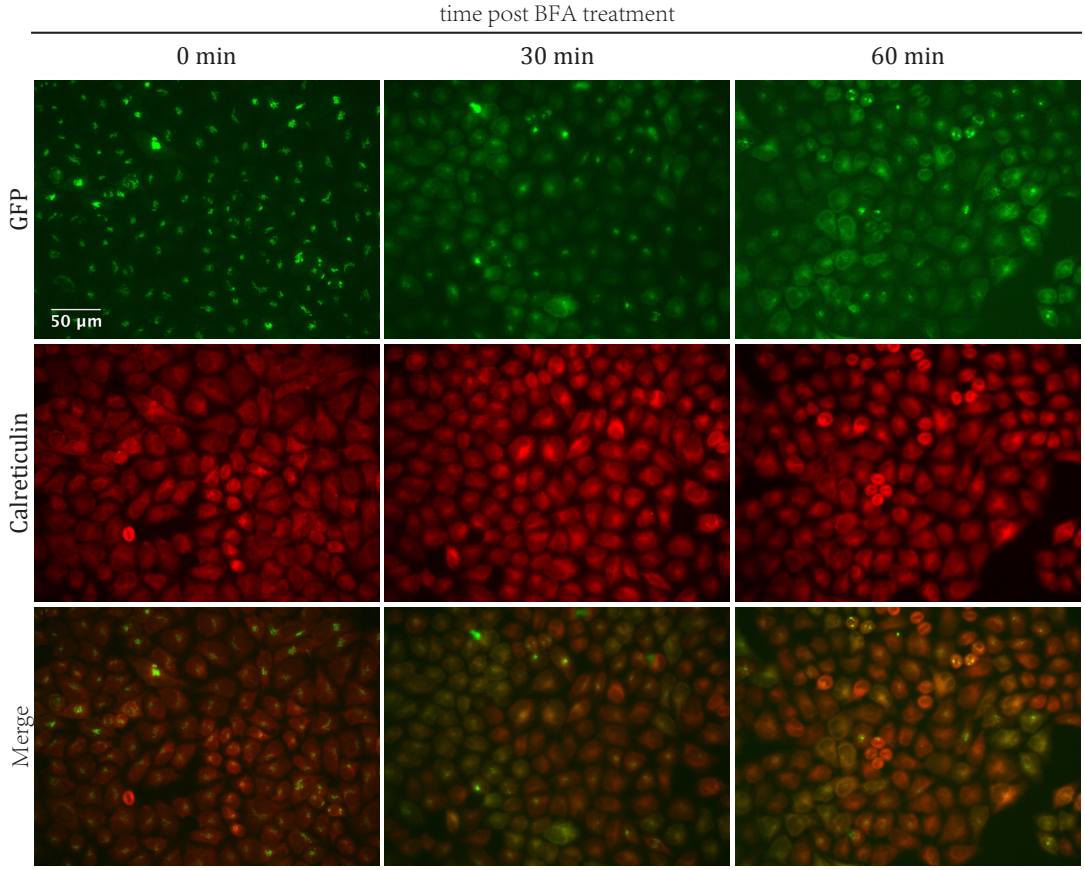

Figure 23 Immunofluorescent images for Golgi fragmentation cells
Cells mentioned in Figure 19 and 20 were co-labeled with Calreticulin antibody (ER marker, red) after fixation.

In order to examine the Golgi fragmentation and reassembly more detail, cells were labeled by Calreticulin (ER marker) (Fig.23A). During disassembly, the Golgi marker assumed an ER-like staining pattern over time, consistent with the collapse of the Golgi and its coalescence with the ER, as reported[57]. Using the ER marker as a reference, this was assessed based on a scoring system in which the status Golgi fragmentation was assigned to three categories: no fragmentation, partial fragmentation (remaining a little Golgi apparatus structure; having a perinuclear ER like shape) or total fragmentation, where the Golgi and ER

staining coalesced (Fig.24A). Five randomly selected fields from each coverslip were captured by 40x lens. Cells in these fields were counted manually and classified into the three Golgi morphology types (Fig.24B). This more detailed assessment also indicated no obvious difference in the level of Golgi fragmentation or Golgi reassembly between RHBDD2 KD and unc93b1 KD cells.

In conclusion, RHBDD2 appeared dispensable in controlling BFA induced Golgi fragmentation and Golgi reassembly. However, it is important to note that this result was based on an incomplete knockdown of RHBDD2. Ideally, cells genetically null for RHBDD2 (for example, obtained from RHBDD2 KO mice or from cells targeted via CRISPR/Cas9) will be used in the future to re-examine this within the context of a complete absence of RHBDD2 protein.

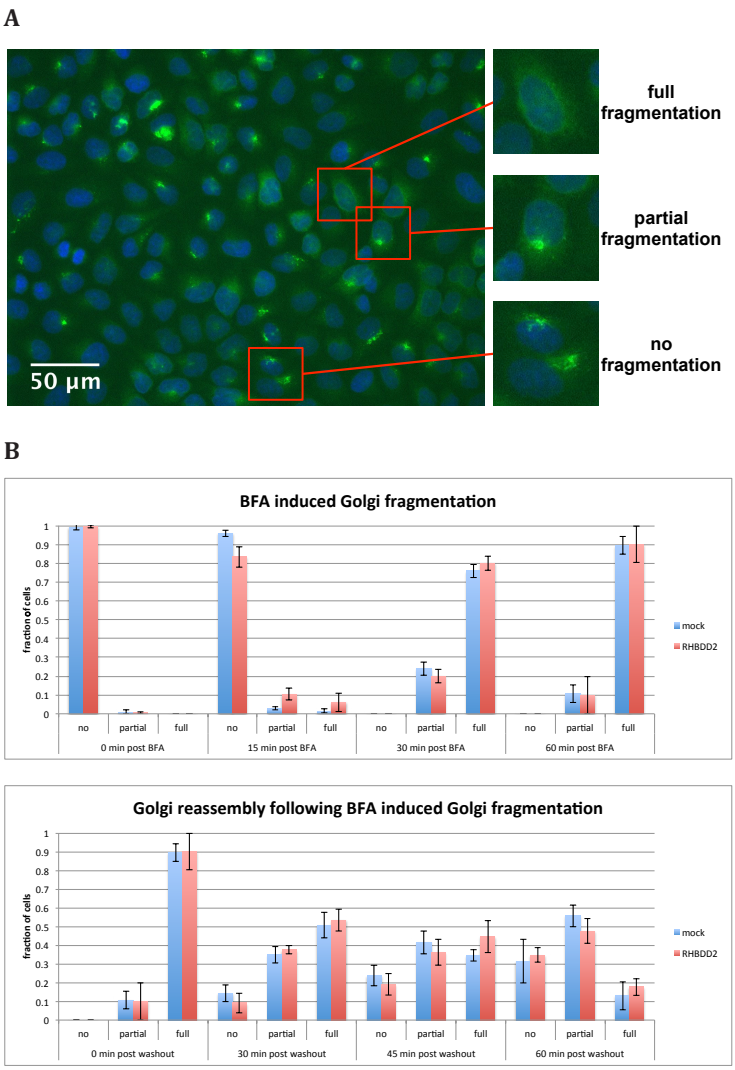

Figure 24 semi-quantification of Golgi fragmentation and reassembly
(A) A scoring system was set based on the Golgi morphology: no fragmentation – the Golgi structure is complete and showing a strong signal; partial fragmentation – the signal shows both Golgi like and ER like morphology; full fragmentation – the signal shows only a ER like morphology. (B) Five decentralized fields of each coverslip were captured by 40x lens on Leica DMRA2 microscopy. Cells were manually classified and quantified to make the histogram.

4. Discussion

In this project, I focused on elucidating the function of RHBDD2. My work began though by revisiting the membrane topology of RHBDD2. A thorough comparison with the sequences of other Rhomboid superfamily proteins enabled me to predict that RHBDD2 contains six putative transmembrane domains, with cytoplasmic N and C termini (Fig.11C). This prediction is at odds with several prior studies that argue that Derlins have six TMDs [50], iRhoms and active Rhomboids have seven TMDs[51] [52]. Time-permitting, my prediction would have been tested experimentally. The presence of five versus six TMDs can be distinguished by determining the accessibility of the C terminus of the protein; by permeabilizing cells expressing RHBDD2 with Triton-X100 (which permeabilizes the plasma membrane and internal membranes) versus Digitonin, which can only permeabilize the plasma membrane. If Digitonin permeabilized cells are accessible to staining with anti-HA antibodies, it implies that the C terminus localizes to the cytoplasm, meaning that RHBDD2 has six TMDs. Conversely, if staining is only achieved following TX-100 permeabilization the RHBDD2 C-terminus is should localize to the Golgi lumen implying that RHBDD2 has five TMDs.

Two major foci of this thesis were (1) to investigate how the RHBDD2 R85H mutant found in some retinitis pigmentosa patients causes disease at a cellular level; (2) to investigate the wild type role of RHBDD2 at the cellular and physiological levels. Dealing firstly with how the R85H mutation causes retinitis pigmentosa, I can conclude that the mutant protein, when overexpressed in mouse retinal pigment epithelial cells, does not trigger a constitutive induction of ER stress. Furthermore, I observed minimal differences in drug induced ER stress in cells expressing WT versus mutant RHBDD2. Clearly, the effects on a number of ER stress-induced pathways and their transcriptional targets of the

UPR (Perk, ATF6, ATF4, etc.) would be needed to assemble a fuller picture. Nonetheless, this allows one to tentatively speculate that the defect observed in the patients may not be caused by cell death of photoreceptors, caused by misfolded mutant RHBDD2 R85H. Immunoflurescence analysis and colocalization experiments demonstrated that the R85H mutatant protein exhibited the same localization—the Golgi apparatus—as the WT RHBDD2 (Fig.15A) Ideally, these comparisons would have been based on the endogenous WT versus RHBDD2 R85H mutated proteins (for example, generated at the endogenous locus, using CRISPR/Cas9) rather than the overexpression model used here. Nonetheless, these data add further weight to the notion that the disease in RP patients may not be due to the ER retention of the mutated protein, again suggesting that ER stress may not explain the disease phenotype.

The second goal of the thesis was to attempt to define the physiological role of RHBDD2. One way in which this was approached was at the organismal level, by attempting to make RHBDD2 null mice. As described, a strategy was adopted to make RHBDD2 KO mice via CRISPR. In the initial experiment, only five putative founder animals were born, an abnormally small yield of pups from this experimental procedure; unfortunately all pups died. Two of these mice genotyped as heterozygous and three of them as wild type (Fig.17C and 17D). Thus, the death of animals probably cannot be attributed to mutation in RHBDD2, but possibly other sporadic reasons. As discussed above, a second targeting attempt identified two chimeric founder animals harbouring the desired mutation; these will be used to establish an RHBDD2-null colony. Further work will involve characterization of the phenotype of these mutant mice.

In an alternative approach to define the function of RHBDD2, IP/mass spectrometry were performed. The rationale was to immunoprecipitate the binding partners of RHBDD2, subsequently identify those proteins and use this information to hypothesize about the possible function of RHBDD2. These experiments revealed that the Golgins (GM160, Golgin-84, Golgin-45) co-immunoprecipitated with RHBDD2 under crosslinker condition (Supplementary Table 6). As Golgins play a key role as membrane tethers, we hypothesized that RHBDD2 may be involved in the maintenance of Golgi structure or Golgi homeostasis. Components of COPII vesicles (Sec24A, Sec24B

and Sec24D in the crosslinking IPs; Sec16A, Sec23A and Sec24C in the non-crosslinking IPs) were captured under both with or without crosslinker conditions, thus indicating RHBDD2 may paly a role in COPII dependent ER-to-Golgi anterograde transport (Supplementary Table 7). Both golgins and Sec proteins didn't show difference between RHBDD2 WT and R85H samples. However, the total hits number is reduced (Supplementary Table 2,3 and 4,5) in mutant samples, indicating a change in its binding properties, possibly caused by a conformational change in the mutant protein.

To address the role of RHBDD2 in the maintenance of the structure of the Golgi apparatus and in Golgi fragmentation and reassembly experiments, RNAi-based knockdown (KD) experiments were performed. The choice of RNAi as the loss of function approach was dictated by the limited time constraints of the master thesis. The results showed no detectable difference in the kinetics of Golgi disassembly, or assembly, between KD cells and cells treated with a control siRNA. However, considering the modest knockdown efficiency of RHBDD2 (Fig.20B), the lack of phenotype could be explained by incomplete ablation of RHBDD2 at the protein level. Further experiments would ideally be conducted using cells in which RHBDD2 was ablated CRISPR, or using cells isolated from RHBDD2 KO mice.

For more precise experiments, addressing the pathological role of the R85H mutation, it is needed to generate endogenous R85H mutant cell line in order to assess the phathology under endogenous expression conditions.

The physiological role of RHBDD2 remains unknown. Considering the components of COPII vesicles in IP samples (Supplementory Table 1-10), it is worth to test the cargo trafficking in the early secretory pathway. In addition, because TMEM115 has an impact on glycolsylation in Golgi apparatus, it is also worth to further test the lectin binding in KO cells.

5. Abbreviation

ER, endoplasmic reticulum

COPII, coat protein complex II

COPI, coat protein complex I

ERAD, ER-associated degradation

UPR, unfolded protein response

RP, Retinitis Pigmentosa

WT, wild type

EV, empty vector

Tg, thapsigargin

Tm, tunicamycin

BFA, Brefeldin A

CRISPR, clustered regularly interspaced short palindromic repeats

IP, immunoprecipitation

KD, knockdown

TMD, transmembrane domain

REP, retinal pigment epithelium

6. References

1. Howell, G. J., Holloway, Z. G., Cobbold, C., Monaco, A. P. & Ponnambalam, S. 1-69 (Elsevier, 2006).
2. Adrain, C. & Freeman, M. Regulation of receptor tyrosine kinase ligand processing. *Cold Spring Harb Perspect Biol* **6**, (2014).
3. Jahn, T. R. & Radford, S. E. The Yin and Yang of protein folding. *FEBS J* **272**, 5962-5970 (2005).
4. Ellgaard, L. & Helenius, A. Quality control in the endoplasmic reticulum. *Nat Rev Mol Cell Biol* **4**, 181-191 (2003).
5. Spang, A. Retrograde traffic from the Golgi to the endoplasmic reticulum. *Cold Spring Harb Perspect Biol* **5**, (2013).
6. Appenzeller-Herzog, C. & Hauri, H. P. The ER-Golgi intermediate compartment (ERGIC): in search of its identity and function. *J Cell Sci* **119**, 2173-2183 (2006).
7. Vembar, S. S. & Brodsky, J. L. One step at a time: endoplasmic reticulum-associated degradation. *Nat Rev Mol Cell Biol* **9**, 944-957 (2008).
8. Pickart, C. M. Mechanisms underlying ubiquitination. *Annu Rev Biochem* **70**, 503-533 (2001).
9. Greenblatt, E. J., Olzmann, J. A. & Kopito, R. R. Derlin-1 is a rhomboid pseudoprotease required for the dislocation of mutant alpha-1 antitrypsin from the endoplasmic reticulum. *Nat Struct Mol Biol* **18**, 1147-1152 (2011).
10. Wahlman, J. et al. Real-time fluorescence detection of ERAD substrate retrotranslocation in a mammalian in vitro system. *Cell* **129**, 943-955 (2007).
11. Schekman, R. Cell biology: a channel for protein waste. *Nature* **429**, 817-818 (2004).

12. Araki, E., Oyadomari, S. & Mori, M. Endoplasmic reticulum stress and diabetes mellitus. *INTERNAL MEDICINE-TOKYO-JAPANESE SOCIETY OF INTERNAL MEDICINE-* **42**, 7-14 (2003).
13. Hetz, C. The unfolded protein response: controlling cell fate decisions under ER stress and beyond. *Nat Rev Mol Cell Biol* **13**, 89-102 (2012).
14. Ahmedli, N. B. et al. Dynamics of the rhomboid-like protein RHBDD2 expression in mouse retina and involvement of its human ortholog in retinitis pigmentosa. *J Biol Chem* **288**, 9742-9754 (2013).
15. Pelham, H. R. & Rothman, J. E. The debate about transport in the Golgi--two sides of the same coin? *Cell* **102**, 713-719 (2000).
16. Klumperman, J. Architecture of the mammalian Golgi. *Cold Spring Harb Perspect Biol* **3**, (2011).
17. Alcalde, J., Bonay, P., Roa, A., Vilaro, S. & Sandoval, I. V. Assembly and disassembly of the Golgi complex: two processes arranged in a cis-trans direction. *The Journal of cell biology* **116**, 69-83 (1992).
18. Slusarewicz, P., Nilsson, T., Hui, N., Watson, R. & Warren, G. Isolation of a matrix that binds medial Golgi enzymes. *J Cell Biol* **124**, 405-413 (1994).
19. Ramirez, I. B. & Lowe, M. Golgins and GRASPs: holding the Golgi together. *Semin Cell Dev Biol* **20**, 770-779 (2009).
20. Wong, M. & Munro, S. Membrane trafficking. The specificity of vesicle traffic to the Golgi is encoded in the golgin coiled-coil proteins. *Science* **346**, 1256898 (2014).
21. Mayer, U. & Nusslein-Volhard, C. A group of genes required for pattern formation in the ventral ectoderm of the Drosophila embryo. *Genes Dev* **2**, 1496-1511 (1988).
22. Urban, S. & Wolfe, M. S. Reconstitution of intramembrane proteolysis in vitro reveals that pure rhomboid is sufficient for catalysis and specificity. *Proceedings of the National Academy of Sciences of the United States of America* **102**, 1883-1888 (2005).
23. Lemberg, M. K. et al. Mechanism of intramembrane proteolysis investigated with purified rhomboid proteases. *The EMBO journal* **24**, 464-472 (2005).

24. Lemberg, M. K. & Freeman, M. Functional and evolutionary implications of enhanced genomic analysis of rhomboid intramembrane proteases. *Genome research* **17**, 1634-1646 (2007).
25. Ong, Y. S., Tran, T. H., Gounko, N. V. & Hong, W. TMEM115 is an integral membrane protein of the Golgi complex involved in retrograde transport. *J Cell Sci* **127**, 2825-2839 (2014).
26. McIlwain, D. R. et al. iRhom2 regulation of TACE controls TNF-mediated protection against Listeria and responses to LPS. *Science* **335**, 229-232 (2012).
27. Zettl, M., Adrain, C., Strisovsky, K., Lastun, V. & Freeman, M. Rhomboid family pseudoproteases use the ER quality control machinery to regulate intercellular signaling. *Cell* **145**, 79-91 (2011).
28. Christianson, J. C. et al. Defining human ERAD networks through an integrative mapping strategy. *Nature cell biology* **14**, 93-105 (2012).
29. Sawalha, A. H. et al. A putative functional variant within the UBAC2 gene is associated with increased risk of Behçt' disease. *Arthritis & Rheumatism* **63**, 3607-3612 (2011).
30. Fleig, L. et al. Ubiquitin-dependent intramembrane rhomboid protease promotes ERAD of membrane proteins. *Mol Cell* **47**, 558-569 (2012).
31. Liu, J. et al. Rhbdd3 controls autoimmunity by suppressing the production of IL-6 by dendritic cells via K27-linked ubiquitination of the regulator NEMO. *Nat Immunol* **15**, 612-622 (2014).
32. Lacunza, E. et al. Identification of signaling pathways modulated by RHBDD2 in breast cancer cells: a link to the unfolded protein response. *Cell Stress Chaperones* **19**, 379-388 (2014).
33. Lacunza, E. et al. RHBDD2: a 5-fluorouracil responsive gene overexpressed in the advanced stages of colorectal cancer. *Tumour Biol* **33**, 2393-2399 (2012).
34. Jiang, H., Xiong, S. & Xia, X. Retinitis pigmentosaassociated rhodopsin mutant T17M induces endoplasmic reticulum (ER) stress and sensitizes cells to ER stress-induced cell death. *Mol Med Rep* **9**, 1737-1742 (2014).
35. Wang, J. et al. A mutation in the insulin 2 gene induces diabetes with severe pancreatic beta-cell dysfunction in the Mody mouse. *J Clin Invest* **103**, 27-37 (1999).
36. Hamel, C. Retinitis pigmentosa. *Orphanet J Rare Dis* **1**, 40 (2006).

37. Mendes, H. F., van der Spuy, J., Chapple, J. P. & Cheetham, M. E. Mechanisms of cell death in rhodopsin retinitis pigmentosa: implications for therapy. *Trends Mol Med* **11**, 177-185 (2005).
38. ZY. The CRISPR Craze. (2013).
39. Deltcheva, E. et al. CRISPR RNA maturation by trans-encoded small RNA and host factor RNase III. *Nature* **471**, 602-607 (2011).
40. Jinek, M. et al. A programmable dual-RNA-guided DNA endonuclease in adaptive bacterial immunity. *Science* **337**, 816-821 (2012).
41. Greenblatt, E. J., Olzmann, J. A. & Kopito, R. R. Derlin-1 is a rhomboid pseudoprotease required for the dislocation of mutant alpha-1 antitrypsin from the endoplasmic reticulum. *Nat Struct Mol Biol* **18**, 1147-1152 (2011).
42. Lemberg, M. K. & Freeman, M. Functional and evolutionary implications of enhanced genomic analysis of rhomboid intramembrane proteases. *Genome Res* **17**, 1634-1646 (2007).
43. Urban, S. & Freeman, M. Substrate specificity of rhomboid intramembrane proteases is governed by helix-breaking residues in the substrate transmembrane domain. *Mol Cell* **11**, 1425-1434 (2003).
44. Adrain, C. & Freeman, M. New lives for old: evolution of pseudoenzyme function illustrated by iRhoms. *Nat Rev Mol Cell Biol* **13**, 489-498 (2012).
45. Short, B. et al. A GRASP55-rab2 effector complex linking Golgi structure to membrane traffic. *J Cell Biol* **155**, 877-883 (2001).
46. Sohda, M. et al. The interaction of two tethering factors, p115 and COG complex, is required for Golgi integrity. *Traffic* **8**, 270-284 (2007).
47. Klausner, R. D., Donaldson, J. G. & Lippincott-Schwartz, J. Brefeldin A: insights into the control of membrane traffic and organelle structure. *J Cell Biol* **116**, 1071-1080 (1992).

1. Howell, G. J., Holloway, Z. G., Cobbold, C., Monaco, A. P. & Ponnambalam, S. 1-69 (Elsevier, 2006).
2. Adrain, C. & Freeman, M. Regulation of receptor tyrosine kinase ligand processing. *Cold Spring Harb Perspect Biol* **6**, (2014).

3. Jahn, T. R. & Radford, S. E. The Yin and Yang of protein folding. *FEBS J* **272**, 5962-5970 (2005).
4. Ellgaard, L. & Helenius, A. Quality control in the endoplasmic reticulum. *Nat Rev Mol Cell Biol* **4**, 181-191 (2003).
5. Brandizzi, F. & Barlowe, C. Organization of the ER-Golgi interface for membrane traffic control. *Nat Rev Mol Cell Biol* **14**, 382-392 (2013).
6. Spang, A. Retrograde traffic from the Golgi to the endoplasmic reticulum. *Cold Spring Harb Perspect Biol* **5**, (2013).
7. Appenzeller-Herzog, C. & Hauri, H. P. The ER-Golgi intermediate compartment (ERGIC): in search of its identity and function. *J Cell Sci* **119**, 2173-2183 (2006).
8. Vembar, S. S. & Brodsky, J. L. One step at a time: endoplasmic reticulum-associated degradation. *Nat Rev Mol Cell Biol* **9**, 944-957 (2008).
9. Pickart, C. M. Mechanisms underlying ubiquitination. *Annu Rev Biochem* **70**, 503-533 (2001).
10. Greenblatt, E. J., Olzmann, J. A. & Kopito, R. R. Derlin-1 is a rhomboid pseudoprotease required for the dislocation of mutant alpha-1 antitrypsin from the endoplasmic reticulum. *Nat Struct Mol Biol* **18**, 1147-1152 (2011).
11. Wahlman, J. et al. Real-time fluorescence detection of ERAD substrate retrotranslocation in a mammalian in vitro system. *Cell* **129**, 943-955 (2007).
12. Schekman, R. Cell biology: a channel for protein waste. *Nature* **429**, 817-818 (2004).
13. Araki, E., Oyadomari, S. & Mori, M. Endoplasmic reticulum stress and diabetes mellitus. *INTERNAL MEDICINE-TOKYO-JAPANESE SOCIETY OF INTERNAL MEDICINE-* **42**, 7-14 (2003).
14. Hetz, C. The unfolded protein response: controlling cell fate decisions under ER stress and beyond. *Nat Rev Mol Cell Biol* **13**, 89-102 (2012).
15. He, L., Skirkanich, J., Moronetti, L., Lewis, R. & Lamitina, T. The cystic-fibrosis-associated DeltaF508 mutation confers post-transcriptional destabilization on the C. elegans ABC transporter PGP-3. *Dis Model Mech* **5**, 930-939 (2012).

16. Ahmedli, N. B. et al. Dynamics of the rhomboid-like protein RHBDD2 expression in mouse retina and involvement of its human ortholog in retinitis pigmentosa. *J Biol Chem* **288**, 9742-9754 (2013).
17. Boden, G. Endoplasmic reticulum stress: another link between obesity and insulin resistance/inflammation? *Diabetes* **58**, 518-519 (2009).
18. Malhotra, V. & Mayor, S. Cell biology: the Golgi grows up. *Nature* **441**, 939-940 (2006).
19. Pelham, H. R. & Rothman, J. E. The debate about transport in the Golgi--two sides of the same coin? *Cell* **102**, 713-719 (2000).
20. Klumperman, J. Architecture of the mammalian Golgi. *Cold Spring Harb Perspect Biol* **3**, (2011).
21. Alcalde, J., Bonay, P., Roa, A., Vilaro, S. & Sandoval, I. V. Assembly and disassembly of the Golgi complex: two processes arranged in a cis-trans direction. *The Journal of cell biology* **116**, 69-83 (1992).
22. Wong, M. & Munro, S. Membrane trafficking. The specificity of vesicle traffic to the Golgi is encoded in the golgin coiled-coil proteins. *Science* **346**, 1256898 (2014).
23. Slusarewicz, P., Nilsson, T., Hui, N., Watson, R. & Warren, G. Isolation of a matrix that binds medial Golgi enzymes. *J Cell Biol* **124**, 405-413 (1994).
24. Ramirez, I. B. & Lowe, M. Golgins and GRASPs: holding the Golgi together. *Semin Cell Dev Biol* **20**, 770-779 (2009).
25. Chen, Y. A. & Scheller, R. H. SNARE-mediated membrane fusion. *Nat Rev Mol Cell Biol* **2**, 98-106 (2001).
26. Mayer, U. & Nusslein-Volhard, C. A group of genes required for pattern formation in the ventral ectoderm of the Drosophila embryo. *Genes Dev* **2**, 1496-1511 (1988).
27. Urban, S. & Wolfe, M. S. Reconstitution of intramembrane proteolysis in vitro reveals that pure rhomboid is sufficient for catalysis and specificity. *Proceedings of the National Academy of Sciences of the United States of America* **102**, 1883-1888 (2005).
28. Wu, Z. et al. Structural analysis of a rhomboid family intramembrane protease reveals a gating mechanism for substrate entry. *Nat Struct Mol Biol* **13**, 1084-1091 (2006).

29. Lemberg, M. K. et al. Mechanism of intramembrane proteolysis investigated with purified rhomboid proteases. *The EMBO journal* **24**, 464-472 (2005).
30. Adrain, C. & Freeman, M. New lives for old: evolution of pseudoenzyme function illustrated by iRhoms. *Nat Rev Mol Cell Biol* **13**, 489-498 (2012).
31. Lemberg, M. K. & Freeman, M. Functional and evolutionary implications of enhanced genomic analysis of rhomboid intramembrane proteases. *Genome research* **17**, 1634-1646 (2007).
32. Xu, B. et al. WNK1, a novel mammalian serine/threonine protein kinase lacking the catalytic lysine in subdomain II. *J Biol Chem* **275**, 16795-16801 (2000).
33. Ong, Y. S., Tran, T. H., Gounko, N. V. & Hong, W. TMEM115 is an integral membrane protein of the Golgi complex involved in retrograde transport. *J Cell Sci* **127**, 2825-2839 (2014).
34. McIlwain, D. R. et al. iRhom2 regulation of TACE controls TNF-mediated protection against Listeria and responses to LPS. *Science* **335**, 229-232 (2012).
35. Zettl, M., Adrain, C., Strisovsky, K., Lastun, V. & Freeman, M. Rhomboid family pseudoproteases use the ER quality control machinery to regulate intercellular signaling. *Cell* **145**, 79-91 (2011).
36. Lloyd, S. J., Raychaudhuri, S. & Espenshade, P. J. Subunit architecture of the Golgi Dsc E3 ligase required for sterol regulatory element-binding protein (SREBP) cleavage in fission yeast. *J Biol Chem* **288**, 21043-21054 (2013).
37. Christianson, J. C. et al. Defining human ERAD networks through an integrative mapping strategy. *Nature cell biology* **14**, 93-105 (2012).
38. Sawalha, A. H. et al. A putative functional variant within the UBAC2 gene is associated with increased risk of Behçt' disease. *Arthritis & Rheumatism* **63**, 3607-3612 (2011).
39. Fleig, L. et al. Ubiquitin-dependent intramembrane rhomboid protease promotes ERAD of membrane proteins. *Mol Cell* **47**, 558-569 (2012).
40. Liu, J. et al. Rhbdd3 controls autoimmunity by suppressing the production of IL-6 by dendritic cells via K27-linked ubiquitination of the regulator NEMO. *Nat Immunol* **15**, 612-622 (2014).
41. Wang, Y. et al. A novel member of the Rhomboid family, RHBDD1, regulates BIK-mediated apoptosis. *Cell Mol Life Sci* **65**, 3822-3829 (2008).

42. Lacunza, E. et al. Identification of signaling pathways modulated by RHBDD2 in breast cancer cells: a link to the unfolded protein response. *Cell Stress Chaperones* **19**, 379-388 (2014).
43. Lacunza, E. et al. RHBDD2: a 5-fluorouracil responsive gene overexpressed in the advanced stages of colorectal cancer. *Tumour Biol* **33**, 2393-2399 (2012).
44. Hamel, C. Retinitis pigmentosa. *Orphanet J Rare Dis* **1**, 40 (2006).
45. Mendes, H. F., van der Spuy, J., Chapple, J. P. & Cheetham, M. E. Mechanisms of cell death in rhodopsin retinitis pigmentosa: implications for therapy. *Trends Mol Med* **11**, 177-185 (2005).
46. Jiang, H., Xiong, S. & Xia, X. Retinitis pigmentosaassociated rhodopsin mutant T17M induces endoplasmic reticulum (ER) stress and sensitizes cells to ER stress-induced cell death. *Mol Med Rep* **9**, 1737-1742 (2014).
47. ZY. The CRISPR Craze. (2013).
48. Deltcheva, E. et al. CRISPR RNA maturation by trans-encoded small RNA and host factor RNase III. *Nature* **471**, 602-607 (2011).
49. Jinek, M. et al. A programmable dual-RNA-guided DNA endonuclease in adaptive bacterial immunity. *Science* **337**, 816-821 (2012).
50. Greenblatt, E. J., Olzmann, J. A. & Kopito, R. R. Derlin-1 is a rhomboid pseudoprotease required for the dislocation of mutant alpha-1 antitrypsin from the endoplasmic reticulum. *Nat Struct Mol Biol* **18**, 1147-1152 (2011).
51. Lemberg, M. K. & Freeman, M. Functional and evolutionary implications of enhanced genomic analysis of rhomboid intramembrane proteases. *Genome Res* **17**, 1634-1646 (2007).
52. Urban, S. & Freeman, M. Substrate specificity of rhomboid intramembrane proteases is governed by helix-breaking residues in the substrate transmembrane domain. *Mol Cell* **11**, 1425-1434 (2003).
53. Lykke-Andersen, J., Shu, M. D. & Steitz, J. A. Human Upf proteins target an mRNA for nonsense-mediated decay when bound downstream of a termination codon. *Cell* **103**, 1121-1131 (2000).
54. Kozak, M. Constraints on reinitiation of translation in mammals. *Nucleic Acids Res* **29**, 5226-5232 (2001).
55. Darido, C. & Jane, S. M. Golgi Feels Its Own Wound. *Adv Wound Care (New Rochelle)* **2(3)**, 87-92 (2013).

56. Short, B. et al. A GRASP55-rab2 effector complex linking Golgi structure to membrane traffic. *J Cell Biol* **155**, 877-883 (2001).
57. Klausner, R. D., Donaldson, J. G. & Lippincott-Schwartz, J. Brefeldin A: insights into the control of membrane traffic and organelle structure. *J Cell Biol* **116**, 1071-1080 (1992).
58. http://www.ebi.ac.uk/Tools/msa/clustalo/
59. http://www.ebi.ac.uk/Tools/msa/muscle/
60. http://www.ebi.ac.uk/Tools/msa/tcoffee/
61. http://www.uniprot.org
62. http://topcons.cbr.su.se
63. http://crispr.mit.edu/
64. http://biogps.org/#goto=genereport&id=215160
65. Terns, M. P. & Terns, R. M. CRISPR-based adaptive immune systems. Curr Opin Microbiol 14, 321-327 (2011).

7. Supplemantary Information

Figure S1 Map of gRNA basic plasmid

Dr. Moisés Mallo
Instituto Gulbenkian de Ciência
Rua da Quinta Grande, 6
2780-156 Oeiras
Portugal
Email: mallo@igc.gulbenkian.pt

TYPE:
BOX:
POSITION:

Made by: MOISES MALLO
Date: 7-10-2013

Plasmid Name: g RNA basic

Description: The sequence containing the lead RNA for CRISPR, cloned into the PstI/BamHI sites of pUTB7. Then the seed RNA can be cloned into the BbsI site

Size:
Vector: ~ 1.5 KS
Insert:

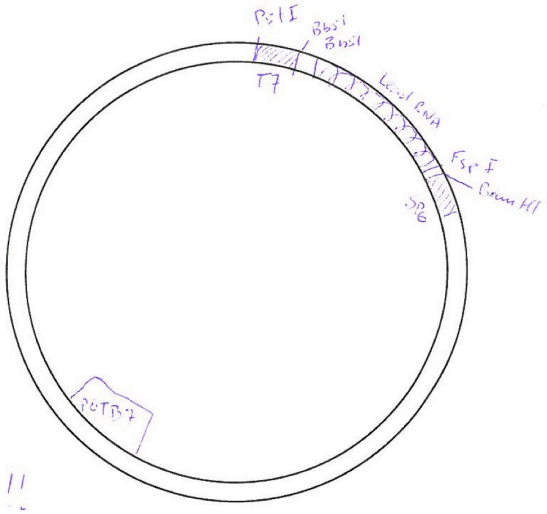

Resistance = CHLORAMFENICOL II

```
PstI      T7 promoter          BbsI    BbsI
CTGCAGTAATACGACTCACTATAGGGacGTCTTCGAGAAGACctGTTTTAGAGCTAGAAATAGCAAGTTAAAATAAGGCTAGTCCGTTA
||||||||||||||||||||||||||||||||||||||||||||||||||||||||||||||||||||||||||||||||||||||||||
GACGTCATTATGCTGAGTGATATCCCtgCAGAAGCTCTTCTGgaCAAAATCTCGATCTTTATCGTTCAATTTTATTCCGATCAGGCAAT

                                  FspI BamHI
TCAACTTGAAAAAGTGGCACCGAGTCGGTGCGCAGGATCC
|||||||||||||||||||||||||||||||||||||||
AGTTGAACTTTTTCACCGTGGCTCAGCCACGCGTCCTAGG

General structure of gRNAs

AGGGNNNNNNNNNNNNNNNNNNN
    NNNNNNNNNNNNNNNNNNNNCAAA                N= 20 nucleotides
```

To use it, desing primers with the structure shown above, clone into the BbsI site and confirm by sequencing with SP6. Then cut with FspI and transcribe with T7

Abbreviation for following tables:

G, Golgi apparatus; N, nucleus; C, cytoplasm; Ex, extracellular; M, membrane; Mi, mitochondria; IC, intermediate compartment between ER and Golgi; CM, cell membrane; NM, nucleus membrane; A, autophagosome; E, endosome; L, lysosome; Ph, phagosome; SP, spindle pole; P, peroxisome; Me, melanosome

Table 1 Unique RHBDD2 hits in first IP (with crosslinker)

First IP Accession	Protein name	#Peptides with crosslinker RHBDD2	TMD	localization	function
Q7RTS9	Dymeclin	1	6	G; C	Golgi organization; bone development
Q08378	Golgin subfamily A member 3 (golgin-160)	2	0	G; C	Golgi organization
Q15643	Thyroid receptor-interacting protein 11	2	0	G; C	Golgi organization; enhances THRB-modulated transcription
Q8WTW3	Conserved oligomeric Golgi complex subunit 1	1	0	G	Golgi organization; intra-Golgi transport
Q14746	Conserved oligomeric Golgi complex subunit 2	1	0	G	Golgi organization; intra-Golgi transport
Q9Y2V7	Conserved oligomeric Golgi complex subunit 6	1	0	G	Golgi organization; intra-Golgi transport
Q8TBA6	Golgin subfamily A member 5 (golgin-84)	13	1	G	Golgi organization; intra-Golgi transport
Q9H2G9	Golgin-45	3	0	G	Golgi organization; anterograde transport
P20340	Ras-related protein Rab-6A	1	0	Golgi	Golgi organization; Golgi-to-ER retrograde transport; endosome-to-Golgi retrograde transport
Q15363	Transmembrane emp24 domain-containing protein 2	1	2	G; ER; IC	Golgi organization; COPI and COPII dependent transport; Golgi-to-plasma membrane transport
O95159	Zinc finger protein-like 1	1	1	G	Golgi organization; interacts with GM130; ER-to-Golgi transport
Q9H8Y8	Golgi reassembly-stacking protein 2	2	0	G	Golgi organization; intracellular transport; lipid-anchor
Q9H4A6	Golgi phosphoprotein 3	1	1	G; Mi	Golgi organization; Golgi-to-plasma membrane transport; Localization of Golgi enzyme
Q9BQQ3	Golgi reassembly-stacking protein 1	1	0	G	Golgi organization; interacte with GM130, mediate docking of transport vesicles
Q96L58	Beta-1,3-galactosyltransferase 6	1	1	G	glycosylation; Beta-1,4-galactosyltransferase
Q9UBV7	Beta-1,4-galactosyltransferase 7	1	1	G	glycosylation; Beta-1,4-galactosyltransferase
Q8IZ52	Chondroitin sulfate synthase 2	1	1	G	glycosylation; metal binding transferase
O75063	Glycosaminoglycan xylosylkinase	1	1	G	glycosylation; regulate the amount of mature GAG (sulfated glycosaminoglycans) chains
O60476	Mannosyl-oligosaccharide 1,2-alpha-mannosidase IB	1	2	G	glycosylation; Asn-linked oligosaccharides
Q10471	Polypeptide N-acetylgalactosaminyltransferase 2	1	1	G	glycosylation; O-linked oligosaccharide biosynthesis
Q6P996	Pyridoxal-dependent decarboxylase domain-containing protein 1	1	0	G	glycosylation; carboxy-lyase activity
Q8WVQ1	Soluble calcium-activated nucleotidase 1	1	1	ER; G	glycosylation; calcium-dependent nucleotidase with a preference for UDP
Q12893	Transmembrane protein 115	1	6	G	glycosylation; Golgi-to-ER retrograde transport
Q7Z392	Trafficking protein particle complex subunit 11	1	0	G	ER-to-Golgi transport
O43617	Trafficking protein particle complex subunit 3	2	1	ER; G	ER-to-Golgi transport
Q8IUR0	Trafficking protein particle complex subunit 5	1	1	ER; G	ER-to-Golgi transport
Q8TD16	Protein bicaudal D homolog 2	1	0	G; C	COPI independent Golgi-to-ER retrograde transport
O95249	Golgi SNAP receptor complex member 1	2	1	G	intra-Golgi; ER-to-Golgi transport; belongs to t-SNAREs
Q96JA3	Pleckstrin homology domain-containing family A member 8	1	0	G; C	Golgi-to-plasma membrane transport
Q9P2W9	Syntaxin-18	1	1	ER; G	Golgi-to-ER retrograde transport
P82094	TATA element modulatory factor	3	0	G; C; N	RAB6-dependent retrograde transport (Golgi-to-ER and endosome-to-Golgi retrograde transport)
Q5VIR6	Vacuolar protein sorting-associated protein 53 homolog	1	0	G; E	endosome-to-trans-Golgi transport; endocytic recycling
Q9H4A5	Golgi phosphoprotein 3-like	1	1	G	antagonize Golgi-to-plasma membrane transport
Q9NZ52	ADP-ribosylation factor-binding protein GGA3	1	0	G	protein sorting
P98194	Calcium-transporting ATPase type 2C member 1	3	10	G	magnesium-dependent ATPase activity coupled with the transport of calcium
Q92896	Golgi apparatus protein 1	2	2	G	binds fibroblast growth factor and E-selectin
Q02818	Nucleobindin-1	2	1	G; C	calcium homeostasis of Golgi
Q8IUH4	Palmitoyltransferase ZDHHC13	1	6	G	magnesium transport; palmitoyltransferase for HD and GAD2
Q9BZG1	Ras-related protein Rab-34	1	0	G; Ph; C	localization of lysosomes; maturation of phagosomes; protein transport
Q8NFA0	Ubiquitin carboxyl-terminal hydrolase 32	3	0	G; M	ubiquitination
Q8TAD4	Zinc transporter 5	2	16	G	zinc transporter that transports zinc into Golgi lumens
Q92538	Golgi-specific brefeldin A-resistance guanine nucleotide exchange factor 1	3	1	G; IC	Golgi organization; COPI dependent retrograde transport
Q12907	Vesicular integral-membrane protein VIP36	1	2	G; ER; IC	glycosylation; transport and sorting of glycoproteins; interacts with glycans
Q96KG9	N-terminal kinase-like protein	1	0	G; IC; C	COPI dependent retrograde transport
O95486	Protein transport protein Sec24A	8	0	G; ER; IC	COPII dependent anterograde transport
O95487	Protein transport protein Sec24B	7	0	G; ER; IC	COPII dependent anterograde transport
O94855	Protein transport protein Sec24D	1	0	G; ER; IC	COPII dependent anterograde transport
P32019	Type II inositol 1,4,5-trisphosphate 5-phosphatase	2	0	G; C; IC	metal ion binding; dephosphorylation
Q96RQ1	Endoplasmic reticulum-Golgi intermediate compartment protein 2	1	2	IC; N	transport between ER and Golgi
Q5VYK3	Proteasome-associated protein ECM29 homolog	1	0	ER; IC	ERAD; binds compartment specific proteins, may couple the proteasome to different compartments
P55735	Protein SEC13 homolog	1	0	ER; IC	COPII dependent anterograde transport
Q8WVT3	Trafficking protein particle complex subunit 12	1	1	IC	ER-to-Golgi transport
Q6DD88	Atlastin-3	1	2	ER	GTPase activity; ER organization
Q9UKM7	Endoplasmic reticulum mannosyl-oligosaccharide 1,2-alpha-mannosidase	1	1	ER	glycosylation; glycoprotein quality control
Q96IW7	Vesicle-trafficking protein SEC22a	2	4	ER	transport between ER and Golgi
P62913	60S ribosomal protein L11	1	0	N	rRNA maturation; 60S ribosomal subunits formation; Promotes nucleolar location of PML
Q9BPX3	Condensin complex subunit 3	1	1	N	chromosome assembly and segregation during cell division
Q99829	Copine-1	1	0	N; C	membrane traffick
Q9Y6G9	Cytoplasmic dynein 1 light intermediate chain 1	1	0	N; C	microtubule motor activity
P33992	DNA replication licensing factor MCM5	1	0	N	APTase coupled with DNA replication, initiation and elongation
P29692	Elongation factor 1-delta	1	0	N	activate transcription factor binding; direct DNA-binding at HSE
P26641	Elongation factor 1-gamma	1	1	N; C; E; M	probably anchor the complex to other cellular components
Q00839	Heterogeneous nuclear ribonucleoprotein U	1	0	N; C; CM	promotes MYC mRNA stabilization; the circadian regulation of the core clock component
Q92830	Histone acetyltransferase KAT2A	1	0	N	promote transcriptional activation
P39880	Homeobox protein cut-like 1	2	0	N	regulates mammalian development
Q9BZD4	Kinetochore protein Nuf2	1	0	N	chromosome segregation and spindle checkpoint activity
Q03252	Lamin-B2	2	0	NM	components of inner nuclear membrane
Q9BV20	Methylthioribose-1-phosphate isomerase	1	1	N; C	Catalyzes the interconversion of MTR-1-P into MTRu-1-P; promotes cell invasion
O95248	Myotubularin-related protein 5	1	2	N	phosphatase regulator activity; GTPase activity
Q9Y217	Myotubularin-related protein 6	4	0	N	Phosphatase that acts on lipids with a phosphoinositol headgroup
O00308	NEDD4-like E3 ubiquitin-protein ligase WWP2	1	0	N	ubiquitination
Q8N1F7	Nuclear pore complex protein Nup93	6	2	N	plays a role in the nuclear pore complex assembly
Q6DKJ4	Nucleoredoxin	1	0	C; N	regulator of the Wnt signaling pathway
P11171	Protein 4.1	1	0	C; N	major structural element of the membrane skeleton
Q69YN4	Protein virilizer homolog	1	0	N	mRNA splicing regulation
Q7L7V1	Putative pre-mRNA-splicing factor ATP-dependent RNA helicase DHX32	1	0	N; Mi	ATP binding
Q9Y3I0	tRNA-splicing ligase RtcB homolog	1	0	N; C	joins spliced tRNA halves to mature-sized tRNAs; act as an RNA ligase
Q6PI48	Aspartate--tRNA ligase, mitochondrial	1	0	Mi	aspartate-tRNA(Asn) ligase activity
Q9UJS0	Calcium-binding mitochondrial carrier protein Aralar2	1	0	Mi	calcium binding; transporter activity
P56556	NADH dehydrogenase [ubiquinone] 1 alpha subcomplex subunit 6	1	0	Mi	functions in respiratory chain
Q9H974	Queuine tRNA-ribosyltransferase subunit QTRTD1	1	0	C; Mi	interacts with QTRT1 to form an active queuine tRNA-ribosyltransferase
Q13637	Ras-related protein Rab-32	2	0	Mi; Ph	anchor specific protein to mitochondrion; maturation of phagosomes
O43464	Serine protease HTRA2, mitochondrial	1	1	Mi	proteolytic activity
Q9BWD1	Acetyl-CoA acetyltransferase	1	0	C	acetyl-CoA C-acetyltransferase activity
Q13085	Acetyl-CoA carboxylase 1	2	0	C	biotin carboxyl carrier protein; biotin carboxylase; carboxyltransferase
Q4L235	Acyl-CoA synthetase family member 4	1	0	?	fatty acid metabolism
Q9H4A4	Aminopeptidase B	1	0	Ex	exopeptidase
O96018	Amyloid beta A4 precursor protein-binding family A member 3	1	1	C	formation of beta-APP; inhibit activity of HIF1AN
Q6AI12	Ankyrin repeat domain-containing protein 40	2	0	?	?
Q9NZT1	Calmodulin-like protein 5	1	0	Ex	calcium binding
Q05193	Dynamin-1	1	0	C	microtubule-associated force-producing protein; GTPase activity; vesicular trafficking
Q96PU5	E3 ubiquitin-protein ligase NEDD4-like	1	0	C	ubiquitination
Q8IYI6	Exocyst complex component 8	1	0	C	docking of exocytic vesicles on plasma membrane
O00178	GTP-binding protein 1	1	0	C	promotes degradation of mRNA; GTPase activity
P27816	Microtubule-associated protein 4	1	0	C	promotes microtubule assembly
Q86UY6	N-alpha-acetyltransferase 40	1	0	?	acetylation
Q8NEB9	Phosphatidylinositol 3-kinase catalytic subunit type 3	1	0	A	multiple membrane trafficking pathways: autophagosome formation, endocytic trafficking
Q99570	Phosphoinositide 3-kinase regulatory subunit 4	1	0	A	multiple membrane trafficking pathways: autophagosome formation, endocytic trafficking
Q15102	Platelet-activating factor acetylhydrolase IB subunit gamma	1	0	C	catalytic subunit that plays an important role during the development of brain
Q2KHT3	Protein CLEC16A	2	3	E; L	regulates mitochondrial quality control
Q9NRY5	Protein FAM114A2	1	0	?	purine nucleotide binding
Q4ADV7	Protein RIC1 homolog	1	2	C	fusion of endosome-derived vesicles with the Golgi compartment
Q96GX2	Putative ataxin-7-like protein 3B	1	0	?	?
P08134	Rho-related GTP-binding protein RhoC	1	0	CM	myosin contractile ring formation; apical junction formation
P23921	Ribonucleoside-diphosphate reductase large subunit	1	0	C	provides the precursors necessary for DNA synthesis
Q9HD45	Transmembrane 9 superfamily member 3	1	10	M	?
Q92544	Transmembrane 9 superfamily member 4	1	10	M	?
Q8NBN3	Transmembrane protein 87A	1	8	M	?
Q96FW1	Ubiquitin thioesterase OTUB1	1	0	C	ubiquitination
Q8IYS2	Uncharacterized protein KIAA2013	1	2	M	?
Q9H270	Vacuolar protein sorting-associated protein 11 homolog	1	0	A; E; L; C	SNARE-mediated membrane fusion; vesicle-mediated protein trafficking
Q96RL7	Vacuolar protein sorting-associated protein 13A	1	0	C	post-Golgi transport
Q7Z7G8	Vacuolar protein sorting-associated protein 13B	2	0	?	sorting in post Golgi membrane traffic
Q5MNZ6	WD repeat domain phosphoinositide-interacting protein 3	3	0	C; A	autophagosome assembly
Q9HAD4	WD repeat-containing protein 41	2	0	L	?

Table 2 Unique RHBDD2 hits in second IP (with crosslinker)

Second IP Accession	Protein name	#Peptides with crosslinker RHBDD2	TMD	localization	function
Q08379	Golgin subfamily A member 2 (GM130)	9	0	G; SP	Golgi organization; spindle pole assembly; centrosome organization
Q08378	Golgin subfamily A member 3 (golgin-160)	2	0	G; C	Golgi organization
Q15643	Thyroid receptor-interacting protein 11	1	0	G; C	Golgi organization; enhances THRB-modulated transcription
Q9H8Y8	Golgi reassembly-stacking protein 2	3	0	G	Golgi organization; intracellular transport; lipid-anchor
Q8TBA6	Golgin subfamily A member 5 (golgin-84)	9	1	G	Golgi organization; intra-Golgi transport
Q9H2G9	Golgin-45	1	0	G	Golgi organization; anterograde transport
P20340	Ras-related protein Rab-6A	5	0	G	Golgi organization; Golgi-to-ER retrograde transport; endosome-to-Golgi retrograde transport
O95159	Zinc finger protein-like 1	3	1	G	Golgi organization; interacts with GM130; ER-to-Golgi transport
O14617	AP-3 complex subunit delta-1	1	0	G; C	post-Golgi transport; budding of vesicles from the Golgi membrane
O60763	General vesicular transport factor p115	7	0	G; C	intra-Golgi transport; docking of transport vesicles
Q9H4A5	Golgi phosphoprotein 3-like	2	1	G	antagonize Golgi-to-plasma membrane transport
O14653	Golgi SNAP receptor complex member 2	3	1	G	intra-Golgi transport
Q8IUH4	Palmitoyltransferase ZDHHC13	4	6	G	magnesium transport; palmitoyltransferase for HD and GAD2
Q8IUH5	Palmitoyltransferase ZDHHC17	3	6	G; C	involved in sorting or targeting proteins and initiating events of endocytosis; Mg2+ transport
Q13948	Protein CASP	3	1	G	intra-Golgi transport
P53992	Protein transport protein Sec24C	12	0	G; ER; C	COPII dependent anterograde transport
P61106	Ras-related protein Rab-14	1	0	G; E; Ph	transport between Golgi and endosomes
P82094	TATA element modulatory factor	1	0	G; C; N	RAB6-dependent retrograde transport (Golgi-to-ER and endosome-to-Golgi retrograde transport)
Q8TAD4	Zinc transporter 5	3	16	G	zinc transporter that transports zinc into Golgi lumens
Q10469	Alpha-1,6-mannosyl-glycoprotein 2-beta-N-acetylglucosaminyltransferase	2	0	G	glycosylation; conversion of ligo-mannose to complex N-glycans
Q6P996	Pyridoxal-dependent decarboxylase domain-containing protein 1	4	0	G	glycosylation; carboxy-lyase activity
Q8WVQ1	Soluble calcium-activated nucleotidase 1	1	1	ER; G	glycosylation; calcium-dependent nucleotidase with a preference for UDP
P78381	UDP-galactose translocator	1	8	G	glycosylation; transports nucleotide sugars from the cytosol into Golgi
Q9BXS5	AP-1 complex subunit mu-1	2	0	G; C	protein sorting in trans-Golgi and endosomes
P01111	GTPase Nras	1	0	G; CM	binds GDP/GTP and possess intrinsic GTPase activity
O15027	Protein transport protein Sec16A	1	0	ER; G	defines endoplasmic reticulum exit sites; ER-to-Golgi transport; transitional ER organization
Q92974	Rho guanine nucleotide exchange factor 2	2	0	G; C	activates Rho-GTPases by promoting the exchange of GDP for GTP
Q6NTF9	Rhomboid domain-containing protein 2	1	6	G	RHBDD2
Q9Y5Z9	UbiA prenyltransferase domain-containing protein 1	1	9	ER; G; Mi; C; N	mediates the formation of menaquinone-4 (MK-4) and coenzyme Q10
Q9NZC7	WW domain-containing oxidoreductase	1	0	C; G; Mi; N	a tumor suppressor and plays a role in apoptosis; bone development
Q9NRZ7	1-acyl-sn-glycerol-3-phosphate acyltransferase gamma	1	5	ER	acyl donor for fatty acid
Q6IAN0	Dehydrogenase/reductase SDR family member 7B	1	2	ER	oxidoreductase activity
Q9UKM7	Endoplasmic reticulum mannosyl-oligosaccharide 1,2-alpha-mannosidase	1	1	ER	glycosylation; glycoprotein quality control
Q9BS26	Endoplasmic reticulum resident protein 44	1	0	ER	mediates thiol-dependent retention
O95864	Fatty acid desaturase 2	2	4	ER	lipid metabolic pathway
O00165	HCLS1-associated protein X-1	1	0	Mi; ER; N; C	involved in cell survival and migration; endocytosis pathway; regulates calcium pools
Q9Y5Y5	Peroxisomal membrane protein PEX16	1	0	ER; P	peroxisome membrane biogenesis; peroxisome assembly
P55084	Trifunctional enzyme subunit beta, mitochondrial	3	0	Mi; ER	lipid metabolism; fatty acid beta-oxidation pathway
Q96IW7	Vesicle-trafficking protein SEC22a	2	4	ER	transport between ER and Golgi
Q96RQ1	Endoplasmic reticulum-Golgi intermediate compartment protein 2	1	2	IC; N	transport between ER and Golgi
O95486	Protein transport protein Sec24A	2	0	G; ER; IC	COPII dependent anterograde transport
O95487	Protein transport protein Sec24B	6	0	G; ER; IC	COPII dependent anterograde transport
O94855	Protein transport protein Sec24D	2	0	G; ER; IC	COPII dependent anterograde transport
P61019	Ras-related protein Rab-2A	4	0	ER; G; IC	ER-to-Golgi transport
Q9Y6Y8	SEC23-interacting protein	4	0	ER; IC	organization of endoplasmic reticulum exit sites
Q13190	Syntaxin-5	2	1	G; IC	Golgi organization; ER-to-Golgi transport
Q9Y3Q3	Transmembrane emp24 domain-containing protein 3	1	1	G; ER; IC	vesicular protein trafficking
P32019	Type II inositol 1,4,5-trisphosphate 5-phosphatase	5	0	G; C; IC	metal ion binding; dephosphorylation
Q9Y676	28S ribosomal protein S18b, mitochondrial	2	0	Mi	mitochondrial translation; structural constituent of ribosome
Q9NX20	39S ribosomal protein L16, mitochondrial	1	0	Mi	component of the large subunit of mitochondrial ribosome
Q53H12	Acylglycerol kinase, mitochondrial	1	0	Mi	involved in the pathway glycerolipid metabolism
P30566	Adenylosuccinate lyase	1	0	C; Mi	catalyzes two non-sequential steps in de novo AMP synthesis
P61221	ATP-binding cassette sub-family E member 1	2	0	C; Mi	interact with Rnase L; regulate mRNA turnover; chaperone for post-translational events
Q9UG63	ATP-binding cassette sub-family F member 2	1	0	Mi; M	ATPase activity; transporter activity
Q9H078	Caseinolytic peptidase B protein homolog	1	0	Mi	regulate ATPase and be related to secretion/protein trafficking process
P49916	DNA ligase 3	1	0	Mi; N	correct defective DNA strand-break repair and sister chromatid exchange
Q9HAV7	GrpE protein homolog 1, mitochondrial	1	0	Mi	PAM complex; translocation of transit peptide-containing proteins
Q9Y241	HIG1 domain family member 1A, mitochondrial	1	2	Mi	catalyzes the reduction of oxygen to water in the mitochondrial respiratory
O14925	Mitochondrial import inner membrane translocase subunit Tim23	2	3	Mi	mediates the translocation of transit peptide-containing proteins
Q3ZCQ8	Mitochondrial import inner membrane translocase subunit TIM50	2	1	Mi	mediates the translocation of transit peptide-containing proteins
Q9BT17	Mitochondrial ribosome-associated GTPase 1	1	0	Mi	regulates mitochondrial ribosome assembly and translational activity; GTPase activity
P56556	NADH dehydrogenase [ubiquinone] 1 alpha subcomplex subunit 6	2	0	Mi	functions in respiratory chain
P49821	NADH dehydrogenase [ubiquinone] flavoprotein 1, mitochondrial	1	1	Mi	core subunit of the mitochondrial membrane respiratory chain NADH dehydrogenase
P19404	NADH dehydrogenase [ubiquinone] flavoprotein 2, mitochondrial	1	0	Mi	core subunit of the mitochondrial membrane respiratory chain NADH dehydrogenase
O75251	NADH dehydrogenase [ubiquinone] iron-sulfur protein 7, mitochondrial	1	0	Mi	core subunit of the mitochondrial membrane respiratory chain NADH dehydrogenase
Q96I59	Probable asparagine--tRNA ligase, mitochondrial	1	0	Mi	asparagine-tRNA ligase activity; ATP binding
P31040	Succinate dehydrogenase [ubiquinone] flavoprotein subunit, mitochondrial	2	0	Mi	involved in mitochondrial electron transport chain; tumor suppressor
P62888	60S ribosomal protein L30	2	0	C; Ex; N; M	structural constituent of ribosome
O14646	Chromodomain-helicase-DNA-binding protein 1	2	0	N; C	regulates polymerase I and II transcription; regulates DNA replication;
P11802	Cyclin-dependent kinase 4	1	0	C; N; M	phosphorylates and inhibits members of the retinoblastoma protein family
P00374	Dihydrofolate reductase	1	0	C; N	folate metabolism; contributes to mitochondrial thymidylate biosynthesis pathway
P26358	DNA (cytosine-5)-methyltransferase 1	3	0	N	preferentially methylates hemimethylated DNA
P18858	DNA ligase 1	2	0	N	seals nicks in double-stranded DNA during DNA replication, DNA recombination and DNA repair
P28340	DNA polymerase delta catalytic subunit	1	0	N	DNA synthesis and an exonucleolytic activity
Q13642	Four and a half LIM domains protein 1	1	0	C; N	involved in muscle development or hypertrophy
Q9BQ67	Glutamate-rich WD repeat-containing protein 1	1	0	N	poly(A) RNA binding
Q9NZI8	Insulin-like growth factor 2 mRNA-binding protein 1	3	0	N; C	mRNA binding; translation regulator activity
Q15046	Lysine--tRNA ligase	2	0	C; N; CM	Catalyzes the specific attachment of an amino acid to its cognate tRNA
Q9UKD2	mRNA turnover protein 4 homolog	3	0	N; C	ribosome assembly
Q9Y217	Myotubularin-related protein 6	1	0	N	Phosphatase that acts on lipids with a phosphoinositol headgroup
O00308	NEDD4-like E3 ubiquitin-protein ligase WWP2	2	0	N	ubiquitination
Q8N1F7	Nuclear pore complex protein Nup93	4	2	N	plays a role in the nuclear pore complex assembly
Q6DKJ4	Nucleoredoxin	1	0	C; N	regulator of the Wnt signaling pathway
O75182	Paired amphipathic helix protein Sin3b	1	0	N	acts as a transcriptional repressor
Q8IYS1	Peptidase M20 domain-containing protein 2	1	0	Ex; N	enzyme activity
O00541	Pescadillo homolog	1	0	N	maturation of ribosomeal RNAs and formation of the 60S ribosome
O15162	Phospholipid scramblase 1	3	1	N; M	mediates accelerated bidirectional transbilayer migration; fibrin clot formation
Q9UQ80	Proliferation-associated protein 2G4	1	0	C; N	a ERBB3-regulated signal transduction pathway; ribosome assembly
P46087	Putative ribosomal RNA methyltransferase NOP2	2	0	N	methylates the C5 position of cytosine 4447 in 28S rRNA
P56182	Ribosomal RNA processing protein 1 homolog A	1	0	N	generation of 28S rRNA
Q5H9R7	Serine/threonine-protein phosphatase 6 regulatory subunit 3	1	0	C; N	a scaffolding PP6 subunit; maintains immune self-tolerance
P62314	Small nuclear ribonucleoprotein Sm D1	1	0	C; N	splicing of cellular pre-mRNA
P23246	Splicing factor, proline- and glutamine-rich	1	0	C; N	DNA- and RNA binding protein, involved in several nuclear processes
Q6ZRP7	Sulfhydryl oxidase 2	1	1	NM; CM	catalyzes the oxidation of sulfhydryl groups in peptide and protein
P42285	Superkiller viralicidic activity 2-like 2	1	0	N	involved in pre-mRNA splicing
Q9BUZ4	TNF receptor-associated factor 4	1	0	N; C	links members of TNFR family to different signaling pathways
P61088	Ubiquitin-conjugating enzyme E2 N	2	0	N; C	catalyzes the synthesis of polyubiquitin chains; acts with E3 ligases
Q15008	26S proteasome non-ATPase regulatory subunit 6	1	0	C	ATPase for ubiquitination
P51857	3-oxo-5-beta-steroid 4-dehydrogenase	1	0	C	catalyzes the reduction of substrate concentration
P63220	40S ribosomal protein S21	1	0	C	structural constituent of ribosome
P63173	60S ribosomal protein L38	1	0	C	structural constituent of ribosome
Q9BWD1	Acetyl-CoA acetyltransferase, cytosolic	2	0	C	acetyl-CoA C-acetyltransferase activity
P59998	Actin-related protein 2/3 complex subunit 4	1	0	C	regulation of actin polymerization; formation of branched actin networks
Q9NVJ2	ADP-ribosylation factor-like protein 8B	2	0	C; E	plays a role in lysosome motility and chromosome segregation
O96018	Amyloid beta A4 precursor protein-binding family A member 3	1	0	C	formation of beta-APP; enhance the activity of HIF1A in macrophages
P04114	Apolipoprotein B-100	1	0	C	constituent of chylomicrons (apo B-48), LDL (apo B-100) and VLDL (apo B-100); secreted protein
P05089	Arginase-1	1	0	C	synthesizes L-ornithine and urea from L-arginine
Q96PU5	E3 ubiquitin-protein ligase NEDD4-like	2	0	C	ubiquitination
Q9HC35	Echinoderm microtubule-associated protein-like 4	1	0	C	may modify the assembly dynamics of microtubules
P05198	Eukaryotic translation initiation factor 2 subunit 1	1	0	C	forms a ternary complex with GTP and initiator tRNA

O00303	Eukaryotic translation initiation factor 3 subunit F	1	0	C	component of eIF-3 complex, which is required for the initiation of protein synthesis
Q92990	Glomulin	1	0	C	membrane anchoring protein; development of the vasculature
Q06210	Glutamine--fructose-6-phosphate aminotransferase [isomerizing] 1	1	0	C; Ex	controls flux of glucose into the hexosamine pathway; regulate precursors for glycosylation
P49915	GMP synthase [glutamine-hydrolyzing]	1	0	C	involved in the de novo synthesis of guanine nucleotides
Q86YM7	Homer protein homolog 1	1	0	C	postsynaptic density scaffolding protein;
Q6YN16	Hydroxysteroid dehydrogenase-like protein 2	1	0	P	no steroid dehydrogenase activity
Q15181	Inorganic pyrophosphatase	2	0	C	inorganic diphosphatase activity
Q9H9A6	Leucine-rich repeat-containing protein 40	1	0	M	?
Q9H1A3	Methyltransferase-like protein 9	1	1	?	?
P60660	Myosin light polypeptide 6	1	0	C; Ex; M	regulatory light chain of myosin; does not bind calcium
Q96QG7	Myotubularin-related protein 9	1	0	C	pseudophosphatase
O43808	Peroxisomal membrane protein PMP34	1	5	P; C	peroxisomal transporter for multiple cofactors
P00558	Phosphoglycerate kinase 1	1	0	C	a glycolytic enzyme; a polymerase alpha cofactor protein
O15067	Phosphoribosylformylglycinamidine synthase	1	0	C	purines biosynthetic pathway
Q8WWH5	Probable tRNA pseudouridine synthase 1	1	0	?	synthesis of pseudouridine from uracil in transfer RNAs
Q6ZRT6	Proline-rich protein 23B	1	0	?	?
O60879	Protein diaphanous homolog 2	1	0	C; E	oogenesis; regulates endosome dynamics and motility of early endosomes
Q9UBU6	Protein FAM8A1	1	3	M	autosomal highly conserved protein
Q8N8P6	Putative uncharacterized protein FLJ39060	1	0	?	?
Q96C36	Pyrroline-5-carboxylate reductase 2	1	0	C	housekeeping enzyme that catalyzes the last step in proline biosynthesis
Q15042	Rab3 GTPase-activating protein catalytic subunit	1	0	C	GTPase that has specificity for Rab3 subfamily
Q14964	Ras-related protein Rab-39A	2	0	CM; Ph; L	maturation and acidification of phagosomes
P62070	Ras-related protein R-Ras2	1	0	C	GTPase activity; transduces growth inhibitory signals across cell membrane
Q92546	Retrograde Golgi transport protein RGP1 homolog	2	0	C; M	a GEF that activates Rab6A; fusion of endosome-derived vesicles with Golgi apparatus
P08134	Rho-related GTP-binding protein RhoC	1	0	CM	myosin contractile ring formation; apical junction formation
P60891	Ribose-phosphate pyrophosphokinase 1	1	0	C	catalyzes the synthesis of PRPP that is essential for nucleotide synthesis
P49458	Signal recognition particle 9 kDa protein	1	0	C	targets secretory proteins to ER
P50225	Sulfotransferase 1A1	1	0	C	catalyzes the sulfate conjugation of catecholamines, phenolic drugs and neurotransmitters
Q14232	Translation initiation factor eIF-2B subunit alpha	1	0	C; CM; M	catalyzes the exchange of eukaryotic initiation factor 2-bound GDP for GTP
Q99805	Transmembrane 9 superfamily member 2	1	9	E	functions as a channel or small molecule transporter.
Q92544	Transmembrane 9 superfamily member 4	1	10	M	?
P22102	Trifunctional purine biosynthetic protein adenosine-3	4	0	C; Ex	synthesizes glycinamide
P23258	Tubulin gamma-1 chain	1	0	Centrosome	major constituent of microtubules
Q9HA47	Uridine-cytidine kinase 1	1	0	C	phosphorylates uridine and cytidine to uridine monophosphate and cytidine monophosphate
Q96A05	V-type proton ATPase subunit E 2	1	0	C	ATPase that is essential for assembly or catalytic function
Q5MNZ6	WD repeat domain phosphoinositide-interacting protein 3	4	0	C; A	autophagosome assembly
Q92536	Y+L amino acid transporter 2	1	12	CM	involved in the sodium-independent uptake of amino acids

Table 3 Unique R85H hits in second IP (with crosslinker)

Second IP Accession	Protein name	#Peptides with crosslinker R85H	TMD	localization	function
Q08379	Golgin subfamily A member 2 (GM130)	7	0	G; SP	Golgi organization; spindle pole assembly; centrosome organization
Q08378	Golgin subfamily A member 3 (golgin-160)	2	0	G; C	Golgi organization
Q9BSR8	Protein YIPF4	1	5	G	Golgi organization
Q15643	Thyroid receptor-interacting protein 11	4	0	G; C	Golgi organization; enhances THRB-modulated transcription
Q9H8Y8	Golgi reassembly-stacking protein 2	3	0	G	Golgi organization; intracellular transport; lipid-anchor
Q8TBA6	Golgin subfamily A member 5 (golgin-84)	9	1	G	Golgi organization; intra-Golgi transport
Q9H2G9	Golgin-45	1	0	G	Golgi organization; anterograde transport
P20340	Ras-related protein Rab-6A	3	0	G	Golgi organization; Golgi-to-ER retrograde transport; endosome-to-Golgi retrograde transport
O60763	General vesicular transport factor p115	5	0	G; C	intra-Golgi transport; docking of transport vesicles
O14653	Golgi SNAP receptor complex member 2	3	1	G	intra-Golgi transport
Q8IUH4	Palmitoyltransferase ZDHHC13	3	6	G	magnesium transport; palmitoyltransferase for HD and GAD2
Q8IUH5	Palmitoyltransferase ZDHHC17	3	6	G; C	involved in sorting or targeting proteins and initiating events of endocytosis; Mg2+ transport
Q13948	Protein CASP	2	1	G	intra-Golgi transport
P53992	Protein transport protein Sec24C	10	0	G; ER; C	COPII dependent anterograde transport
P61106	Ras-related protein Rab-14	2	0	G; E; Ph	transport between Golgi and endosomes
Q9Y3E0	Vesicle transport protein GOT1B	1	4	G	ER-to-Golgi transport; fusion of ER-derived transport vesicles with Golgi
Q8TAD4	Zinc transporter 5	2	16	G	zinc transporter that transports zinc into Golgi lumens
Q9BXS5	AP-1 complex subunit mu-1	1	0	G; C	protein sorting in trans-Golgi and endosomes
Q9NZC7	WW domain-containing oxidoreductase	1	0	C; G; Mi; N	a tumor suppressor and plays a role in apoptosis; bone development
Q10469	Alpha-1,6-mannosyl-glycoprotein 2-beta-N-acetylglucosaminyltransferase	1	0	G	glycosylation; conversion of ligo-mannose to complex N-glycans
Q96L58	Beta-1,3-galactosyltransferase 6	1	1	G	glycosylation; Beta-1,4-galactosyltransferase
Q6P996	Pyridoxal-dependent decarboxylase domain-containing protein 1	1	0	G	glycosylation; carboxy-lyase activity
P78381	UDP-galactose translocator	1	8	G	glycosylation; transports nucleotide sugars from the cytosol into Golgi
P55084	Trifunctional enzyme subunit beta, mitochondrial	1	0	Mi; ER	lipid metabolism; fatty acid beta-oxidation pathway
O95486	Protein transport protein Sec24A	1	0	G; ER; IC	COPII dependent anterograde transport
O95487	Protein transport protein Sec24B	3	0	G; ER; IC	COPII dependent anterograde transport
O94855	Protein transport protein Sec24D	2	0	G; ER; IC	COPII dependent anterograde transport
P61019	Ras-related protein Rab-2A	3	0	ER; G; IC	ER-to-Golgi transport
Q9Y6Y8	SEC23-interacting protein	2	0	ER; IC	organization of endoplasmic reticulum exit sites
Q13190	Syntaxin-5	2	1	G; IC	Golgi organization; ER-to-Golgi transport
P46783	40S ribosomal protein S10	1	0	C; N	component of the 40S ribosomal subunit
P62888	60S ribosomal protein L30	1	0	C; Ex; N; M	structural constituent of ribosome
Q9NRL2	Bromodomain adjacent to zinc finger domain protein 1A	1	0	N	component of the ACF complex; facilitate the DNA replication process; transcription repression
P28340	DNA polymerase delta catalytic subunit	1	0	N	DNA synthesis and an exonucleolytic activity
P19474	E3 ubiquitin-protein ligase TRIM21	2	0	C; N	ubiquitination
Q13642	Four and a half LIM domains protein 1	1	0	C; N	involved in muscle development or hypertrophy
Q9BQ67	Glutamate-rich WD repeat-containing protein 1	1	0	N	poly(A) RNA binding
Q9NVN8	Guanine nucleotide-binding protein-like 3-like protein	1	0	N	prevents ubiquitination; processing of ribosomal pre-rRNA
Q99729	Heterogeneous nuclear ribonucleoprotein A/B	1	0	N; C	binds single-stranded RNA
Q14103	Heterogeneous nuclear ribonucleoprotein D0	2	0	N; C	RNA binding; mRNA turnover; telomere elongation; circadian regulation of translation
Q9Y2U8	Inner nuclear membrane protein Man1	1	2	N	a specific repressor of TGF-beta, activin, and BMP signaling
Q9NZI8	Insulin-like growth factor 2 mRNA-binding protein 1	2	0	N; C	mRNA binding; translation regulator activity
P40126	L-dopachrome tautomerase	1	1	Melanosome	regulates eumelanin and phaeomelanin levels.
Q9NU22	Midasin	3	0	N	nuclear chaperone required for maturation and nuclear export of pre-60S ribosome subunits
Q96T76	MMS19 nucleotide excision repair protein homolog	1	0	N; SP	mediates the incorporation of iron-sulfur cluster into apoproteins
Q9Y217	Myotubularin-related protein 6	3	0	N	Phosphatase that acts on lipids with a phosphoinositol headgroup
O75182	Paired amphipathic helix protein Sin3b	1	0	N	acts as a transcriptional repressor
Q8IYS1	Peptidase M20 domain-containing protein 2	1	0	Ex; N	enzyme activity
O15162	Phospholipid scramblase 1	2	1	N; M	mediates accelerated bidirectional transbilayer migration; fibrin clot formation
Q9UQ80	Proliferation-associated protein 2G4	1	0	C; N	a ERBB3-regulated signal transduction pathway; ribosome assembly
Q9BRX2	Protein pelota homolog	1	0	N; C	chromosome segregation; recognizes stalled ribosomes; triggers mRNA endonucleolytic cleavage
P46060	Ran GTPase-activating protein 1	1	0	C; N	GTPase activator for the nuclear Ras-related regulatory protein Ran
Q9H0N0	Ras-related protein Rab-6C	1	0	N; C	centrosome duplication
P56182	Ribosomal RNA processing protein 1 homolog A	1	0	N	generation of 28S rRNA
Q15019	Septin-2	1	0	C; Spindle	filament-forming cytoskeletal GTPase
Q5H9R7	Serine/threonine-protein phosphatase 6 regulatory subunit 3	1	0	C; N	a scaffolding PP6 subunit; maintains immune self-tolerance
P23246	Splicing factor, proline- and glutamine-rich	2	0	C; N	DNA- and RNA binding protein, involved in several nuclear processes
Q9NTJ3	Structural maintenance of chromosomes protein 4	1	0	C; N	conversion of interphase chromatin into mitotic-like condense chromosomes
Q96SB8	Structural maintenance of chromosomes protein 6	1	0	N	involved in DNA double-strand breaks by homologous recombination
Q6ZRP7	Sulfhydryl oxidase 2	1	1	NM; CM	catalyzes the oxidation of sulfhydryl groups in peptide and protein
Q9Y3I0	tRNA-splicing ligase RtcB homolog	1	0	N; C	joins spliced tRNA halves to mature-sized tRNAs; act as an RNA ligase
P23258	Tubulin gamma-1 chain	1	0	Centrosome	major constituent of microtubules
P07101	Tyrosine 3-monooxygenase	1	0	C; Mi; N	physiology of adrenergic neurons
P61088	Ubiquitin-conjugating enzyme E2 N	1	0	N; C	catalyzes the synthesis of polyubiquitin chains; acts with E3 ligases
Q53H12	Acylglycerol kinase, mitochondrial	1	0	Mi	involved in the pathway glycerolipid metabolism
P61221	ATP-binding cassette sub-family E member 1	1	0	C; Mi	interact with Rnase L; regulate mRNA turnover; chaperone for post-translational events
Q9H078	Caseinolytic peptidase B protein homolog	2	0	Mi	regulate ATPase and be related to secretion/protein trafficking process
P31930	Cytochrome b-c1 complex subunit 1, mitochondrial	1	0	Mi	ubiquitination; mitochondrial respiratory chain
P99999	Cytochrome c	1	0	Mi	electron carrier protein; plays a role in apoptosis
O60313	Dynamin-like 120 kDa protein, mitochondrial	1	0	Mi	mitochondrial fusion and regulation of apoptosis
Q3ZCQ8	Mitochondrial import inner membrane translocase subunit TIM50	1	1	Mi	mediates the translocation of transit peptide-containing proteins
P56556	NADH dehydrogenase [ubiquinone] 1 alpha subcomplex subunit 6	2	0	Mi	functions in respiratory chain
O75251	NADH dehydrogenase [ubiquinone] iron-sulfur protein 7, mitochondrial	1	0	Mi	core subunit of the mitochondrial membrane respiratory chain NADH dehydrogenase
Q15008	26S proteasome non-ATPase regulatory subunit 6	1	0	C	ATPase for ubiquitination
P05089	Arginase-1	1	0	C	synthesizes L-ornithine and urea from L-arginine
P35613	Basigin	1	1	CM	targets the monocarboxylate transporters SLC16A1, SLC16A3 and SLC16A8 to the plasma membrane
P07814	Bifunctional glutamate/proline--tRNA ligase	1	0	C	catalyzes the attachment of the cognate amino acid to the tRNA; component of the GAIT
Q9HC35	Echinoderm microtubule-associated protein-like 4	1	0	C	may modify the assembly dynamics of microtubules
P05198	Eukaryotic translation initiation factor 2 subunit 1	1	0	C	forms a ternary complex with GTP and initiator tRNA
P34932	Heat shock 70 kDa protein 4	1	0	C	ATP binding; chaperone-mediated protein complex assembly; response to UPR
Q9NZL4	Hsp70-binding protein 1	1	0	C	interferes with ubiquitination and inhibits chaperone-assisted degradation of immature CFTR
Q96FN5	Kinesin-like protein KIF12	1	0	C	ATP binding; microtubule motor activity
P11279	Lysosome-associated membrane glycoprotein 1	1	1	CM; E; L	a receptor for Lassa virus protein; implicated in tumor cell metastasis
Q6NT16	MFS-type transporter SLC18B1	1	12	M	transmembrane transport
Q8WUY8	N-acetyltransferase 14	1	2	M	binds the 5'-GGACTACAG-3' sequence of coproporphyrinogen oxidase promoter
P50897	Palmitoyl-protein thioesterase 1	1	0	L	removes thioester-linked fatty acyl groups during lysosomal degradation
Q9H5Z1	Probable ATP-dependent RNA helicase DHX35	1	0	C	involved in pre-mRNA splicing
O60610	Protein diaphanous homolog 1	2	0	C	assembly of F-actin structures
O60879	Protein diaphanous homolog 2	1	0	C; E	oogenesis; regulates endosome dynamics and motility of early endosomes
Q9UBU6	Protein FAM8A1	1	3	M	autosomal highly conserved protein
Q96AA3	Protein RFT1 homolog	1	12	M	glycosylation; N-linked oligosaccharide assembly; translocation of oligosaccharide
Q6PL24	Protein TMED8	1	0	M	transport
Q96C36	Pyrroline-5-carboxylate reductase 2	2	0	C	housekeeping enzyme that catalyzes the last step in proline biosynthesis
Q14964	Ras-related protein Rab-39A	3	0	CM; Ph; L	maturation and acidification of phagosomes
Q96E17	Ras-related protein Rab-3C	1	0	C	protein transport
P62070	Ras-related protein R-Ras2	1	0	C	GTPase activity; transduces growth inhibitory signals across cell membrane
P08134	Rho-related GTP-binding protein RhoC	1	0	CM	myosin contractile ring formation; apical junction formation
P31153	S-adenosylmethionine synthase isoform type-2	2	0	C	catalyzes the formation of S-adenosylmethionine from methionine and ATP
P02549	Spectrin alpha chain, erythrocytic 1	1	0	C	major constituent of the cytoskeletal network underlying the erythrocyte plasma membrane
P22102	Trifunctional purine biosynthetic protein adenosine-3	5	0	C; Ex	synthesizes glycinamide
Q5MNZ6	WD repeat domain phosphoinositide-interacting protein 3	2	0	C; A	autophagosome assembly

Table 4 Unique RHBDD2 hits in third IP (without crosslinker)

Third IP Accession	Protein name	#Peptides with crosslinker RHBDD2	TMD	localization	function
Q9H3P7	Golgi resident protein GCP60	1	0	G; Mi	Golgi organization; transport between ER and Golgi
O15027	Protein transport protein Sec16A	1	0	ER; G	defines endoplasmic reticulum exit sites; ER-to-Golgi transport; transitional ER organization
Q15436	Protein transport protein Sec23A	1	0	ER; G	COPII dependent anterograde transport
P53992	Protein transport protein Sec24C	1	0	G; ER; C	COPII dependent anterograde transport
Q8WVM8	Sec1 family domain-containing protein 1	1	0	C; ER; G	SNARE-pin assembly; Golgi-to-ER retrograde transport
Q5VIR6	Vacuolar protein sorting-associated protein 53 homolog	1	0	G; E	endosome to Golgi transport; lysosomal sorting; endocytic recycling
Q14697	Neutral alpha-glucosidase AB	1	1	G; ER	glycosylation; dleaves glucose residues from oligosaccharide precursor of immature glycoproteins
Q12904	Aminoacyl tRNA synthase complex-interacting multifunctional protein 1	2	0	N; C; ER; G	binds tRNA; inflammatory cytokine activity; regulates TGF-beta signaling; glucose homeostasis;
O95197	Reticulon-3	1	3	G; ER	involved in membrane trafficking; ER stress pathway
Q6NTF9	Rhomboid domain-containing protein 2	2	6	G	RHBDD2
P27797	Calreticulin	2	0	ER; C; Ex; CM	promotes folding, oligomeric assembly and quality control in the ER calreticulin/calnexin cycle
Q99942	E3 ubiquitin-protein ligase RNF5	1	3	ER; M; Mi	E2-dependent E3 ubiquitin-protein ligase activity
P30519	Heme oxygenase 2	1	1	ER	cleaves the heme ring at the alpha methene bridge to form biliverdin
P33121	Long-chain-fatty-acid--CoA ligase 1	1	2	Mi; ER	activates long-chain fatty acids for cellular lipids synthesis and degradation
O00264	Membrane-associated progesterone receptor component 1	1	1	ER	receptor for progesterone
Q969V3	Nicalin	2	1	ER	antagonizes Nodal signaling and subsequent organization of axial structures
P13667	Protein disulfide-isomerase A4	1	0	ER; Me	catalyzes the rearrangement of -S-S- bonds in proteins
P60468	Protein transport protein Sec61 subunit beta	1	1	ER	necessary for protein translocation in the endoplasmic reticulum
Q15293	Reticulocalbin-1	2	0	ER	regulates calcium-dependent activities in ER
O76094	Signal recognition particle subunit SRP72	1	0	C; ER	targets secretory proteins to the rough endoplasmic reticulum membrane
Q8N0U8	Vitamin K epoxide reductase complex subunit 1-like protein 1	1	4	ER	involved in vitamin K metabolism
Q9P003	Protein cornichon homolog 4	1	3	ER; IC; M	COPII dependent anterograde transport
O00231	26S proteasome non-ATPase regulatory subunit 11	1	0	N; C	involved in the ATP-dependent degradation of ubiquitinated proteins
O00487	26S proteasome non-ATPase regulatory subunit 14	1	0	C; Ex; N	involved in the ATP-dependent degradation of ubiquitinated proteins
O43427	Acidic fibroblast growth factor intracellular-binding protein	1	0	N; M	involved in mitogenic function of FGF1
P08758	Annexin A5	2	0	C; N	acts as an indirect inhibitor of the thromboplastin-specific complex
O95400	CD2 antigen cytoplasmic tail-binding protein 2	1	0	C; N	involved in pre-mRNA splicing as component of the U5 snRNP complex
Q99459	Cell division cycle 5-like protein	2	0	N; C	DNA-binding protein involved in cell cycle control
O00299	Chloride intracellular channel protein 1	1	0	N; C; CM	inserts into membranes and form chloride ion channels
Q8N684	Cleavage and polyadenylation specificity factor subunit 7	1	0	N	plays a key role in pre-mRNA 3'-processing
P25685	DnaJ homolog subfamily B member 1	2	0	C; N	interacts with HSP70 and can stimulate its ATPase activity
P63167	Dynein light chain 1, cytoplasmic	1	0	C; N; Mi	involved in linking dynein to cargos and to adapter proteins that regulate dynein function
Q9UBQ5	Eukaryotic translation initiation factor 3 subunit K	2	0	C; N	required for several steps in the initiation of protein synthesis
P51858	Hepatoma-derived growth factor	1	0	C; N	mitogenic activity for fibroblasts; acts as a transcriptional repressor
Q68E01	Integrator complex subunit 3	1	0	N	involved in the snRNA U1 and U2 transcription and in their 3'-box-dependent processing
Q96T76	MMS19 nucleotide excision repair protein homolog	1	0	N; SP	mediates the incorporation of iron-sulfur cluster into apoproteins
Q7L9L4	MOB kinase activator 1B	1	0	C; N	activator of LATS1/2 in the Hippo signaling pathway
Q9Y217	Myotubularin-related protein 6	1	0	N	Phosphatase that acts on lipids with a phosphoinositol headgroup
Q8WX92	Negative elongation factor B	1	0	N	negatively regulates the elongation of transcription by RNA polymerase II
P43490	Nicotinamide phosphoribosyltransferase	2	0	C; Ex; N	involved in the rate limiting component in the mammalian NAD biosynthesis pathway
Q9Y266	Nuclear migration protein nudC	1	0	C; N	neurogenesis and neuronal migration; formation of mitotic spindles and chromosome separation
Q12769	Nuclear pore complex protein Nup160	2	0	N	involved in poly(A)+RNA transport
Q9Y5B6	PAX3- and PAX7-binding protein 1	2	0	N	involved in myogenesis
P15259	Phosphoglycerate mutase 2	1	0	C; Ex; N	2,3-bisphosphoglycerate-dependent phosphoglycerate mutase activity
O15162	Phospholipid scramblase 1	4	1	N; M	mediates accelerated ATP-independent bidirectional transbilayer migration; fibrin clot formation
Q99471	Prefoldin subunit 5	1	0	N; C	binds specifically to cytosolic chaperonin (c-CPN) and transfers target proteins to it
Q9UHI6	Probable ATP-dependent RNA helicase DDX20	3	0	N; C	plays a catalyst role in the assembly of small nuclear ribonucleoproteins (snRNPs)
P43487	Ran-specific GTPase-activating protein	2	0	C; N	inhibits GTP exchange on Ran
Q13283	Ras GTPase-activating protein-binding protein 1	1	0	C; CM; N	a regulated effector of stress granule assembly
P35250	Replication factor C subunit 2	1	0	N	ATP binding; DNA binding
P35244	Replication protein A 14 kDa subunit	1	0	N	binds and stabilizes single-stranded DNA intermediates
P27694	Replication protein A 70 kDa DNA-binding subunit	1	0	N	binds and stabilizes single-stranded DNA intermediates
O75792	Ribonuclease H2 subunit A	1	0	N	degrades the RNA of RNA:DNA hybrids
P36873	Serine/threonine-protein phosphatase PP1-gamma catalytic subunit	1	0	C; N; Mi	associates with over 200 regulatory proteins to form highly specific holoenzymes
Q9Y3F4	Serine-threonine kinase receptor-associated protein	1	0	C; N	plays a catalyst role in the assembly of small nuclear ribonucleoproteins (snRNPs)
P42224	Signal transducer and activator of transcription 1-alpha/beta	1	0	C; N	mediates cellular responses to interferons, cytokines and other growth factors
P23246	Splicing factor, proline- and glutamine-rich	2	0	C; N	DNA- and RNA binding protein, involved in several nuclear processes
Q9GZT3	SRA stem-loop-interacting RNA-binding protein, mitochondrial	1	0	Mi; N	acts as a nuclear receptor corepressor
Q7KZF4	Staphylococcal nuclease domain-containing protein 1	1	0	C; N	functions as a bridging factor between STAT6 and the basal transcription factor
Q9NTJ3	Structural maintenance of chromosomes protein 4	2	0	C; N	conversion of interphase chromatin into mitotic-like condense chromosomes
Q9UBT2	SUMO-activating enzyme subunit 2	2	0	C; N	acts as a E1 ligase for SUMO1, SUMO2, SUMO3, and probably SUMO4
P00441	Superoxide dismutase [Cu-Zn]	1	0	C; N	destroys radicals which are normally produced and which are toxic to biological systems
Q13148	TAR DNA-binding protein 43	1	0	N	regulates transcription and splicing; regulates CFTR splicing
Q9NXF1	Testis-expressed sequence 10 protein	1	0	N; C; NM	functions as a component of the Five Friends of Methylated CHTOP (5FMC) complex
P20290	Transcription factor BTF3	1	0	C; N	prevents inappropriate targeting of non-secretory polypeptides to ER
Q12923	Tyrosine-protein phosphatase non-receptor type 13	1	0	C; N	regulates negatively FAS-induced apoptosis and NGFR-mediated pro-apoptotic signaling
Q9Y4Y9	U6 snRNA-associated Sm-like protein LSm5	1	0	N	plays a role in U6 snRNP assembly and function
P61088	Ubiquitin-conjugating enzyme E2 N	1	0	N; C	catalyzes the synthesis of polyubiquitin chains; acts with E3 ligases
O15294	UDP-N-acetylglucosamine--peptide N-acetylglucosaminyltransferase 110 kDa subunit	1	0	Mi; M; C; N; CM	catalyzes a single N-acetylglucosamine from UDP-GlcNAc transfer to a serine or threonine residue
P54727	UV excision repair protein RAD23 homolog B	1	0	N; C	multiubiquitin chain receptor involved in modulation of proteasomal degradation
Q9UNX4	WD repeat-containing protein 3	1	0	N	poly(A) RNA binding; snoRNA binding
P61604	10 kDa heat shock protein, mitochondrial	1	0	Mi	mitochondrial protein biogenesis
Q9Y305	Acyl-coenzyme A thioesterase 9, mitochondrial	3	0	Mi	catalyzes the hydrolysis of acyl-CoAs to the free fatty acid and coenzyme A
P30566	Adenylosuccinate lyase	2	0	C; Mi	catalyzes two non-sequential steps in de novo AMP synthesis
Q6PI48	Aspartate--tRNA ligase, mitochondrial	1	0	Mi	aspartate-tRNA(Asn) ligase activity
P30049	ATP synthase subunit delta, mitochondrial	2	0	Mi	produces ATP from ADP in the presence of a proton gradient across the membrane
O76031	ATP-dependent Clp protease ATP-binding subunit clpX-like, mitochondrial	3	0	Mi	hydrolyzes ATP; targets specific substrates for degradation by the Clp complex
P50416	Carnitine O-palmitoyltransferase 1, liver isoform	2	2	Mi	mitochondrial uptake of long-chain fatty acids and beta-oxidation in the mitochondrion
O75390	Citrate synthase, mitochondrial	1	0	Mi	involved in step 1 of the subpathway that synthesizes isocitrate from oxaloacetate
O43169	Cytochrome b5 type B	1	1	Mi	functions as an electron carrier for several membrane bound oxygenases
P14406	Cytochrome c oxidase subunit 7A2, mitochondrial	1	1	Mi	the terminal oxidase in mitochondrial electron transport
P10515	Dihydrolipoyllysine-residue acetyltransferase component of pyruvate dehydrogenase complex, mitochondrial	2	0	Mi	catalyzes the overall conversion of pyruvate to acetyl-CoA and CO2
Q96RP9	Elongation factor G, mitochondrial	1	0	Mi	catalyzes the GTP-dependent ribosomal translocation step during translation elongation
Q8NFF5	FAD synthase	1	0	Mi; C	Catalyzes the adenylation of flavin mononucleotide
Q92947	Glutaryl-CoA dehydrogenase, mitochondrial	1	0	Mi	catalyzes the oxidative decarboxylation of glutaryl-CoA to crotonyl-CoA and CO2
Q9HC38	Glyoxalase domain-containing protein 4	1	0	Mi	?
P26440	Isovaleryl-CoA dehydrogenase, mitochondrial	1	0	Mi	synthesizes (S)-3-hydroxy-3-methylglutaryl-CoA from 3-isovaleryl-CoA
P40926	Malate dehydrogenase, mitochondrial	6	0	Mi	malate dehydrogenase (NADP+) activity
Q13505	Metaxin-1	1	0	M; Mi	involved in transport of proteins into the mitochondrion
Q7L0Y3	Mitochondrial ribonuclease P protein 1	1	0	Mi	functions in mitochondrial tRNA maturation
Q6UB35	Monofunctional C1-tetrahydrofolate synthase, mitochondrial	3	0	Mi	provides the missing metabolic reaction required to link mitochondria and cytoplasm
Q16718	NADH dehydrogenase [ubiquinone] 1 alpha subcomplex subunit 5	1	0	Mi	accessory subunit of the mitochondrial membrane respiratory chain NADH dehydrogenase
P04181	Ornithine aminotransferase, mitochondrial	1	0	Mi	involved in synthesis of L-glutamate 5-semialdehyde from L-ornithine
P30044	Peroxiredoxin-5, mitochondrial	1	0	Mi; C; P	involved in intracellular redox signaling
Q14409	Putative glycerol kinase 3	2	1	Mi; C	regulation of glycerol uptake and metabolism
P45954	Short/branched chain specific acyl-CoA dehydrogenase, mitochondrial	1	0	Mi	plays a role in controlling the metabolic flux of valproic acid in the development of toxicity
Q8N442	Translation factor GUF1, mitochondrial	1	0	Mi	promotes mitochondrial protein synthesis
P62273	40S ribosomal protein S29	1	0	C; Ex	zinc binding; structural constituent of ribosome
P05387	60S acidic ribosomal protein P2	1	0	C; M; Ex	plays a role in elongation step of protein synthesis
Q16877	6-phosphofructo-2-kinase/fructose-2,6-bisphosphatase 4	1	0	C	synthesis and degradation of fructose 2,6-bisphosphate
Q13085	Acetyl-CoA carboxylase 1	1	0	C	catalyzes the rate-limiting reaction in the biogenesis of long-chain fatty acids
P59998	Actin-related protein 2/3 complex subunit 4	1	0	C	regulation of actin polymerization; formation of branched actin networks
P07741	Adenine phosphoribosyltransferase	2	0	C	catalyzes a salvage reaction resulting in the formation of AMP
Q01518	Adenylyl cyclase-associated protein 1	1	0	C; M	regulates filament dynamics; mRNA localization; establishment of cell polarity
O00170	AH receptor-interacting protein	1	0	C	a positive role in AHR-mediated (aromatic hydrocarbon receptor) signaling
Q9P2R3	Ankyrin repeat and FYVE domain-containing protein 1	1	0	E; C	proposed effector of Rab5
P63010	AP-2 complex subunit beta	1	0	CM; M	functions in protein transport via transport vesicles in different membrane traffic pathways
P35613	Basigin	2	1	CM	targets the monocarboxylate transporters SLC16A1, SLC16A3 and SLC16A8 to the plasma membrane

Q9UDT6	CAP-Gly domain-containing linker protein 2	1	0	C	links microtubules to DLB; operates brain-specific organellle translocations
O75534	Cold shock domain-containing protein E1	1	0	C	internal initiation of translation of human rhinovirus RNA; involved in mRNA turnover
Q14008	Cytoskeleton-associated protein 5	1	0	SP; C	Binds to the plus end of microtubules and regulates microtubule dynamics and organization
Q96KP4	Cytosolic non-specific dipeptidase	1	0	C	hydrolyzes a variety of dipeptides; tumor suppressor
Q2NKX8	DNA excision repair protein ERCC-6-like	1	0	centromere	acts as an essential component of the spindle assembly checkpoint
P24534	Elongation factor 1-beta	2	0	C	translation elongation factor activity
Q14152	Eukaryotic translation initiation factor 3 subunit A	1	0	C	required for several steps in the initiation of protein synthesis
Q99613	Eukaryotic translation initiation factor 3 subunit C	1	0	C	required for several steps in the initiation of protein synthesis
O00303	Eukaryotic translation initiation factor 3 subunit F	1	0	C	required for several steps in the initiation of protein synthesis
Q04637	Eukaryotic translation initiation factor 4 gamma 1	1	0	C; M	involved in the recognition of the mRNA cap
Q9UPT5	Exocyst complex component 7	1	0	C; CM	involved in the docking of exocytic vesicles with fusion sites on the plasma membrane
Q96PY5	Formin-like protein 2	1	0	C	plays a role in the regulation of cell morphology and cytoskeletal organization
Q96QA5	Gasdermin-A	1	0	C	induces apoptosis
Q06210	Glutamine--fructose-6-phosphate aminotransferase [isomerizing] 1	1	0	C; Ex	controls the flux of glucose into the hexosamine pathway; regulate precursors for glycosylation
P47897	Glutamine--tRNA ligase	2	0	C	brain development
P34932	Heat shock 70 kDa protein 4	1	0	C	ATP binding; chaperone-mediated protein complex assembly; response to UPR
Q9NZL4	Hsp70-binding protein 1	1	0	C	interferes with ubiquitination and inhibits chaperone-assisted degradation of immature CFTR
P49441	Inositol polyphosphate 1-phosphatase	1	0	C	involved in the pathway phosphatidylinositol signaling pathway
O75449	Katanin p60 ATPase-containing subunit A1	1	0	C; SP	severs microtubules in an ATP-dependent manner
Q04760	Lactoylglutathione lyase	2	0	C; Ex	involved in regulates TNF-induced transcriptional activity of NF-kappa-B; osteoclastogenesis
Q99538	Legumain	2	1	L	hydrolysis of asparaginyl bonds
Q8IVV2	Lipoxygenase homology domain-containing protein 1	1	0	C; M	involved in hearing
P13473	Lysosome-associated membrane glycoprotein 2	1	1	CM; E; L	implicated in tumor cell metastasis
P14174	Macrophage migration inhibitory factor	1	0	Ex; C	involved in the innate immune response to bacterial pathogens
O75352	Mannose-P-dolichol utilization defect 1 protein	2	6	M	required for normal utilization of mannose-dolichol phosphate (Dol-P-Man)
Q15691	Microtubule-associated protein RP/EB family member 1	1	0	C	promotes cytoplasmic microtubule nucleation and elongation; involved in spindle function
P29966	Myristoylated alanine-rich C-kinase substrate	1	0	C; M	the most prominent cellular substrate for protein kinase C
Q01804	OTU domain-containing protein 4	1	0	?	deubiquitinating enzyme that specifically hydrolyzes 'Lys-48'-linked polyubiquitin
Q9NVE7	Pantothenate kinase 4	1	0	C	physiological regulation of the intracellular CoA concentration
Q3KNS1	Patched domain-containing protein 3	1	7	M	sperm development or sperm function
Q9UBV8	Peflin	1	0	C; M	calcium binding
P18669	Phosphoglycerate mutase 1	2	0	C; Ex; M	2,3-bisphosphoglycerate-dependent phosphoglycerate mutase activity
P46020	Phosphorylase b kinase regulatory subunit alpha, skeletal muscle isoform	1	0	CM	catalyzes the phosphorylation of serine in certain substrates, including troponin I
A2RTX5	Probable threonine--tRNA ligase 2, cytoplasmic	2	0	C	ATP binding; threonine-tRNA ligase activity
P07737	Profilin-1	2	0	C	binds to actin and affects the structure of the cytoskeleton
Q15185	Prostaglandin E synthase 3	1	0	C	catalyzes the oxidoreduction of prostaglandin endoperoxide H2 (PGH2) to prostaglandin E2 (PGE2)
O60678	Protein arginine N-methyltransferase 3	1	0	C	methylates the guanidino nitrogens of arginyl residues in some proteins
Q8N9Q2	Protein SREK1IP1	1	0	?	involved in the control of cellular survival.
P0C7P4	Putative cytochrome b-c1 complex subunit Rieske-like protein 1	2	0	M	metal ion binding
Q8I2P2	Putative protein FAM10A4	2	0	C	?
Q9UET6	Putative tRNA (cytidine(32)/guanosine(34)-2'-O)-methyltransferase	2	0	C	methylates the 2'-O-ribose of nucleotides at positions 32 and 34 of the tRNA anticodon loop
Q96C36	Pyrroline-5-carboxylate reductase 2	2	0	C	housekeeping enzyme that catalyzes the last step in proline biosynthesis
Q6IAA8	Ragulator complex protein LAMTOR1	1	0	E; L; CM	involved in amino acid sensing and activation of mTORC1
Q9Y2Q5	Ragulator complex protein LAMTOR2	1	0	E; L	involved in amino acid sensing and activation of mTORC1
Q0VGL1	Ragulator complex protein LAMTOR4	1	0	L	involved in amino acid sensing and activation of mTORC1
P62491	Ras-related protein Rab-11A	2	0	CM; L	key regulators of intracellular membrane trafficking
P20339	Ras-related protein Rab-5A	1	0	CM; E; C; M; Me	key regulators of intracellular membrane trafficking
P51148	Ras-related protein Rab-5C	2	0	CM; E; Me	involved in vesicular traffic
A6NIZ1	Ras-related protein Rap-1b-like protein	1	0	C; CM	Activated by GEF EPAC2 in a cAMP-dependent manner
P13489	Ribonuclease inhibitor	2	0	C	inhibits RNASE1, RNASE2 and ANG; plays a role in redox homeostasis
Q15019	Septin-2	3	0	C; Spindle	filament-forming cytoskeletal GTPase
Q96K37	Solute carrier family 35 member E1	1	10	M	putative transporter
Q01082	Spectrin beta chain, non-erythrocytic 1	2	0	C	involved in secretion, interacts with calmodulin in a calcium-dependent manner
P16949	Stathmin OS=Homo sapiens GN=STMN1 PE=1 SV=3 - [STMN1_HUMAN]	1	0	C	involved in the regulation of the microtubule (MT) filament system by destabilizing microtubule
P26639	Threonine--tRNA ligase, cytoplasmic	2	0	C	ATP binding; protein homodimerization activity; threonine-tRNA ligase activity
O14545	TRAF-type zinc finger domain-containing protein 1	1	0	?	negative feedback regulator that controls excessive innate immune responses
P37837	Transaldolase	2	0	C	balance of metabolites in the pentose-phosphate pathway
P54577	Tyrosine--tRNA ligase, cytoplasmic	2	0	C	catalyzes the attachment of tyrosine to tRNA(Tyr)
P45974	Ubiquitin carboxyl-terminal hydrolase 5	1	0	L	cleaves multiubiquitin polymers with a marked preference for branched polymers
Q9HA47	Uridine-cytidine kinase 1	1	0	C	phosphorylates uridine and cytidine to uridine monophosphate and cytidine monophosphate

Table 5 Unique R85H hits in third IP (without crosslinker)

Third IP Accession	Protein name	#Peptides with crosslinker R85H	TMD	localization	function
Q15436	Protein transport protein Sec23A	2	0	ER; G	COPII dependent anterograde transport
P53992	Protein transport protein Sec24C	1	0	G; ER; C	COPII dependent anterograde transport
O95197	Reticulon-3	1	3	G; ER	involved in membrane trafficking; ER stress pathway
Q14697	Neutral alpha-glucosidase AB	1	1	G; ER	glycosylation; dleaves glucose residues from oligosaccharide precursor of immature glycoproteins
Q10471	Polypeptide N-acetylgalactosaminyltransferase 2	1	1	G; Ex	glycosylation; catalyzes the initial reaction in O-linked oligosaccharide biosynthesis
Q6P996	Pyridoxal-dependent decarboxylase domain-containing protein 1	1	0	G	glycosylation; carboxy-lyase activity
Q12904	Aminoacyl tRNA synthase complex-interacting multifunctional protein 1	2	0	N; C; ER; G	binds tRNA; inflammatory cytokine activity; regulates TGF-beta signaling; glucose homeostasis;
Q6NTF9	Rhomboid domain-containing protein 2	1	6	G	RHBDD2
P55061	Bax inhibitor 1	1	7	ER	modulates UPR signaling; ER calcium homeostasis; suppressor of apoptosis
Q99942	E3 ubiquitin-protein ligase RNF5	1	3	ER; M; Mi	E2-dependent E3 ubiquitin-protein ligase activity
Q969N2	GPI transamidase component PIG-T	1	1	ER	essential for transfer of GPI to proteins; formation of carbonyl intermediates
Q969V3	Nicalin	1	1	ER	antagonizes Nodal signaling and subsequent organization of axial structures
Q96JJ7	Protein disulfide-isomerase TMX3	1	1	ER	participates in the folding of proteins containing disulfide bonds
Q9HCN8	Stromal cell-derived factor 2-like protein 1	1	0	ER	ER-associated misfolded protein catabolic process; regulation of apoptosis process
Q8NFQ8	Torsin-1A-interacting protein 2	2	1	ER; NM	ER organization; TOR1A transport between nucleus and ER; ATPase activity
P55084	Trifunctional enzyme subunit beta, mitochondrial	1	0	Mi; ER	lipid metabolism; fatty acid beta-oxidation pathway
Q9P003	Protein cornichon homolog 4	1	3	ER; IC; M	COPII dependent anterograde transport
P21953	2-oxoisovalerate dehydrogenase subunit beta, mitochondrial	1	0	Mi	catalyzes the overall conversion of alpha-keto acids to acyl-CoA and CO2
P30566	Adenylosuccinate lyase	1	0	C; Mi	catalyzes two non-sequential steps in de novo AMP synthesis
Q6PI48	Aspartate--tRNA ligase, mitochondrial	1	0	Mi	aspartate-tRNA(Asn) ligase activity
P30049	ATP synthase subunit delta, mitochondrial	1	0	Mi	produces ATP from ADP in the presence of a proton gradient across the membrane
O76031	ATP-dependent Clp protease ATP-binding subunit clpX-like, mitochondrial	3	0	Mi	hydrolyzes ATP; targets specific substrates for degradation by the Clp complex
Q8NE86	Calcium uniporter protein, mitochondrial	2	2	Mi	calcium uniporter that mediates calcium uptake into mitochondria
P31327	Carbamoyl-phosphate synthase [ammonia], mitochondrial	1	0	Mi; N	involved in the urea cycle of ureotelic animals
P50416	Carnitine O-palmitoyltransferase 1, liver isoform	2	2	Mi	mitochondrial uptake of long-chain fatty acids and beta-oxidation in the mitochondrion
O43169	Cytochrome b5 type B	1	1	Mi	functions as an electron carrier for several membrane bound oxygenases
Q8NFF5	FAD synthase	1	0	Mi; C	Catalyzes the adenylation of flavin mononucleotide
Q92947	Glutaryl-CoA dehydrogenase, mitochondrial	2	0	Mi	catalyzes the oxidative decarboxylation of glutaryl-CoA to crotonyl-CoA and CO2
P26440	Isovaleryl-CoA dehydrogenase, mitochondrial	1	0	Mi	synthesizes (S)-3-hydroxy-3-methylglutaryl-CoA from 3-isovaleryl-CoA
Q8IXI2	Mitochondrial Rho GTPase 1	1	1	Mi	involved in mitochondrial trafficking
Q6UB35	Monofunctional C1-tetrahydrofolate synthase, mitochondrial	1	0	Mi	provides the missing metabolic reaction required to link mitochondria and cytoplasm
Q16718	NADH dehydrogenase [ubiquinone] 1 alpha subcomplex subunit 5	1	0	Mi	accessory subunit of the mitochondrial membrane respiratory chain NADH dehydrogenase
Q14318	Peptidyl-prolyl cis-trans isomerase FKBP8	2	1	Mi	inactive Ppiase; becomes active when bound to calmodulin and calcium
Q9GZT3	SRA stem-loop-interacting RNA-binding protein, mitochondrial	1	0	Mi; N	acts as a nuclear receptor corepressor
O00231	26S proteasome non-ATPase regulatory subunit 11	1	0	N; C	involved in the ATP-dependent degradation of ubiquitinated proteins
Q13363	C-terminal-binding protein 1	1	0	C; N	corepressor targeting diverse transcription regulators such as GLIS2 or BCL6
Q16527	Cysteine and glycine-rich protein 2	1	0	N	drastically down-regulated in response to PDGF-BB or cell injury
P28340	DNA polymerase delta catalytic subunit	1	0	N	DNA synthesis and an exonucleolytic activity
Q9UHW5	GPN-loop GTPase 3	1	0	N	required for proper localization of RNA polymerase II (RNAPII)
Q15477	Helicase SKI2W	1	0	N; C	involved in exosome-mediated RNA decay and associates with transcriptionally active genes
P02788	Lactotransferrin	1	0	Ex; C; N	iron binding transport proteins which can bind two Fe3+ ions
Q96T76	MMS19 nucleotide excision repair protein homolog	4	0	N; SP	mediates the incorporation of iron-sulfur cluster into apoproteins
Q8WX92	Negative elongation factor B	1	0	N	negatively regulates the elongation of transcription by RNA polymerase II
Q9BW27	Nuclear pore complex protein Nup85	1	0	N; C	essential component of the nuclear pore complex (NPC)
O15162	Phospholipid scramblase 1	2	1	N; M	mediates accelerated ATP-independent bidirectional transbilayer migration; fibrin clot formation
Q14558	Phosphoribosyl pyrophosphate synthase-associated protein 1	1	0	N	plays a negative regulatory role in 5-phosphoribose 1-diphosphate synthesis
Q9UHI6	Probable ATP-dependent RNA helicase DDX20	4	0	N; C	plays a catalyst role in the assembly of small nuclear ribonucleoproteins (snRNPs)
P15056	Serine/threonine-protein kinase B-raf	1	0	N; C; CM	involved in the transduction of mitogenic signals from the cell membrane to the nucleus
O15084	Serine/threonine-protein phosphatase 6 regulatory ankyrin repeat subunit A	1	0	N	involved in the recognition of phosphoprotein substrates
P62306	Small nuclear ribonucleoprotein F	1	0	C; N	core component of the spliceosomal U1, U2, U4 and U5 small nuclear ribonucleoproteins (snRNPs)
Q13148	TAR DNA-binding protein 43	1	0	N	regulates transcription and splicing; regulates CFTR splicing
Q8NI27	THO complex subunit 2	1	0	N	required for efficient export of polyadenylated RNA and spliced mRNA
Q9UBB9	Tuftelin-interacting protein 11	2	0	C; N	involved in pre-mRNA splicing; spliceosome disassembly during late-stage splicing events
P11172	Uridine 5'-monophosphate synthase	3	0	C; N	orotate phosphoribosyltransferase activity; orotidine-5'-phosphate decarboxylase activity
Q9BZH6	WD repeat-containing protein 11	1	0	M; C; N	?
Q9UNX4	WD repeat-containing protein 3	1	0	N	poly(A) RNA binding; snoRNA binding
Q9NU02	Ankyrin repeat and EF-hand domain-containing protein 1	2	0	?	calcium binding
Q9P2R3	Ankyrin repeat and FYVE domain-containing protein 1	2	0	E; C	proposed effector of Rab5
Q7L1Q6	Basic leucine zipper and W2 domain-containing protein 1	1	0	C; M	enhances histone H4 gene transcription but does not seem to bind DNA directly
P35613	Basigin	1	1	CM	targets the monocarboxylate transporters SLC16A1, SLC16A3 and SLC16A8 to the plasma membrane
Q9UDT6	CAP-Gly domain-containing linker protein 2	1	0	C	links microtubules to DLB; operates brain-specific organellle translocations
Q96KP4	Cytosolic non-specific dipeptidase	1	0	C	hydrolyzes a variety of dipeptides; tumor suppressor
P60981	Destrin	1	0	C; Ex	severs actin filaments (F-actin) and binds to actin monomers (G-actin)
P24534	Elongation factor 1-beta	1	0	C	translation elongation factor activity
Q9UPT5	Exocyst complex component 7	1	0	C; CM	involved in the docking of exocytic vesicles with fusion sites on the plasma membrane
Q96QA5	Gasdermin-A	1	0	C	induces apoptosis
Q06210	Glutamine--fructose-6-phosphate aminotransferase [isomerizing] 1	1	0	C; Ex	controls the flux of glucose into the hexosamine pathway; regulate precursors for glycosylation
P47897	Glutamine--tRNA ligase	2	0	C	brain development
Q8NEV9	Interleukin-27 subunit alpha	1	0	Ex	fuctions in innate immunity
Q99538	Legumain	1	1	L	hydrolysis of asparaginyl bonds
Q9H9A6	Leucine-rich repeat-containing protein 40	1	0	M	?
Q9P260	LisH domain and HEAT repeat-containing protein KIAA1468	1	0	?	?
O75352	Mannose-P-dolichol utilization defect 1 protein	1	6	M	required for normal utilization of mannose-dolichol phosphate (Dol-P-Man)
Q9NVE7	Pantothenate kinase 4	1	0	C	physiological regulation of the intracellular CoA concentration
P56589	Peroxisomal biogenesis factor 3	2	1	P	involved in peroxisome biosynthesis and integrity
A2RTX5	Probable threonine--tRNA ligase 2, cytoplasmic	1	0	C	ATP binding; threonine-tRNA ligase activity
O60678	Protein arginine N-methyltransferase 3	1	0	C	methylates the guanidino nitrogens of arginyl residues in some proteins
Q8WUH1	Protein Churchill	1	0	?	mediates FGF signaling during neural development
Q8TCG1	Protein CIP2A	1	0	C; M	inhibits PP2A and stabilizes MYC in human malignancies
Q9H7Z3	Protein NRDE2 homolog	1	0	?	?
Q5JSZ5	Protein PRRC2B	1	0	?	poly(A) RNA binding
Q8N9Q2	Protein SREK1IP1	1	0	?	involved in the control of cellular survival.
P51148	Ras-related protein Rab-5C	1	0	CM; E; Me	involved in vesicular traffic
A6NIZ1	Ras-related protein Rap-1b-like protein	1	0	C; CM	Activated by GEF EPAC2 in a cAMP-dependent manner
P13489	Ribonuclease inhibitor	1	0	C	inhibits RNASE1, RNASE2 and ANG; plays a role in redox homeostasis
Q9NSD5	Sodium- and chloride-dependent GABA transporter 2	1	11	CM	sodium-dependent GABA and taurine transporter
P19623	Spermidine synthase	1	0	C	catalyzes the production of spermidine from putrescine and dcSAM
Q6YHU6	Thyroid adenoma-associated protein	1	0	?	?
Q9UI30	tRNA methyltransferase 112 homolog	1	0	Ex	participates both in methylation of protein and tRNA species
P54577	Tyrosine--tRNA ligase, cytoplasmic	1	0	C	catalyzes the attachment of tyrosine to tRNA(Tyr)
Q9H269	Vacuolar protein sorting-associated protein 16 homolog	1	0	E; L; A	vesicle-mediated protein trafficking to lysosomal compartments; autophagic pathways
Q9UN37	Vacuolar protein sorting-associated protein 4A	2	0	E	involved in late steps of the endosomal multivesicular bodies (MVB) pathway

Table 6 Conserved RHBDD2 WT hits between first IP and second IP (both with crosslinker)

Accession	Protein name	TMD	localization	function
Q08378	Golgin subfamily A member 3 (golgin-160)	0	G; C	Golgi organization
Q15643	Thyroid receptor-interacting protein 11	0	G; C	Golgi organization; enhances THRB-modulated transcription
Q9H8Y8	Golgi reassembly-stacking protein 2	0	G	Golgi organization; intracellular transport; lipid-anchor
Q8TBA6	Golgin subfamily A member 5 (golgin-84)	1	G	Golgi organization; intra-Golgi transport
Q9H2G9	Golgin-45	0	G	Golgi organization; anterograde transport
P20340	Ras-related protein Rab-6A	0	G	Golgi organization; Golgi-to-ER retrograde transport; endosome-to-Golgi retrograde transport
O95159	Zinc finger protein-like 1	1	G	Golgi organization; interacts with GM130; ER-to-Golgi transport
Q9H4A5	Golgi phosphoprotein 3-like	1	G	antagonize Golgi-to-plasma membrane transport
Q8IUH4	Palmitoyltransferase ZDHHC13	6	G	magnesium transport; palmitoyltransferase for HD and GAD2
P82094	TATA element modulatory factor	0	G; C; N	RAB6-dependent retrograde transport (Golgi-to-ER and endosome-to-Golgi retrograde transport)
Q8TAD4	Zinc transporter 5	16	G	zinc transporter that transports zinc into Golgi lumens
Q6P996	Pyridoxal-dependent decarboxylase domain-containing protein 1	0	G	glycosylation; carboxy-lyase activity
Q8WVQ1	Soluble calcium-activated nucleotidase 1	1	ER; G	glycosylation; calcium-dependent nucleotidase with a preference for UDP
Q9UKM7	Endoplasmic reticulum mannosyl-oligosaccharide 1,2-alpha-mannosidase	1	ER	glycosylation; glycoprotein quality control
Q96IW7	Vesicle-trafficking protein SEC22a	4	ER	transport between ER and Golgi
O95486	Protein transport protein Sec24A	0	G; ER; IC	COPII dependent anterograde transport
O95487	Protein transport protein Sec24B	0	G; ER; IC	COPII dependent anterograde transport
O94855	Protein transport protein Sec24D	0	G; ER; IC	COPII dependent anterograde transport
P32019	Type II inositol 1,4,5-trisphosphate 5-phosphatase	0	G; C; IC	metal ion binding; dephosphorylation
Q96RQ1	Endoplasmic reticulum-Golgi intermediate compartment protein 2	2	IC; N	transport between ER and Golgi
Q9Y217	Myotubularin-related protein 6	0	N	Phosphatase that acts on lipids with a phosphoinositol headgroup
O00308	NEDD4-like E3 ubiquitin-protein ligase WWP2	0	N	ubiquitination
Q8N1F7	Nuclear pore complex protein Nup93	2	N	plays a role in the nuclear pore complex assembly
Q6DKJ4	Nucleoredoxin	0	C; N	regulator of the Wnt signaling pathway
P56556	NADH dehydrogenase [ubiquinone] 1 alpha subcomplex subunit 6	0	Mi	functions in respiratory chain
Q9BWD1	Acetyl-CoA acetyltransferase	0	C	acetyl-CoA C-acetyltransferase activity
Q96PU5	E3 ubiquitin-protein ligase NEDD4-like	0	C	ubiquitination
P08134	Rho-related GTP-binding protein RhoC	0	CM	myosin contractile ring formation; apical junction formation
Q92544	Transmembrane 9 superfamily member 4	10	M	?
Q5MNZ6	WD repeat domain phosphoinositide-interacting protein 3	0	C; A	autophagosome assembly

Table 7 Conserved RHBDD2 WT hits between second IP and third IP (with and without crosslinker)

Accession	Protein name	TMD	localization	function
O15027	Protein transport protein Sec16A	0	ER; G	defines endoplasmic reticulum exit sites; ER-to-Golgi transport; transitional ER organization
P53992	Protein transport protein Sec24C	0	G; ER; C	COPII dependent anterograde transport
Q6NTF9	Rhomboid domain-containing protein 2	6	G	RHBDD2
P30566	Adenylosuccinate lyase	0	C; Mi	catalyzes two non-sequential steps in de novo AMP synthesis
Q9Y217	Myotubularin-related protein 6	0	N	Phosphatase that acts on lipids with a phosphoinositol headgroup
O15162	Phospholipid scramblase 1	1	N; M	mediates accelerated bidirectional transbilayer migration; fibrin clot formation
P23246	Splicing factor, proline- and glutamine-rich	0	C; N	DNA- and RNA binding protein, involved in several nuclear processes
P61088	Ubiquitin-conjugating enzyme E2 N	0	N; C	catalyzes the synthesis of polyubiquitin chains; acts with E3 ligases
P59998	Actin-related protein 2/3 complex subunit 4	0	C	regulation of actin polymerization; formation of branched actin networks
O00303	Eukaryotic translation initiation factor 3 subunit F	0	C	component of eIF-3 complex, which is required for the initiation of protein synthesis
Q06210	Glutamine--fructose-6-phosphate aminotransferase [isomerizing] 1	0	C; Ex	controls flux of glucose into the hexosamine pathway; regulate precursors for glycosylation
Q96C36	Pyrroline-5-carboxylate reductase 2	0	C	housekeeping enzyme that catalyzes the last step in proline biosynthesis
Q9HA47	Uridine-cytidine kinase 1	0	C	phosphorylates uridine and cytidine to uridine monophosphate and cytidine monophosphate

Table 8 Conserved R85H mutation hits between second IP and third IP (with and without crosslinker)

Accession	Protein name	TMD	localization	function
Q6P996	Pyridoxal-dependent decarboxylase domain-containing protein 1	0	G	glycosylation; carboxy-lyase activity
P53992	Protein transport protein Sec24C	0	G; ER; C	COPII dependent anterograde transport
P55084	Trifunctional enzyme subunit beta, mitochondrial	0	Mi; ER	lipid metabolism; fatty acid beta-oxidation pathway
P35613	Basigin	1	CM	targets the monocarboxylate transporters SLC16A1, SLC16A3 and SLC16A8 to the plasma membrane
P28340	DNA polymerase delta catalytic subunit	0	N	DNA synthesis and an exonucleolytic activity
Q96T76	MMS19 nucleotide excision repair protein homolog	0	N; SP	mediates the incorporation of iron-sulfur cluster into apoproteins
O15162	Phospholipid scramblase 1	1	N; M	mediates accelerated bidirectional transbilayer migration; fibrin clot formation

Table 9 Conserved RHBDD2 WT and R85H hits in second IP (with crosslinker)

Accession	Protein name	TMD	localization	function
Q08379	Golgin subfamily A member 2 (GM130)	0	G; SP	Golgi organization; spindle pole assembly; centrosome organization
Q08378	Golgin subfamily A member 3 (golgin-160)	0	G; C	Golgi organization
Q15643	Thyroid receptor-interacting protein 11	0	G; C	Golgi organization; enhances THRB-modulated transcription
Q9H8Y8	Golgi reassembly-stacking protein 2	0	G	Golgi organization; intracellular transport; lipid-anchor
Q8TBA6	Golgin subfamily A member 5 (golgin-84)	1	G	Golgi organization; intra-Golgi transport
Q9H2C9	Golgin-45	0	G	Golgi organization; anterograde transport
P20340	Ras-related protein Rab-6A	0	G	Golgi organization; Golgi-to-ER retrograde transport; endosome-to-Golgi retrograde transport
O60763	General vesicular transport factor p115	0	G; C	intra-Golgi transport; docking of transport vesicles
O14653	Golgi SNAP receptor complex member 2	1	G	intra-Golgi transport
Q8IUH4	Palmitoyltransferase ZDHHC13	6	G	magnesium transport; palmitoyltransferase for HD and GAD2
Q8IUH5	Palmitoyltransferase ZDHHC17	6	G; C	involved in sorting or targeting proteins and initiating events of endocytosis; Mg2+ transport
Q13948	Protein CASP	1	G	intra-Golgi transport
P53992	Protein transport protein Sec24C	0	G; ER; C	COPII dependent anterograde transport
P61106	Ras-related protein Rab-14	0	G; E; Ph	transport between Golgi and endosomes
Q8TAD4	Zinc transporter 5	16	G	zinc transporter that transports zinc into Golgi lumens
Q10469	Alpha-1,6-mannosyl-glycoprotein 2-beta-N-acetylglucosaminyltransferase	0	G	glycosylation; conversion of ligo-mannose to complex N-glycans
Q6P996	Pyridoxal-dependent decarboxylase domain-containing protein 1	0	G	glycosylation; carboxy-lyase activity
P78381	UDP-galactose translocator	8	G	glycosylation; transports nucleotide sugars from the cytosol into Golgi
Q9BXS5	AP-1 complex subunit mu-1	0	G; C	protein sorting in trans-Golgi and endosomes
Q9NZC7	WW domain-containing oxidoreductase	0	C; G; Mi; N	a tumor suppressor and plays a role in apoptosis; bone development
O95486	Protein transport protein Sec24A	0	G; ER; IC	COPII dependent anterograde transport
O95487	Protein transport protein Sec24B	0	G; ER; IC	COPII dependent anterograde transport
O94855	Protein transport protein Sec24D	0	G; ER; IC	COPII dependent anterograde transport
P61019	Ras-related protein Rab-2A	0	ER; G; IC	ER-to-Golgi transport
Q9Y6Y8	SEC23-interacting protein	0	ER; IC	organization of endoplasmic reticulum exit sites
Q13190	Syntaxin-5	1	G; IC	Golgi organization; ER-to-Golgi transport
P55084	Trifunctional enzyme subunit beta, mitochondrial	0	Mi; ER	lipid metabolism; fatty acid beta-oxidation pathway
Q53H12	Acylglycerol kinase, mitochondrial	0	Mi	involved in the pathway glycerolipid metabolism
P61221	ATP-binding cassette sub-family E member 1	0	C; Mi	interact with Rnase L; regulate mRNA turnover; chaperone for post-translational events
Q9H078	Caseinolytic peptidase B protein homolog	0	Mi	regulate ATPase and be related to secretion/protein trafficking process
Q3ZCQ8	Mitochondrial import inner membrane translocase subunit TIM50	1	Mi	mediates the translocation of transit peptide-containing proteins
P56556	NADH dehydrogenase [ubiquinone] 1 alpha subcomplex subunit 6	0	Mi	functions in respiratory chain
O75251	NADH dehydrogenase [ubiquinone] iron-sulfur protein 7, mitochondrial	0	Mi	core subunit of the mitochondrial membrane respiratory chain NADH dehydrogenase
P62888	60S ribosomal protein L30	0	C; Ex; N; M	structural constituent of ribosome
P28340	DNA polymerase delta catalytic subunit	0	N	DNA synthesis and an exonucleolytic activity
Q13642	Four and a half LIM domains protein 1	0	C; N	involved in muscle development or hypertrophy
Q9BQ67	Glutamate-rich WD repeat-containing protein 1	0	N	poly(A) RNA binding
Q9NZI8	Insulin-like growth factor 2 mRNA-binding protein 1	0	N; C	mRNA binding; translation regulator activity
Q9Y217	Myotubularin-related protein 6	0	N	Phosphatase that acts on lipids with a phosphoinositol headgroup
O75182	Paired amphipathic helix protein Sin3b	0	N	acts as a transcriptional repressor
Q81YS1	Peptidase M20 domain-containing protein 2	0	Ex; N	enzyme activity
O15162	Phospholipid scramblase 1	1	N; M	mediates accelerated bidirectional transbilayer migration; fibrin clot formation
Q9UQ80	Proliferation-associated protein 2G4	0	C; N	a ERBB3-regulated signal transduction pathway; ribosome assembly
P56182	Ribosomal RNA processing protein 1 homolog A	0	N	generation of 28S rRNA
Q5H9R7	Serine/threonine-protein phosphatase 6 regulatory subunit 3	0	C; N	a scaffolding PP6 subunit; maintains immune self-tolerance
P23246	Splicing factor, proline- and glutamine-rich	0	C; N	DNA- and RNA binding protein, involved in several nuclear processes
P61088	Ubiquitin-conjugating enzyme E2 N	0	N; C	catalyzes the synthesis of polyubiquitin chains; acts with E3 ligases
Q6ZRP7	Sulfhydryl oxidase 2	1	NM; CM	catalyzes the oxidation of sulfhydryl groups in peptide and protein
P23258	Tubulin gamma-1 chain	0	Centrosome	major constituent of microtubules
Q15008	26S proteasome non-ATPase regulatory subunit 6	0	C	ATPase for ubiquitination
P05089	Arginase-1	0	C	synthesizes L-ornithine and urea from L-arginine
Q9HC35	Echinoderm microtubule-associated protein-like 4	0	C	may modify the assembly dynamics of microtubules
P05198	Eukaryotic translation initiation factor 2 subunit 1	0	C	forms a ternary complex with GTP and initiator tRNA
O60879	Protein diaphanous homolog 2	0	C; E	oogenesis; regulates endosome dynamics and motility of early endosomes
Q9UBU6	Protein FAM8A1	3	M	autosomal highly conserved protein
Q96C36	Pyrroline-5-carboxylate reductase 2	0	C	housekeeping enzyme that catalyzes the last step in proline biosynthesis
Q14964	Ras-related protein Rab-39A	0	CM; Ph; L	maturation and acidification of phagosomes
P62070	Ras-related protein R-Ras2	0	C	GTPase activity; transduces growth inhibitory signals across cell membrane
P08134	Rho-related GTP-binding protein RhoC	0	CM	myosin contractile ring formation; apical junction formation
P22102	Trifunctional purine biosynthetic protein adenosine-3	0	C; Ex	synthesizes glycinamide
Q5MNZ6	WD repeat domain phosphoinositide-interacting protein 3	0	C; A	autophagosome assembly

Table 10 Conserved RHBDD2 WT and R85H hits in third IP (without crosslinker)

Accession	Protein name	TMD	localization	function
Q15436	Protein transport protein Sec23A	0	ER; G	COPII dependent anterograde transport
P53992	Protein transport protein Sec24C	0	G; ER; C	COPII dependent anterograde transport
O95197	Reticulon-3	3	G; ER	involved in membrane trafficking; ER stress pathway
Q14697	Neutral alpha-glucosidase AB	1	G; ER	glycosylation; cleaves glucose residues from oligosaccharide precursor of glycoproteins
Q12904	Aminoacyl tRNA synthase complex-interacting multifunctional protein 1	0	N; C; ER; G	binds tRNA; inflammatory cytokine activity; regulates TGF-beta signaling; glucose homeostasis;
Q6NTF9	Rhomboid domain-containing protein 2	6	G	RHBDD2
P13489	Ribonuclease inhibitor	0	C	inhibits RNASE1, RNASE2 and ANG; plays a role in redox homeostasis
Q9P003	Protein cornichon homolog 4	3	ER; IC; M	COPII dependent anterograde transport
Q969V3	Nicalin	1	ER	antagonizes Nodal signaling and subsequent organization of axial structures
Q99942	E3 ubiquitin-protein ligase RNF5	3	ER; M; Mi	E2-dependent E3 ubiquitin-protein ligase activity
P30566	Adenylosuccinate lyase	0	C; Mi	catalyzes two non-sequential steps in de novo AMP synthesis
Q6PI48	Aspartate--tRNA ligase, mitochondrial	0	Mi	aspartate-tRNA(Asn) ligase activity
P30049	ATP synthase subunit delta, mitochondrial	0	Mi	produces ATP from ADP in the presence of a proton gradient across the membrane
O76031	ATP-dependent Clp protease ATP-binding subunit clpX-like, mitochondrial	0	Mi	hydrolyzes ATP; targets specific substrates for degradation by the Clp complex
P50416	Carnitine O-palmitoyltransferase 1, liver isoform	2	Mi	mitochondrial uptake of long-chain fatty acids and beta-oxidation in the mitochondrion
O43169	Cytochrome b5 type B	1	Mi	functions as an electron carrier for several membrane bound oxygenases
Q8NFF5	FAD synthase	0	Mi; C	Catalyzes the adenylation of flavin mononucleotide
Q92947	Glutaryl-CoA dehydrogenase, mitochondrial	0	Mi	catalyzes the oxidative decarboxylation of glutaryl-CoA to crotonyl-CoA and CO2
P26440	Isovaleryl-CoA dehydrogenase, mitochondrial	0	Mi	synthesizes (S)-3-hydroxy-3-methylglutaryl-CoA from 3-isovaleryl-CoA
Q6UB35	Monofunctional C1-tetrahydrofolate synthase, mitochondrial	0	Mi	provides the missing metabolic reaction required to link mitochondria and cytoplasm
Q16718	NADH dehydrogenase [ubiquinone] 1 alpha subcomplex subunit 5	0	Mi	accessory subunit of the mitochondrial membrane respiratory chain NADH dehydrogenase
Q9GZT3	SRA stem-loop-interacting RNA-binding protein, mitochondrial	0	Mi; N	acts as a nuclear receptor corepressor
O00231	26S proteasome non-ATPase regulatory subunit 11	0	N; C	involved in the ATP-dependent degradation of ubiquitinated proteins
Q96T76	MMS19 nucleotide excision repair protein homolog	0	N; SP	mediates the incorporation of iron-sulfur cluster into apoproteins
Q8WX92	Negative elongation factor B	0	N	negatively regulates the elongation of transcription by RNA polymerase II
O15162	Phospholipid scramblase 1	1	N; M	mediates ATP-independent bidirectional transbilayer migration; fibrin clot formation
Q9UHI6	Probable ATP-dependent RNA helicase DDX20	0	N; C	plays a catalyst role in the assembly of small nuclear ribonucleoproteins (snRNPs)
Q13148	TAR DNA-binding protein 43	0	N	regulates transcription and splicing; regulates CFTR splicing
Q9UNX4	WD repeat-containing protein 3	0	N	poly(A) RNA binding; snoRNA binding
Q9P2R3	Ankyrin repeat and FYVE domain-containing protein 1	0	E; C	proposed effector of Rab5
P35613	Basigin	1	CM	targets the monocarboxylate transporters SLC16A1, SLC16A3 and SLC16A8 to the plasma membrane
Q9UDT6	CAP-Gly domain-containing linker protein 2	0	C	links microtubules to DLB; operates brain-specific organellle translocations
Q96KP4	Cytosolic non-specific dipeptidase	0	C	hydrolyzes a variety of dipeptides; tumor suppressor
P24534	Elongation factor 1-beta	0	C	translation elongation factor activity
Q9UPT5	Exocyst complex component 7	0	C; CM	involved in the docking of exocytic vesicles with fusion sites on the plasma membrane
Q96QA5	Gasdermin-A	0	C	induces apoptosis
Q06210	Glutamine--fructose-6-phosphate aminotransferase [isomerizing] 1	0	C; Ex	controls flux of glucose into the hexosamine pathway; regulate precursors for glycosylation
P47897	Glutamine--tRNA ligase	0	C	brain development
Q99538	Legumain	1	L	hydrolysis of asparaginyl bonds
O75352	Mannose-P-dolichol utilization defect 1 protein	6	M	required for normal utilization of mannose-dolichol phosphate (Dol-P-Man)
Q9NVE7	Pantothenate kinase 4	0	C	physiological regulation of the intracellular CoA concentration
A2RTX5	Probable threonine--tRNA ligase 2, cytoplasmic	0	C	ATP binding; threonine-tRNA ligase activity
O60678	Protein arginine N-methyltransferase 3	0	C	methylates the guanidino nitrogens of arginyl residues in some proteins
Q8N9Q2	Protein SREK1IP1	0	?	involved in the control of cellular survival.
P51148	Ras-related protein Rab-5C	0	CM; E; Me	involved in vesicular traffic
A6NIZ1	Ras-related protein Rap-1b-like protein	0	C; CM	Activated by GEF EPAC2 in a cAMP-dependent manner
P54577	Tyrosine--tRNA ligase, cytoplasmic	0	C	catalyzes the attachment of tyrosine to tRNA(Tyr)